Montanuniversität Leoben - University of Leoben

Department Metallurgie - Department of Metallurgy

Nichteisenmetallurgie - Nonferrous Metallurgy

MASTER THESIS

Topic

Characterisation of anode slimes with regard to a multi-metal recovery

submitted by

Christoph Otto

supervised by

Dipl.-Ing. Dr.mont. Stefan Steinlechner

Priv.-Doz. Dipl.-Ing. Dr.mont. Jürgen Antrekowitsch

Leoben, October 2017

NICHTEISENMETALLURGIE
MONTANUNIVERSITÄT
A-8700 LEOBEN

Christoph Otto

October 2016

Characterisation of anode slimes with regard to a multi-metal recovery

During copper production tramp elements, like precious metals are separated in the electrolytic refining step as a by-product called anode slime. The dominating European treatment method of anode slimes for production of precious metals is a pyrometallurgical melting together with lead after an acidic anode slime washing step. This is done for example in a Top Blown Rotary Converter. In this step the less noble elements are oxidized unless a Dore metal is obtained. During this oxidation step increased effort in the off gas- and slag-handling is required, due to present arsenic and antimony. Also the loss of tin is a crucial point for a possible optimization. So, in case of a successful removal of Sn, As and Sb preliminary to this pyrometallurgical oxidation step a significant optimization for a copper producer could be realized.

Therefore, the diploma thesis to be prepared should include following subject areas with the final target to form the base for a removal of selected tramp elements. First of all a detailed literature survey on the present situation of anode slime compositions and production places is required. The origin of the anode slime together with the knowledge of the process of formation builds the base for a detailed characterization of the anode slime sample. As the morphology strongly influences the behaviour in a potential upgrade process, especially the presence of tin, arsenic and antimony in the sample needs to be investigated. Therefore, based on an elemental analysis also the main compounds carrying Sn, As and Sb, utilizing XRD technology, have to be determined. In case of a too low amount of element to be determined via XRD additionally SEM (scanning electron microscope) analysis shall be used. The examined characterization in combination with the carried out literature survey will then form the base for the selection of a suitable process to separate those elements from the rest of the slime. To select or develop a suitable treatment concept additionally an evaluation of existing processes based on literature together with thermodynamic calculation of the behaviour of the target elements shall be performed. Finally tentative trials investigating the main process parameters should show the technical viability to separate Sn, As and Sb from the anode slime.

Leoben, October 2016

Eidesstattliche Erklärung

Ich erkläre an Eides statt, dass ich die vorliegende Arbeit selbstständig verfasst, andere als die angegebenen Quellen und Hilfsmittel nicht benutzt und mich auch sonst keiner unerlaubten Hilfsmittel bedient habe.

Affidavit

I declare in lieu oath, that I wrote this thesis and performed the associated research myself, using only literature cited in this volume.

Datum / Date	Christoph Otto

Acknowledgement

At first I would like to thank Dipl.-Ing. Dr.mont. Stefan Steinlechner and Priv.-Doz. Dipl.-Ing. Dr.mont. Jürgen Antrekowitsch, who supervised this diploma thesis, for their help and many useful proposals during the development of the current investigations, right from the beginning.

Special thanks are also dedicated to Dipl.-Ing. Dr.mont. Holger Schnideritsch and Dipl.-Ing. Josef Fasching, for their help and instruction in the field of SEM-analysis.

And of course I would like to thank my family, especially my wife Lucie, my parents Anneliese and Stefan as well as my grandparents Anna and Otto, for their encouragement and support of all kinds, all throughout my studies at Montanuniversität during the past decade.

Kurzfassung

Die vorliegende Diplomarbeit beschäftigt sich mit den Möglichkeiten der Aufarbeitung von Anodenschlämmen aus der Kupferraffinationselektrolyse im Hinblick auf eine möglichst effiziente Wiedergewinnung der verschiedenen enthaltenen Metalle. Der Fokus wurde dabei auf die Begleitelemente Sn, As und Sb gelegt, da diese einerseits das weitere Recycling stören, aber andererseits auch wiederverwertbar sind, sofern sie in einer reinen Form extrahiert werden können.

Die Literaturrecherche gibt einen Überblick über die anfallenden Reststoffe bei Produktion und Recycling von Kupfer. Detaillierter wird dabei der Anodenschlamm behandelt, insbesondere seine Entstehung während der Elektrolyse. Weiters werden ein Auszug der Zusammensetzungen von Anodenschlämmen aus verschiedenen Kupferhütten weltweit, sowie eine Zusammenfassung jener Phasen, welche Forscher in der Vergangenheit in Anodenschlämmen detektiert haben, präsentiert. Die Prinzipien der im Zuge der Arbeit verwendeten Messverfahren werden kurz beschrieben. Der Stand der Technik im Recycling von Anodenschlamm wird skizziert und im Anschluss sind ausgewählte, pyro- und hydrometallurgische Verfahren vorgestellt, welche derzeit zur Vorbehandlung von Anodenschlämmen angewandt bzw. erforscht werden.

Der erste Teil der experimentellen Arbeit befasste sich mit der detaillierten Charakterisierung von zwei Anodenschlammproben unter Zuhilfenahme der chemischen Analyse, XRD, SEM-EDX sowie stöchiometrischer Berechnungen in Anlehnung an die Literaturrecherche. Lokale Koexistenzen verschiedener Elemente wurden untersucht und am Ende gelang es, einige der unter dem REM sichtbaren Phasen zu identifizieren.

Den zweiten Teil stellten Tastversuche zur Laugung von Sn, As und Sb aus Anodenschlamm in wässriger KOH-Lösung dar. Das Versuchslayout wurde im Hinblick auf die Energieeffizienz bewusst einfach gehalten, d.h. unter Atmosphärendruck und bei moderaten Temperaturen. Im Zuge der Versuchsreihen wurden die Temperatur im Bereich von Umgebungstemperatur bis 80 °C und das Fest/Flüssig-Verhältnis von 1/4 bis 1/20 variiert. Die höchste Ausbringung aller drei Elemente konnte bei 80 °C und einem Fest/Flüssig-Verhältnis von 1/20 erreicht werden, wobei über 80 % des enthaltenen As und Sn sowie knapp 40 % des enthaltenen Sb gelaugt werden konnten. Weiters wurde die Temperaturführung als kritischer Schritt im Prozess erkannt und am Ende Vorschläge zur weiteren Optimierung präsentiert, mit besonderem Fokus auf die separate Laugung von As und Sb.

Abstract

The current diploma thesis deals with the possibilities of the processing of anode slimes from the copper refining electrolysis with regard to an efficient recovery of the contained metals. The focus was laid on the tramp elements Sn, As and Sb, as they disturb the further recyling on the one hand, and are reusable on the other hand, as long as they can be extracted in a pure form.

The literature survey gives an overview of the residues occurring in the production and recycling of copper. The anode slime is dealt with in more detail, especially its formation during the electrolysis. Furthermore, an excerpt of compositions of anode slimes from different copper plants worldwide and a summary of phases detected in anode slimes by researchers in the past are presented. The principles of the measuring methods used within this diploma thesis are briefly described. The state of the art in the recycling of anode slime is sketched, and subsequently, selected pyro- and hydrometallurgical processes are introduced, which are currently applied or investigated for the pretreatment of anode slimes.

The first part of the experimental work dealt with the detailed characterisation of two anode slime samples using chemical analysis, XRD, SEM-EDX and stoichiometric calculations following the literature survey. The local coexistency of different elements was investigated and at the end it was possible to identify some of the phases visible in the SEM images.

Tentative trials on the leaching of Sn, As and Sb from anode slime in aqueous KOH-solution represented the second part. The experimental layout was intentionally kept simple with regard to energy efficiency, i.e. atmospheric pressure and moderate temperatures. In the course of the experimental series the temperature was varied in the range between ambient temperature and 80 °C and the solid/liquid ratio between 1/4 and 1/20. The highest yield of all three elements could be achieved at 80 °C with a solid/liquid ratio of 1/20, where over 80 % of the As and Sn contained as well as nearly 40 % of the Sb contained was leached. Moreover, the temperature control was recognised as a crucial step within the process, and at the end proposals for further optimisation are presented, with special focus on the separate leaching of As and Sb.

Table of contents

1 Introduction

Copper anode slime is a by-product of copper refining electrolysis, where relatively impure anode copper is converted into high purity cathode copper. In general it can be assumed that in the electrolysis process elements that are less noble than copper dissolve in the elctrolyte while all noble ones remain in their metallic state and accumulate as anode slime [1,2]. Ignoble elements can also appear in the anode slime if they form insoluble compounds after their dissolution in the electrolyte [3]. As a consequence, copper anode slime is rich in valuable metals such as Se, Te, As, Sb, Bi, Pb, Au, Ag and Pt, in addition to considerable amounts of Cu [1,2].

The state of the art in treating copper anode slime is based on a three-step process route which consists of pretreatment, concentration and refining. In the pretreatment, base metals which would have negative effects on the subsequent procedures such as Cu, Pb, Sb or As are removed from the slime. Concentration is achieved by smelting or hydrometallurgically by selective dissolution. The final refining is necessary to obtain sellable precious metals [2,4]. However, the selection of the processing method strongly depends on the chemical composition of the particular anode slime. Therefore, a wide variety of methods and research approaches exists.

Pretreatment is the most crucial step in the processing of copper anode slime [5,6]. According to Liu et al., only three pretreatment methods are presently applied on an industrial scale [7]: sulphating roasting [4], acid pressure oxidation leaching [2] and ore dressing.

The emphasis of this diploma thesis is on Sn, As and Sb, whose concentrations are relatively high in the investigated anode slime. As described before, these elements should be removed in the pretreatment step before further processing of the slime to avoid qualitative and environmental problems during the treatment process. Especially the removal of As and Sb has already been the subject of various research activities in recent years [1,7–10]. However, the main problem which remains is the occurence of toxic off-gas or solutions. They have a complex chemistry that prevents a seperate recovery of all constituents, as it is simply not profitable in many cases. Furthermore, these by-products are cost-intensive since they have to be treated as hazardous waste.

Therefore, the aim must be a separate recovery of Sn, As and Sb. In order to reach this goal, detailed knowledge of the chemical behaviour and morphology of these elements is necessary. As a consequence, this diploma thesis focusses on the characterisation of the

provided anode slimes, with special attention to Sn, As and Sb compounds. Not only are the chemical compounds of interest, but also their paragenesis, as one single grain of an anode slime often consists of different chemical compounds which adhere to each other, for instance in a layered form. This fact is crucial, because it can limit the yield of any recovery process, as a shell, which has grown over a primary grain, might prevent the core from dissolution or volatilisation or whatever removal approach.

Once a detailed characterisation can be provided, it can be predicted much more easily which mechanism would work properly in order to remove certain constituents, in this case Sn, As and Sb, with a satisfying rate of yield.

2 Theoretical background and literature study

This chapter deals with the theoretical background concerning copper refining anode slime. It comprises a brief outline of the copper production route and the way of precious metals through it. The effect of anode slime formation itself is also described as well as characterisation and treatment methods for the processing of anode slime.

2.1 Precious metals in residues and by-products of copper production

For the production of copper, both pyro- and hydrometallurgical processes are applied. Sulfidic ores are processed pyrometallurgically, whereas oxidic ores undergo the hydrometallurgical route [11]. In consideration of investigating the electrorefining anode slime, only the pyrometallurgical route is of interest because the winning electrolysis of the hydrometallurgical route does not produce anode slime.

Figure 2-1 shows the flow chart of the pyrometallurgical production of copper. The bold arrows in the chart show the way precious elements – and all of those which are nobler than copper – tend to take within the process. These assumptions are based on simple analysis of the chemical and atmospherical conditions in each process step. The green-coloured panels represent residues that arise in the various different aggregates. Those which are supposed to contain a considerable amount of precious metals – as indicated by the arrows – are printed in bold type.

The result of the process analysis is the following list of potential residues, where precious metals might be contained in a considerable amount:

- Flash smelting dust (Outokumpu-furnace, KIVCET furnace)
- Direct melting dust (Inco, Noranda, TBRC, Ausmelt/Isamelt)
- Matte melting dust (electric furnace, reverberatory furnace)
- Copper converter dust (Peirce-Smith converter)
- Fire refining dust (reverberatory furnace, rotary drum furnace)
- Anode furnace slag
- Anode slime (refining electrolysis cell)

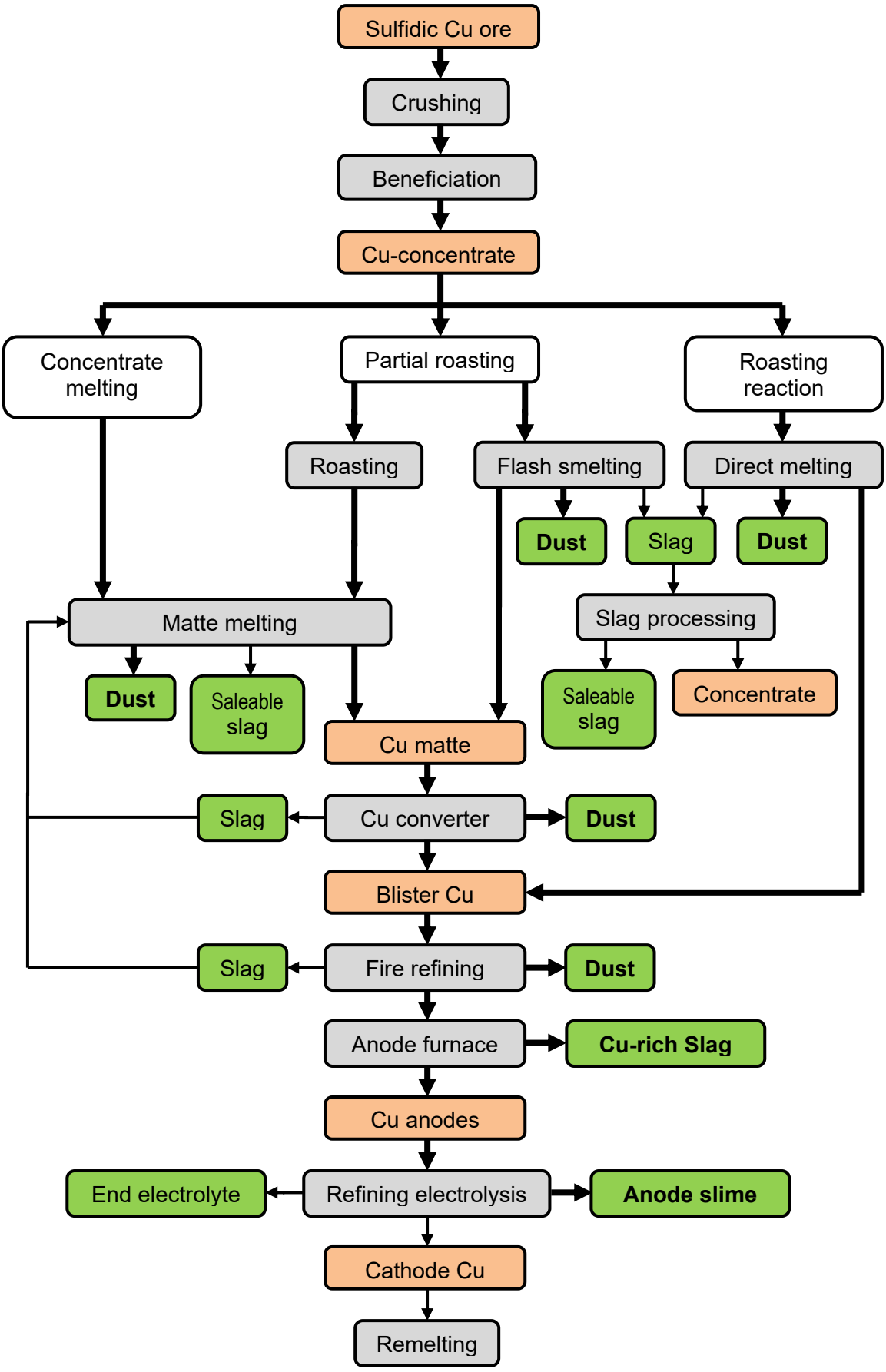

Figure 2-1: Pyrometallurgical copper production [11]

It can be seen that there are many process dusts within the copper production route. According to literature data, they contain large amounts of Cu, Zn, Pb, As and Fe but not high concentrations of precious metals [11–14]. Slags from the copper anode furnace contain more than 40 % Cu. That is why these slags are recycled internally in the copper plants. As stated in literature, in anode furnace slag there is not much precious metal contained, either [11,15]. However, anode slimes, which represent the last by-product in the pyrometallurgical copper production route, are best known for their relatively high content in valuable metals, which is also confirmed by literature data [11,15,16] and the chemical analysis provided together with the anode slime samples used for the investigations in this diploma thesis. An excerpt of these analyses is shown in Table 2-II.

2.2 Anode slime formation

Copper anode slime is a by-product of the electrolytical refining of pyrometallurgically produced copper anodes. The process parameters in the electrorefining cells are adjusted in such a way that theoretically, elements nobler than copper are not dissolved while ignobler ones are dissolved and not deposited on the copper cathode. As a result, on the one hand noble elements (e.g. Au, Ag, PGM) remain as small particles, as the anode matrix successively dissolves. On the other hand, the electrolyte is enriched with ignoble metals. Some of them (e.g. As, Sb, Pb, Ni) tend to react with the sulphatic electrolyte, with dissolved oxygen or with each other. In the process, insoluble compounds can be formed, which are found in the anode slime as well. Copper itself is also able to form metallic particles in the electrolyte by disproportionation of monovalent copper (cuprous Cu^{+}) ions. In this case copper is lost, as these particles do not get deposited on the cathode but can be found in the anode slime [11,17,18].

In summary, the elements and components in an anode slime can be classified according to their behaviour during the electrorefining process [1,19]. This classification is presented in Table 2-I. It is important to note that this list is a coarse classification and does not comprise every possible chemical compound which can appear as a constituent in copper anode slime. Furthermore, the noble elements and copper do not only occur in their elemental form but sometimes in compounds or alloys, as well.

Table 2-I: Classification of elements and components in anode slimes [1,19]

Classification	Elements	Form / phase
Nobler than Cu	Au, Ag, PGM	Elemental
E^0 close to Cu	As, Sb, Bi	Mixed oxides with Pb or arsenates
E^0 lower than Cu	Pb, Sn, Ni, Co, Fe, Zn	$PbSbO_2$, $PbAsO_2$, SnO_2, NiO, Fe_2O_3, $PbSO_4$, $Sn(OH)_2SO_4$
Cu	Cu	Elemental
Chalcogen	S, Se, Te	$(Cu,Ag)_2(Se,Te)$, Cu_2S

According to Wang et al. [17], another approach for the classification of anode slime constituents is based on the different formation mechanisms. Wang's classification is presented below:

- Primary slimes
- Secondary slimes
    - First reaction slimes
    - Second reaction slimes
        - Floating slimes
        - Normal slimes

Primary slimes are chemically unchanged remainings from the anode (e.g. noble metals, sulphides and selenides); secondary slimes result from chemical reactions of primarily dissolved elements. First reaction slimes are the result of a chemical reaction with the electrolyte (e.g. $PbSO_4$, AgCl). As electrolyte is present in a sufficient amount, first reaction slimes build up immediately after the dissolution of the metal component. Second reaction slimes are the product of chemical reactions in the electrolyte, which require dissolved oxygen in the electrolyte. That way high valence oxides are formed, which are the basis for the precipitation of antimonates and arsenato-antimonates [17].

The difference between floating and normal slimes is their hydrodynamic behaviour. While normal slime settles on the ground of the electrolysis cell quite fast, floating slime remains suspended in the electrolyte for very long times without settling and can thus cause severe issues concerning the quality and purity of the copper cathodes since the floating particles get entrapped in the growing surface of the cathode. The reason for the different behaviours of floating and normal slime is not the specific weight, which is approximately 3.55 g/cm³ for both, but the different structures. While normal slime has a crystal structure with a more or less defined surface, floating slime consists of very fine particles with a two-dimensional amorphous structure and irregular shape [3].

According to the formation mechanism, it can be assumed that the chemical composition of the resulting anode slime depends on two important factors:

- Concentrations of tramp elements in the anode Cu
- Parameters of the refining electrolysis

As a consequence, the chemical compositon of anode slimes deriving from different refining plants can vary across a wide range. Table 2-II gives an exemplary overview of the chemical composition of copper refining anode slimes from refining plants around the globe. Elements written in green are considered precious, while those in red are considered hazardous, as their presence can cause environmental issues.

Table 2-II: Chemical compositions of copper anode slimes at various refining plants

Origin of slime (Plant, country)	Cu	Au	Ag	Pt	Pd	Ni	Se	Te	As	Sb	Sn	Pb	Others	Ref.
Slime 1 (crude)	11.5	0.3	5.9	0.01	0.04	3.7	0.6	0.7	2.6	8.2	2.0	12.4	Ba, S, Bi, Cl	
Slime 2 (washed)	7.1	0.4	7.2	0.01	0.06	3.6	1.0	1.0	3.5	11.5	3.3	22.8	Ba, S, Bi	
Norddeutsche Affinerie, Germany	15.5	0.5	13				6.0	1.5	4	6		14		[20]
Outokumpu, Finland	4.2	0.9	7.7				3.3	1.5	4.9	5.1		5.3		[20]
Kazakhmys, Kazakhstan	1.2	0.25	19.5				7.0	1.1	0.85	5.0		35		[20]
Pol'skaya med', Poland	11.8	0.02	32.8				2.3		1.8	0.3		16.5		[20]
Boliden, Sweden	9.8	0.65	21.3				3.3	1.6	0.95	2.6		7.8		[20]
Kennecott, USA	20	0.5	5				5	1	5	1		30		[20]
Noranda, Canada	17	1	25				7	4	1.5	1		10		[20]
Uralelektromed', Russia	2.0	0.7	17.5				9.0	3.5	2.0	12.5		24		[20]
Kyshtym MEZ, Russia	11.7		8.92				5.97	3.3	3.3	24.8		18.0		[20]
Sarkuysan Copper, Turkey	25.80	0.23	2.80			0.29	4.68	0.90	3.93	0.99	8.1	12.93	S, Mg, Cl	[18]
Hindustan Copper Ltd., India	12.3	0.0064	1.5	0.015		36.8	10.5	3.4	0.036	0.01		0.16	Si	[15]
SWIL Ltd., India	1.0		12.0			23.0	1.2		0.3		2.4	11.0		[16]
Nat'l Sarcheshmeh Copper Co., Iran	4.3	0.12	4.5				7.3			2.16		3.54	Ba	[17]

2.3 Constituents of copper anode slime

In the characterisation of the anode slime, the main goal is to find out which chemical compounds are formed by the elements present in the slime. Before starting the investigations it is necessary to know what species to look for primarily. Therefore, the first step regarding the characterisation is a literature survey, in which constituents have already been found in copper anode slimes of other investigations. A summary can be found in the subsequent section. Table 2-III and Table 2-IV show the stoichiometric compounds according to the literature study.

Table 2-III: Chemical compounds in copper anode slimes – summary of literature survey – part 1

Base element	Chemical formula	Comments	References
Cu	Cu		[1,19]
	Cu_2O		[21,22]
	Cu_2S		[1,19]
	$CuSO_4$		[9]
	$CuSO_4 \cdot 5H_2O$		[5,8,19,21,22]
	CuCl		[21]
	$Cu_4(OH)_6SO_4 \cdot 2H_2O$		[5]
	$CuFeS_2$		[5]
	$Cu_2(Se,Te)$		[1,5,7,9,18,19]
Sn	SnO_2		[1,19]
	$Sn(OH)_2SO_4$		[1,19]
As	As_2O_3		[8]
	CuAs		[5]
Sb	Sb_2O_3		[3]
	Sb_2O_4		[8]
	$SbAsO_4$		[8,18,19,23–26]
	$(Sb_2O_3)_x \cdot (As_2O_5)_{1-x}$	floating slime	[5]
	$(Sb_2O_5)_x \cdot (As_2O_5)_{1-x}$	light slime	[5]
Ni	NiO	tiny crystals	[1,19,27,27]
	$NiSO_4 \cdot 2H_2O$		[5]
	$Cu_3Ni_{2-x}SbO_{6-x}$	X = 0.1 – 0.2	[19]
	$(Ni,Fe)Cr_2O_4$		[5]

Table 2-IV: Chemical compounds in copper anode slimes – summary of literature survey – part 2

Base element	Chemical formula	Comments	References
Pb	$PbSO_4$		[1,7,9,18,19,27,28]
	PbO		[8]
	Pb_3O_4		[8]
	$Pb_2As_2O_7$		[8,19]
	$Pb_5(AsO_4)_3(OH,Cl)$		[19]
	$Pb(Sb,As)O_2$		[1,19]
	$PbO(Sb_xAs_{1-x})_2O_5$		[5]
	$Cu_8Pb_{12}As_{10}O_{31}$	empirical formula	[19]
	$Cu_7Pb_{16}As_9O_{33}$	empirical formula	[19]
Si	SiO2		[5,9,18]
	CaFeSiO4		[5]
Ag	Ag	i > 220 A/m²	[1,5,9,19,21,28]
	AgCl		[5]
	$Ag_2(Se,Te)$		[1,9,19,27]
	AgCu(Se,Te)		[9,19,22,27,28]
	$(Cu,Au,Ag)_2(Se,Te)$		[5]
	$(Cu,Ag)_2OSeO_2$		[5]
	AgCuSe	Ag/Se < 1.7 [28]	[7,28]
	Ag_3Sb		[5,8]
Au	Au	elemental	[1,9,19,21]
	AuTe		[5]
Se, Te	Se, Te	elemental	[5]
Ba	$BaSO_4$		[7,9,19,27]
Zn	ZnS		[5]
S	S	elemental	[5]
Bi	$BiAsO_4$		[23–26]
Pt	Pt	elemental	[1,19]
Pd	Pd	elemental	[1,19]
Ca	$CaSO_4 \cdot 2H_2O$	gypsum	[5]
Al	Al_2O_3		[5]
Fe	Fe_2O_3		[1,5,19]
Mg	MgO		[5]

In addition to the chemical compounds listed in the previous table, different non-stoichiometric phases are also mentioned resulting from to the literature study, listed in Table 2-V.

Table 2-V: Non-stoichiometric phases in copper anode slimes – summary of literature survey

Species	Comments	References
Cu-Ag-Pb sulphate		[21]
Cu-Ag-Pb selenite		[21]
Cu-Ag-Pb arsenate		[21]
Cu-Ag-Pb tellurite		[21]
Cu-Pb-As oxide		[19,22]
Pb-Cu-Bi oxide		[27]
Sb-As-Bi-Sn-Pb-Cu oxide		[19,21,22]
Me-SeO_2	Selenites of metals	[5]
Silicates		[27]

2.4 Characterisation methods

This chapter gives a brief description of the analytical methods used for the characterisation of the anode slimes.

2.4.1 Chemical analysis

Chemical analysis was needed to measure the composition of anode slime on a macroscopic as well as on a microscopic scale and of reaction products obtained from the experiments. Energy dispersive X-ray spectrography (SEM-EDX) was applied for the determination of the composition of microscopically small grains in the slime. For measuring the composition of the obtained solution, the filter cakes and the raw material, inductively coupled plasma optical emission spectroscopy (ICP-OES) was used. These analysis was done at an external laboratory.

2.4.2 XRD analysis

X-ray diffractometry was used for the phase identification of anode slime samples. The available X-ray diffractometer contains a mineralogical database, which provided the necessary comparative information. Figure 2-2 shows the basic principle of XRD, Bragg diffraction. As apparent from the figure, constructive interference is only reached if the wavelength of the X-ray beams is equal to d·sinθ or a multiple thereof.

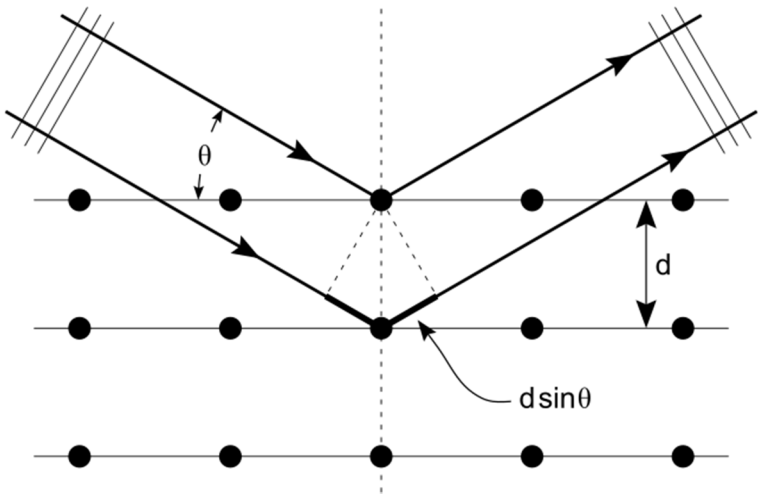

Figure 2-2: Principle of XRD (Bragg diffraction) [29]

As a consequence, each mineral has its own characteristic fingerprint of wavelengths where interference can be observed. These appear as peaks in the corresponding XRD spectra. As a huge variety of different compounds are present in the anode slime samples, the single fingerprint of all constituents will not appear individually but as a cumulative curve. This curve will only give qualitative information on what chemical compounds are most likely contained in the sample. For a quantitative analysis, the results of different techniques have to be combined.

2.4.3 SEM analysis

For the characterisation of the anode slimes, a scanning electron microscope (SEM) including energy dispersive X-ray spectroscopy was utilised. In Figure 2-3 the operating mode of SEM-EDX is shown schematically.

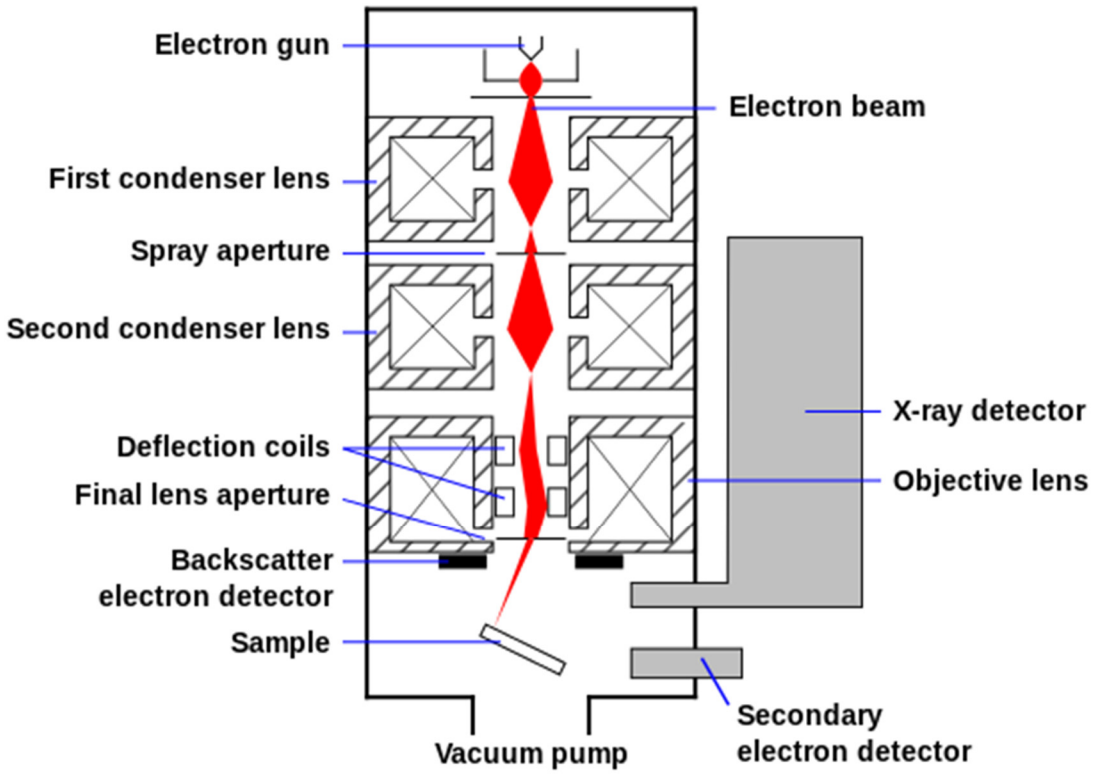

Figure 2-3: Schematic of SEM-EDX [30]

Basically, electrons emitted by the electron gun are accelerated and shot onto the sample surface. The secondary electron detector and the backscatter electron detector are responsible for the creation of the SEM image. The X-ray detector uses the characteristic X-ray emission of the different elements in the sample to determine the chemical compositon of the activated sample area. This technique was used to get information about the chemical composition of microscopic grains in the anode slimes.

2.5 Methods for pretreatment of anode slimes

In agreement with numerous publications about copper anode slime treatment, the processing techniques can be seen as a three-step process [1,2]:

- Pretreatment (removal of base metals)
- Concentration (enrichment of valuable metals)
- Refining (winning of sellable products)

The emphasis within this diploma thesis is the removal of tin, arsenic and antimony. Their content is relatively high compared to the concentration of precious metals. Therefore, they are base metals. Subsequently, the focus is on the pretreatment methods.

As already indicated in the introduction, pretreatment is responsible for removing those elements from the anode slime which would harm the subsequent process steps if they were left in the raw slime [2,4]. Especially the separation of Cu, Se and Te from copper anode slime has been the subject of many publications in the past [2,4,18,31,32]. But also methods for the characterisation and removal of As and Sb phases have been dealt with, as papers published in the last years from all over the world prove [5,8,9,33]. According to Liu et al., only three methods are currently applied industrially [7]:

- Sulfation roasting [4]
- Acid pressure oxidation leaching [2]
- Ore dressing

None of them is currently able to gain As and Sb selectively. As a consequence, alternative methods have been researched which enable such selective separation of these two elements. The following approaches have been published and successfully verified on laboratory scale:

- Selective leaching of As and Sb in KOH [9]
- Vacuum dynamic evaporation and vacuum dynamic flash reduction [8]
- Alkaline pressure oxidative leaching [7]

All those investigated methods focussed mainly on the removal of As and most of them are also able to extract Sb. However, the removal of Sn does not play a role in the papers mentioned. No publications about the removal of Sn from copper anode slimes were found during the literature study for this diploma thesis. The following section gives a brief overview of the research approaches for selective As and Sb removal pointed out above. Special focus is laid on the KOH leaching process because this technique might also have the ability to achieve tin removal, in addition to a possible separation of the removed elements.

2.5.1 Selective leaching of As and Sb in KOH

This pretreatment procedure was published by Fernández et al. in 1996 and consists of several hydro- and pyrometallurgical steps [9]:

- KOH leaching ($p = p_{atm}$; T = 60-100 °C): selective leaching of As and Sb
- Alkaline roasting (K_2CO_3; T = approx. 400-500 °C)
- H_2O leaching (room temperature): selective leaching of Se
- H_2SO_4 leaching: selective leaching of Cu and partly Te
- HCl leaching: selective leaching of Te and partly Cu
- Smelting

The first process step (KOH leaching) is of particular interest concerning the topic of this diploma thesis and is therefore described in detail below. At first it has to be pointed out that in comparison to other investigated techniques, this process works at atmospheric pressure at relatively moderate temperatures, conditions which can be easily set in a laboratory without expensive vacuum or high-pressure apparatusses. With regard to a possible industrial application, this approach is attractive from the economical point of view.

Arsenates of alkaline metals are soluble at room temperature and potassium antimonate is soluble in hot water [9]. This circumstance indicates that beside the selective removal of As and Sb in one step, a separate winning of both at different conditions also seems possible.

Fernández et al. used two different types of anode slimes for their experiments. Firstly, oxidised slime (OXID) which was filtered, dried and stored after its removal from the electrolysis cell, and secondly, non-oxidised slime (NONOXID), which was processed directly after taking it from the cells [9]. The difference between those is the oxidation state of the arsenates and antimonates [3]. The non-oxidised ones are more easily soluble.

Fernández et al. investigated the influence of the KOH concentration of the leaching solution, the process temperature and the solid/liquid (S/L) ratio on the As and Sb yield as well as the influence of the KOH concentration on the (unwanted) Cu and Se yield during KOH leaching. All investigations refer to both OXID and NONOXID samples [9].

The anode slime used for the experiments in this diploma thesis can be considered oxidised, because it was delivered by the industry partner in a dry state and had months of time to oxidise at atmospheric conditions before the experiments were started.

Below, the results of the investigations of Fernández et al. are shown. In Figure 2-4 the effect of the KOH concentration on the As and Sb yield can be seen.

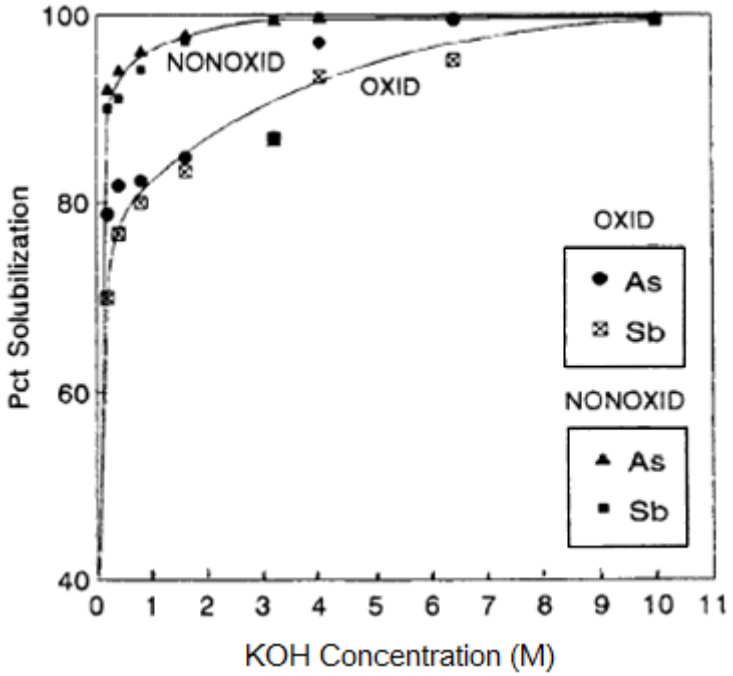

Figure 2-4: Effect of the KOH concentration on the solubilisation of As and Sb from oxidised (OXID) and non-oxidised (NONOXID) anode slimes. Conditions: 80 °C, 30 min, S/L ratio = 1/40, 5 g of anode slime [9]

As little as 0.4 M KOH is enough to leach about 80 % of As and Sb contained in the anode slime and the yield increases with a rising concentration of KOH. It is also clearly visible that As and Sb are better leachable from a non-oxidised slime. The KOH concentration of the solution also has an impact on the carry-over of Cu and Se. The higher the concentration, the more Cu and Se are leached. While As and Sb are better leachable from non-oxidised slime, Cu and Se are leached from non-oxidised slime in smaller amounts than from oxidised slime [9]. Figure 2-5 shows the influence of the process temperature on the As and Sb yield.

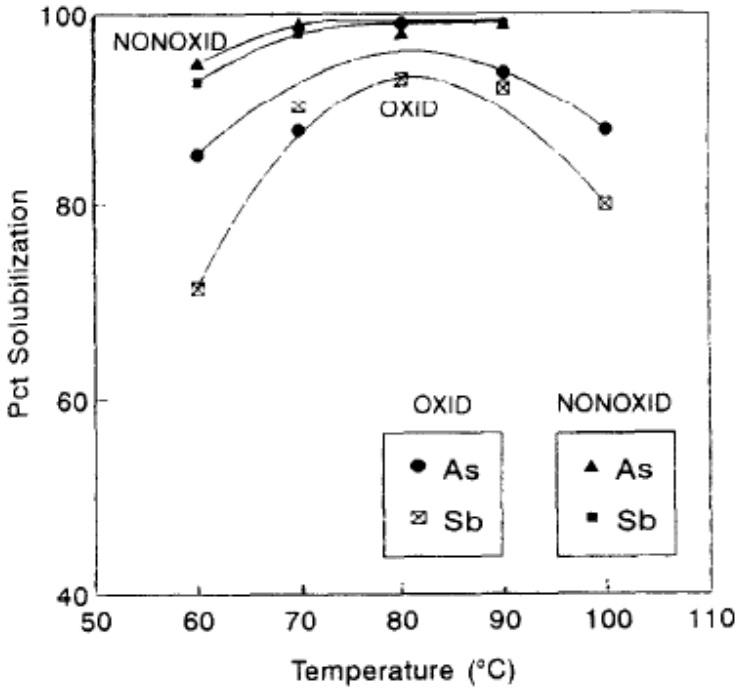

Figure 2-5: Effect of the leaching temperature on the solubilisation of As and Sb from oxidised (OXID) and non-oxidised (NONOXID) anode slimes. Conditions: 4 M KOH, 30 min, S/L ratio = 1/40, 5 g of anode slime [9]

It also becomes obvious from this figure that non-oxidised slimes are more advantageous for the leaching process. But in contrast to the concentration dependency, the temperature shows an optimum value of about 80 °C where the maximum amounts of both As and Sb are removed. Sb is a bit less soluble than As for each tempeature, especially for oxidised slime [9]. Both parameters shown above, KOH concentration and temperature, show an equal effect on both elements, As and Sb. This is not the case for the influence of the S/L ratio which affects these elements in a different way, as shown in Figure 2-6 [9].

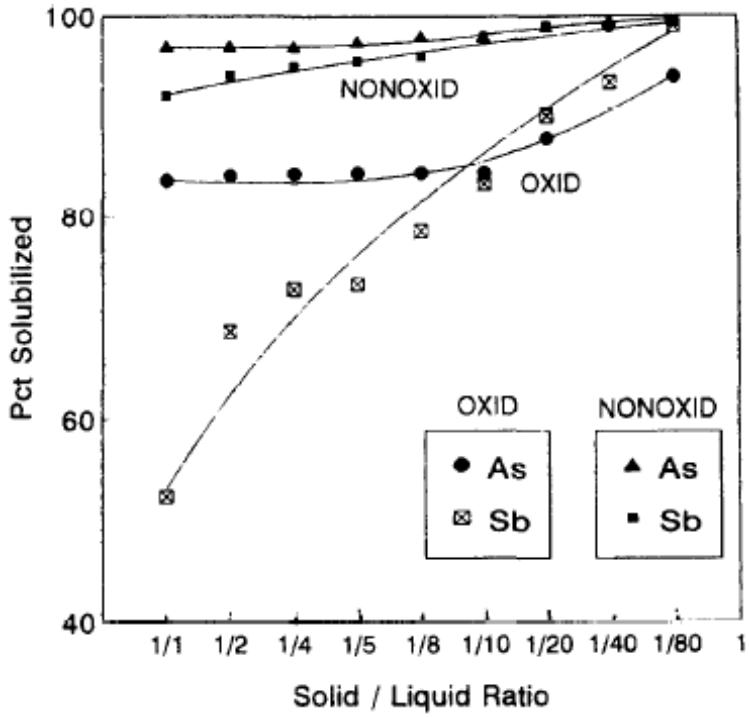

Figure 2-6: Effect of the solid/liquid ratio in the pulp on the solubilisation of As and Sb from oxidised (OXID) and non-oxidised (NONOXID) anode slimes. Conditions: 80 °C, 4 M KOH, 30 min, 5 g of anode slime [9]

For the case of oxidised slime, the solubility of Sb is significantly reduced for high S/L ratios, even at the relatively high temperature of 80 °C. All curves generally show a tendency to a higher yield with decreasing S/L ratios [9].

2.5.2 Vacuum dynamic evaporation/flash reduction

In contrast to the aforedescribed concept, vacuum dynamic evaporation/flash reduction is a pyrometallurgical approach published by Lin et al. in 2012. It is a two-step process that consists of an evaporation and simultanous reduction step of As and Sb oxides from the anode slime. Charcoal powder is used as a reductant. The reduction leads to the transformation of the high valence oxides of As and Sb to the lower valence forms. These are more easily evaporable [8].

Lin's experimental apparatus consisted of a stainless steel pipe, a furnace and a condensation cavity. Slime and reductant is dosed in a porcelain boat and then loaded into the pipe, set under a vacuum and heated up. The process temperatures in Lin's experiments were in a range between 660 and 860 °C; the reductant dosage was under 10 % of the slime amount. The residual gas pressure of the vacuum of 250 Pa allows a continuous air flow that removes the evaporated oxides from the reaction chamber. What remains after the process

is a silver alloy rich in lead, arsenic and antimony and a condensate consisting of As_2O_3 and Sb_2O_3 [8].

Best removal rates of more than 99.9 % can be reached for As under the following process conditions [8]:

- T = 760 °C
- Evaporation time = 60 min
- Air flow rate = 400 ml/min (corresponding to residual gas pressure of 250 Pa)
- 7.5 % reductant dosage

The most considerable disadvantages of this technology are the necessary energy consumption to heat up the slime including the reductant and the necessity of vacuum, which is always a significant cost factor if needed.

2.5.3 Alkaline pressure oxidative leaching (APOL)

Like Fernández's leaching process described above, this approach published by Liu et al. in 2014 also uses alkaline leaching followed by sulphuric acid leaching (SAL). Figure 2-7 shows the basic process layout [7].

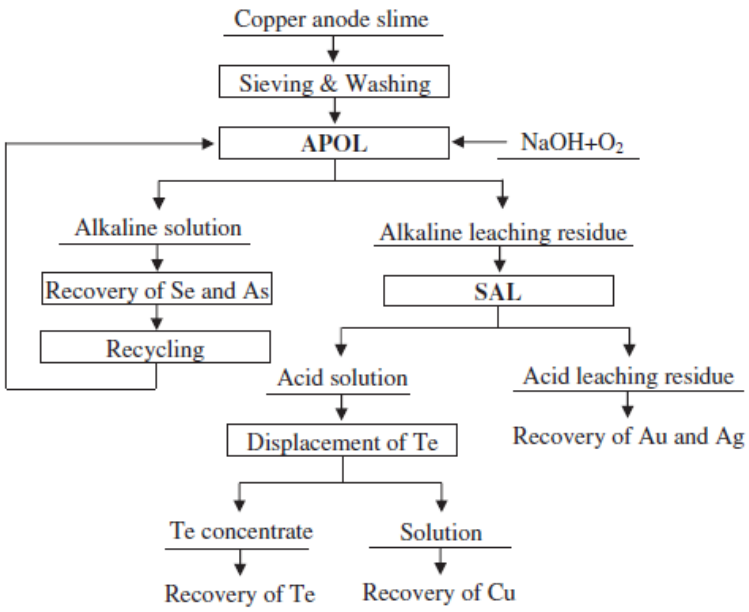

Figure 2-7: Flowsheet of copper anode slime pretreated by the process of alkaline pressure oxidation leaching [7]

In contrast to the other approaches, Sb is not a topic of this research work; Liu et al. focussed on As and Se instead. These can be removed by the alkaline leaching step. For the alkaline leaching step NaOH is utilized and the process is carried out in an autoclave under oxygen atmosphere to achieve oxidative high-pressure conditions. During leaching the slurry in the autoclave is continuously stirred. The optimum conditions for the alkaline pressure oxidation leaching, at which up to 99 % of the As and Se contained could be leached, were the following [7]:

- NaOH concentration = 2 mol/l
- Oxygen partial pressure = 0.7 mPa
- Stirring speed = 750 rpm
- Solid/liquid ratio = 1/5
- T = 200 °C
- Reaction time = 3 h

The subsequent H_2SO_4 leaching was executed under the following conditions [7]:

- H_2SO_4 concentration = 3.6 mol/l
- Stirring speed = 400 rpm
- Solid/liquid ratio = 1/5
- T = 85 °C
- Reaction time = 3 h

That way, 95 % of Cu and 77 % Te are leachable from the remaining residue. One disadvantage of Liu's approach is the necessity for an autoclave to reach pressurised conditions.

2.5.4 Summary

In conclusion, there are two basic principles used to remove As and Sb from copper anode slimes: evaporation and dissolution in alkaline media. In all processes temperature, time and oxygen activity play an important role. The simplest process layout can be realised using KOH leaching because neither autoclaves nor vacuum technology is required. A simple heating plate is sufficient to control the process conditions.

3 Characterisation procedure and results

The first step of the experimental procedure was the chemical analysis and phase characterisation of the anode slime sample. Two different grades of anode slimes were used for the tests. One of them was anode slime in crude condition, straight from the refining electrolysis cell. The other one was basically the same material but washed in sulphatic milieu in a separate step, with different conditions than in the electrolysis cell.

3.1 Chemical analysis

Table 3-I shows the results of the chemical analysis of the anode slime sample materials. The concentrations of Sn, As and Sb are elevated. Cu results from the disproportionation reaction $2\ Cu^{+} \rightarrow Cu + Cu^{2+}$ and from the chemical reaction with other elements. Sulphur is derived from the sulphatic electrolyte, and $BaSO_4$, shown as BaO, is a residue of the mould dressing of the dies in the anode casting wheel.

Table 3-I: Chemical analysis of the anode slimes

Species (concentrations in weight percent)	Crude anode slime	Anode slime washed in sulphatic solution
Cu	11.5	7.1
Sb	8.2	11.5
As	2.6	3.5
Sn	2	3.3
Pb	12.4	22.8
Zn	0.5	0.6
Ni	3.7	3.6
Bi	1.2	1.2
Se	0.6	1
Te	0.7	1
SiO_2	0.4	0.2
BaO	33	8.3
Cl	1	0.7
S	3.4	3.1
Ag	5.9	7.2
Au	0.29	0.43
Pt	0.01	0.01
Pd	0.04	0.06

3.2 XRD analysis

The first step in order to analyse the phase composition of the anode slimes was an X-ray diffraction (XRD) analysis. The characteristic spectra can be seen in Figure 3-1 on the next page. The black line represents the spectrum of the crude anode slime; the red one that of the washed anode slime.

As copper electrowinning takes place in sulphatic milieu, as well as the subsequent washing process, it can be assumed that in both samples basically a similar range of chemical compounds is present, but expected in different concentrations. Based on the available mineralogical databases within the software of the X-ray diffractometer – amongst others – the following minerals or chemical compounds could be detected in the anode slime samples. They are summarised in Table 3-II.

Table 3-II: Suspected chemical compounds according to XRD

Species' name (according to database)	Chemical formula
Anglesite	$PbSO_4$
Tin oxide hydrate	$2SnO{\cdot}H_2O$
Barium telluride	BaTe
Barium phosphorus oxide sulphide hydrate	
Barium calcium sulphate	$Ba_{0,6}Ca_{0,4}SO_4$
Celestine, barian	$(Sr,Ba)SO_4$
Celestine, barian, synthetic	$Ba_{0,25}Sr_{0,75}SO_4$
Silver indium selenide	$AgInSe_2$
Sternbergite	$AgFe_2S_3$
Kurilite	Ag_2Te
Antimony cerium	CeSb
Rosalite, synthetic	$PbSb_2O_5$
Franckeite	$Pb_5Sn_3Sb_2S_{14}$
Antimony arsenic oxide	$As_{0,172}Sb_{0,570}O_{1,113}$

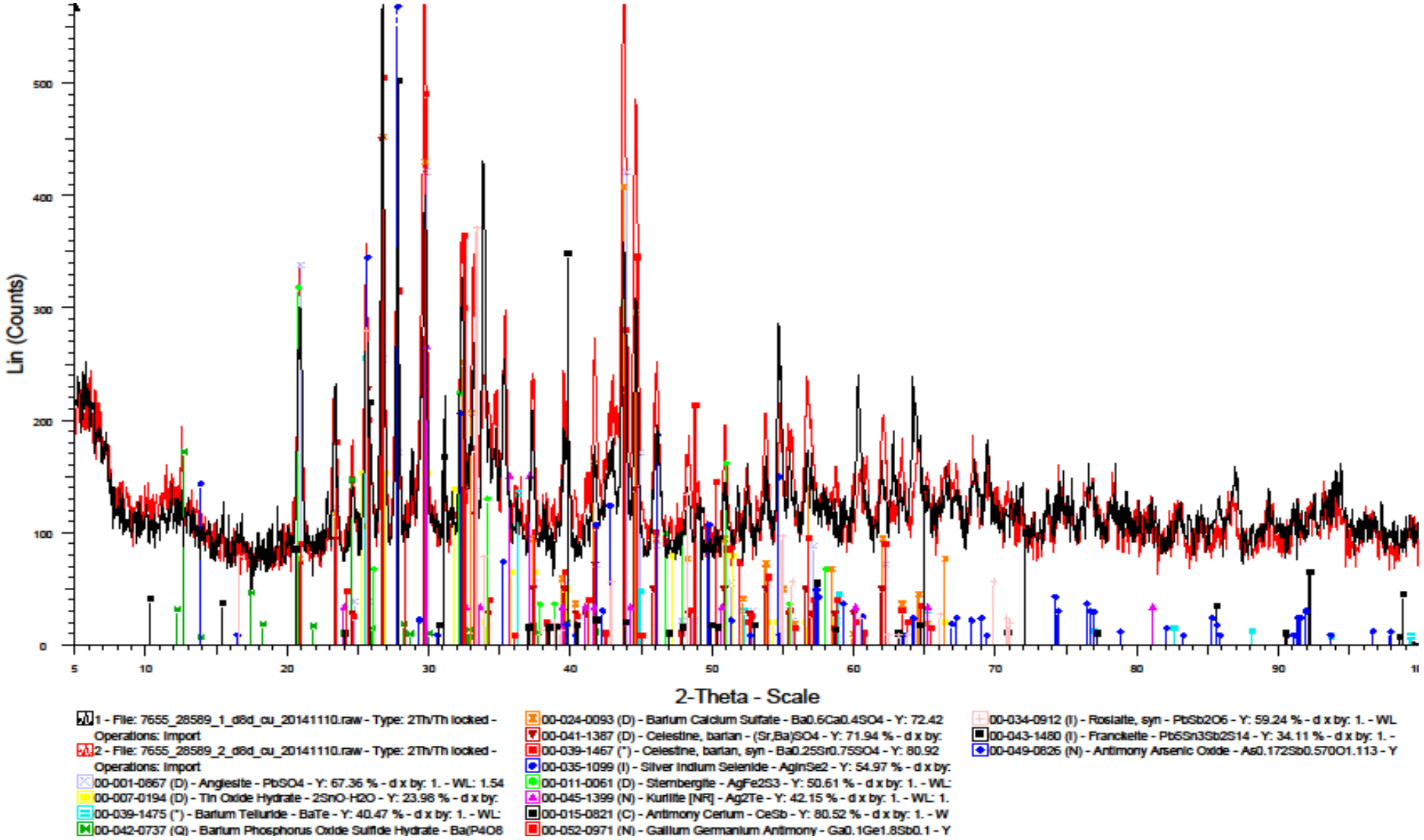

Figure 3-1: XRD spectra of the anode slime samples (crude and washed)

3.3 Sample preparation for SEM analysis

In order to validate the results of the X-ray diffraction analysis, the samples were subjected to scanning electron microscopy (SEM). Two different ways of sample preparation were applied: simple sticking of the dried powdery anode slime samples onto a specimen holder was used for large-scale SEM-EDX measurements; an embedded and ground section of the dried material was prepared to achieve optimum image quality. The preparation of the embedded samples comprised the following steps:

- Mixing of anode slime and embedding compound in a sampling mould
- Bonding of the embedding compound in an exsiccator
- Wet grinding with grain sizes 800, 1200, 2000 and 4000
- Multiple rinsing with isopropanol
- Expelling remaining water under vacuum for 15 min
- Drying in a drying furnace at 105 °C for 48 h
- Sputtering the sample surfaces with carbon

Before sputtering, the crude anode slime sample showed single metallic particles, visible to the naked eye, embedded in a dark grey shaded matrix. The washed slime did not show these and had a dark grey shaded appearance all over the section. This fact underlines the effect of washing anode slime in sulphatic milieu. The sputtering with carbon ensures a good electric conductivity of the sample surface and thus improves the quality of the scanning electron microscopic images.

Both the crude and the washed anode slime were firstly chemically analysed under the SEM to validate the chemical analysis provided (see Table 3-I). To gain possibly accurate results, the sticked samples were used here. Moreover, element-mappings were generated. Afterward, a detailed study of many different grains of the slimes was carried out. Therefore, the embedded samples were utilised to achieve the best possible image quality. The evaluation of the SEM analysis included the following steps:

- Overview mapping of a large-scale area (approx. 0.4 mm²) of the embedded crude anode slime sample
- Element mappings of different areas of the embedded crude and washed anode slime sample
- Finding of correlations, regarding which elements tend to appear together
- Finding of correlations of the elements either with sulphur or oxygen
- Chemical analysis of single grains found in small-scale SEM images

- Calculation of the stoichiometric relations for each spectrum
- Identification of particular chemical compounds on the basis of stoichiometry and the literature study on possible constituents in anode slimes
- Checking the identified compounds for plausibility on the basis of the previously established element mappings
- Comparison with the results of the XRD analysis and literature data

The different evaluation steps and their results are described in detail below.

3.4 Survey SEM-EDX mapping

Figure 3-2 shows the large-scale SEM image of the embedded crude anode slime sample which was utilised for the element mapping. The subsequent two images refer to the same section. The black areas of the sample represent the embedding material, while the different shaded grey-coloured grains are the constituents of the slime.

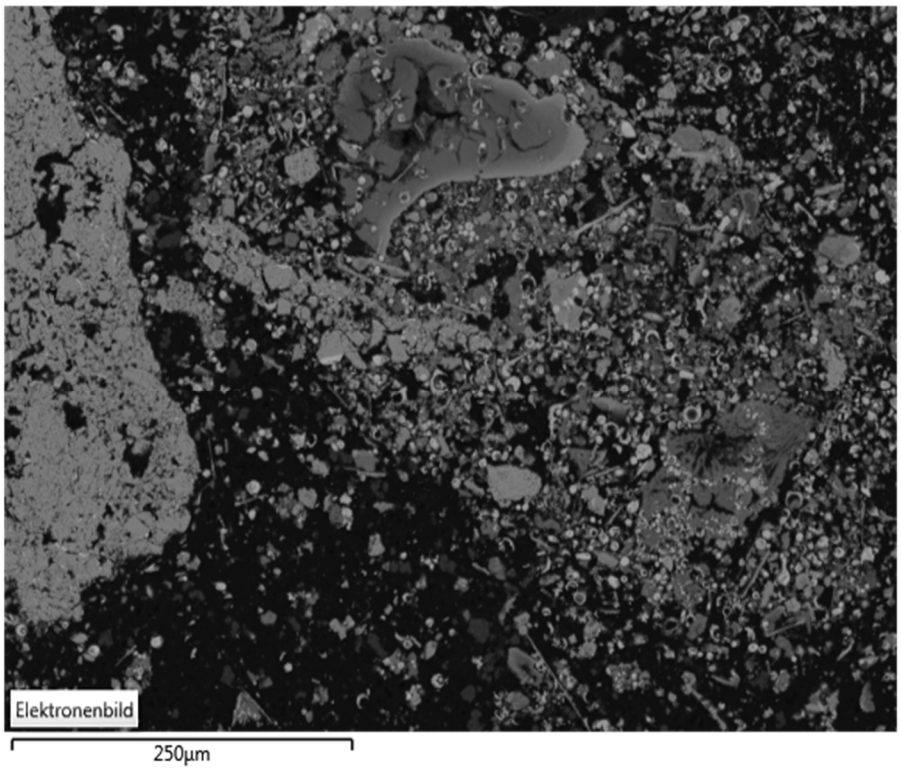

Figure 3-2: Large-scale image of crude slime, embedded sample, 660 x 540 µm (area 1)

The first evaluation step was to find out which elements appear together. Therefore, an element mapping was established. Figure 3-3 and Figure 3-4 show the distribution of the main constituents.

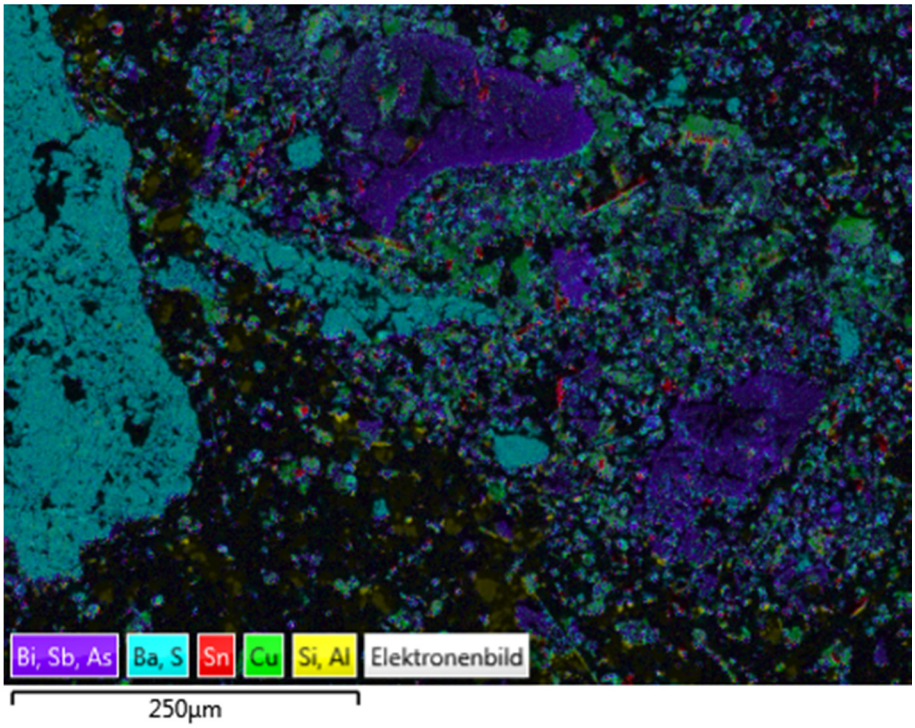

Figure 3-3: Element distribution of Bi, Sb, As, Ba, S, Sn, Cu, Si and Al in crude anode slime

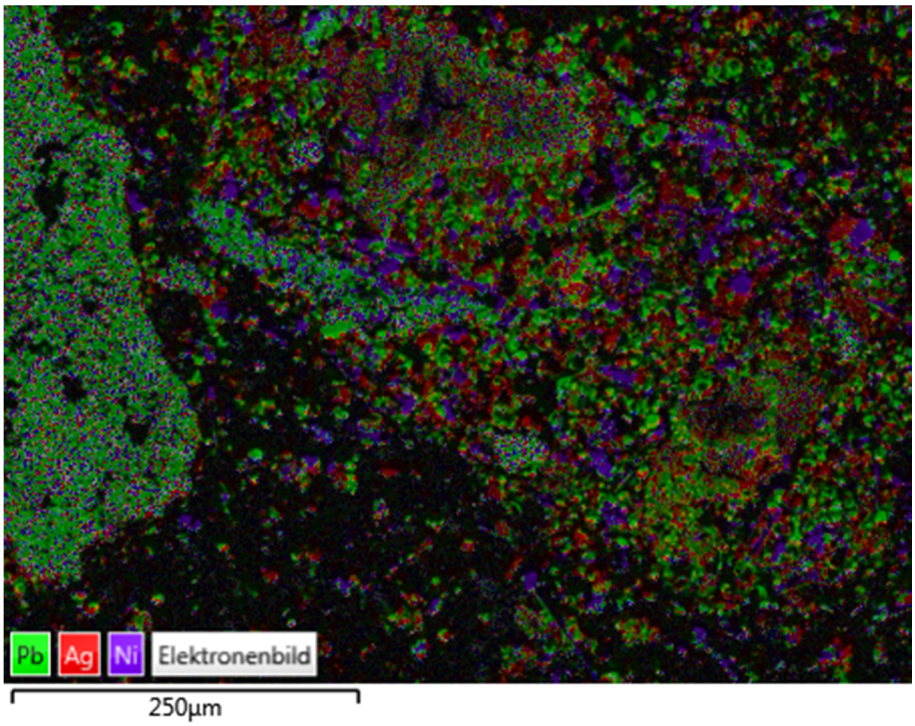

Figure 3-4: Element distribution of Pb, Ag and Ni in crude anode slime

Sn, As and Sb are the elements this thesis is focussed on. As and Sb seem to be associated with each other, while Sn forms a separate phase.

3.5 Systematic study of element correlations

In the second step, a systematic study on the correlations of different elements was carried out. For this purpose, element mappings for each element were generated. The colours represent the concentration of the respective element according to the described value in each single image. The study was done using three different areas out of the embedded slime samples. One large-scale (660 x 540 µm; hereafter referred to as area 1) and one small-scale image (120 x 95 µm; below called area 2), both of the crude slime, and furthermore one image of the washed slime (170 x 140 µm; in the following called area 3) are shown. Area 1 was already presented in Figure 3-2. Area 2 is shown in Figure 3-5; area 3 in Figure 3-6.

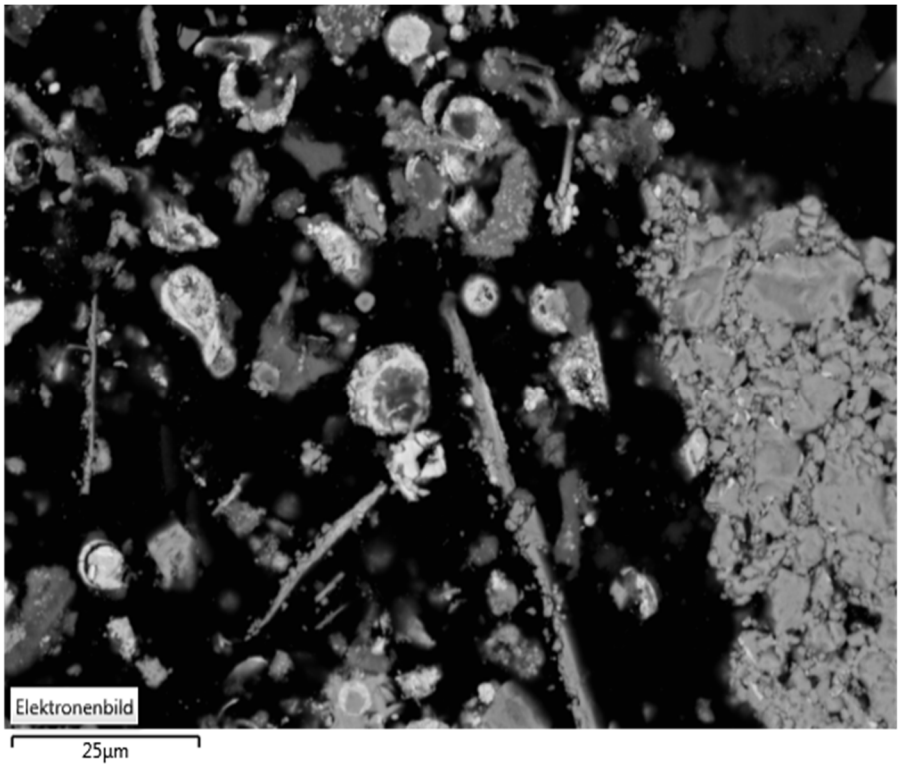

Figure 3-5: Small-scale image of crude slime, embedded sample, 120 x 95 µm (area 2)

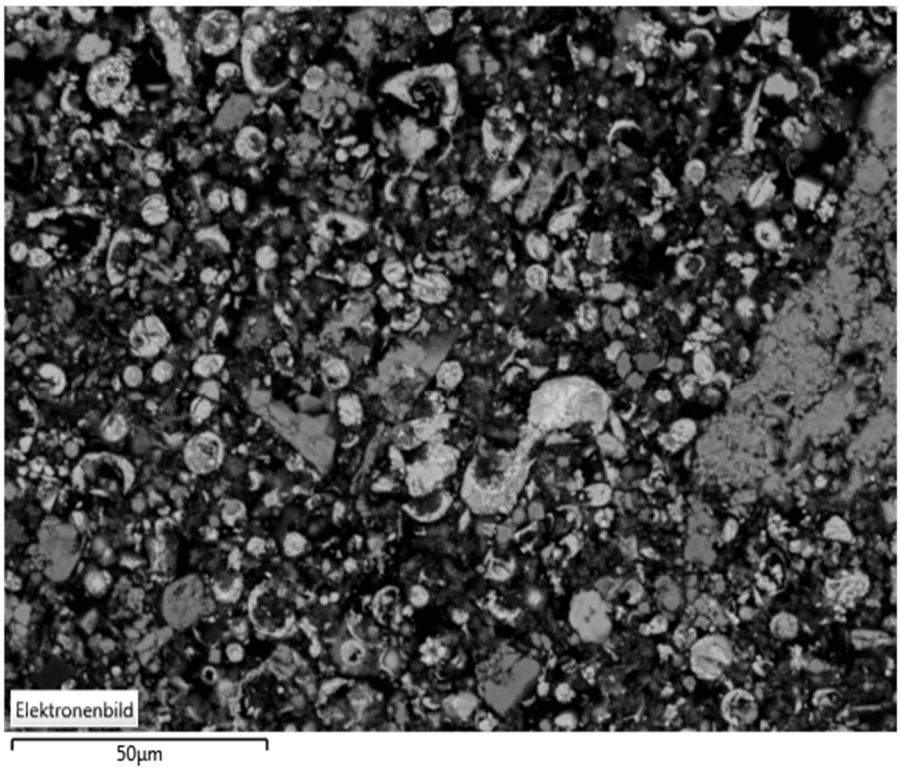

Figure 3-6: Washed slime, embedded sample, 170 x 140 µm (area 3)

Because of the different magnitudes of the three areas, certain differences concerning the similar occurrence of elements seem to exist. Some correlations, such as between Cu, Ni and Sb, only appear on a smaller scale. Therefore, it seemed to be useful to consider all three different areas in the following explanations.

3.5.1 Lead, bismuth, barium and sulphur

Figure 3-7 shows the combined occurrence of Pb, Bi, Ba and S in the crude slime (area 1). It can be seen clearly that Ba occurs in a very distinct way in particles of high concentration, while the concentration in other areas remains rather low. Most likely, Ba appears in a quite pure phase with a low content in other metals. However, Pb and Bi are distributed more wide-spread across the section. The almost perfect correlation of Ba with S indicates that Ba forms a sulphate, which is also true for Pb. Bi seems to correlate with Pb. For areas 2 and 3 the situation looks exactly the same. For that reason, the mappings for these elements in areas 2 and 3 are not presented in images here; those for the washed slime are shown in the appendix (Figure A-1).

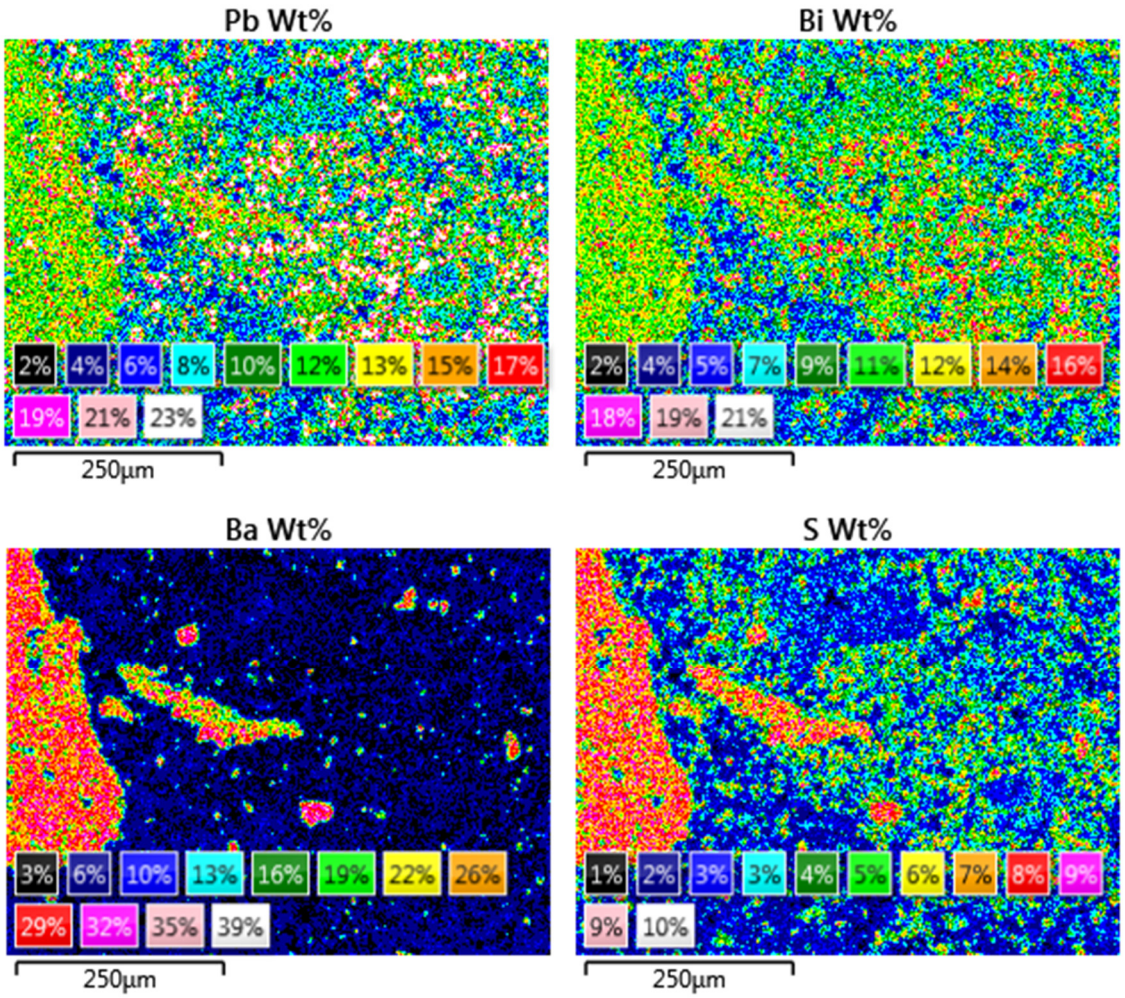

Figure 3-7: Element mappings for Pb, Bi, Ba and S, crude slime (area 1)

3.5.2 Arsenic, antimony, selenium and tellurium

The element mappings for As, Sb, Se and Te in area 1 are presented in Figure 3-8, which is the second group of elements that appears together. The occurrence of As and Sb is more distinct than in the case of Pb, but nevertheless, both elements are widely distributed across the whole section in a noteworthy concentration, except in the area of the Ba-rich particle on the left edge of the image. This might also be one reason why their removal causes issues. Se and Te are also distributed across the whole area, but they are not part of the focus within this thesis. On a smaller scale, those four elements do not show a good correlation. This is an indication that they appear in a greater variety of chemical compounds.

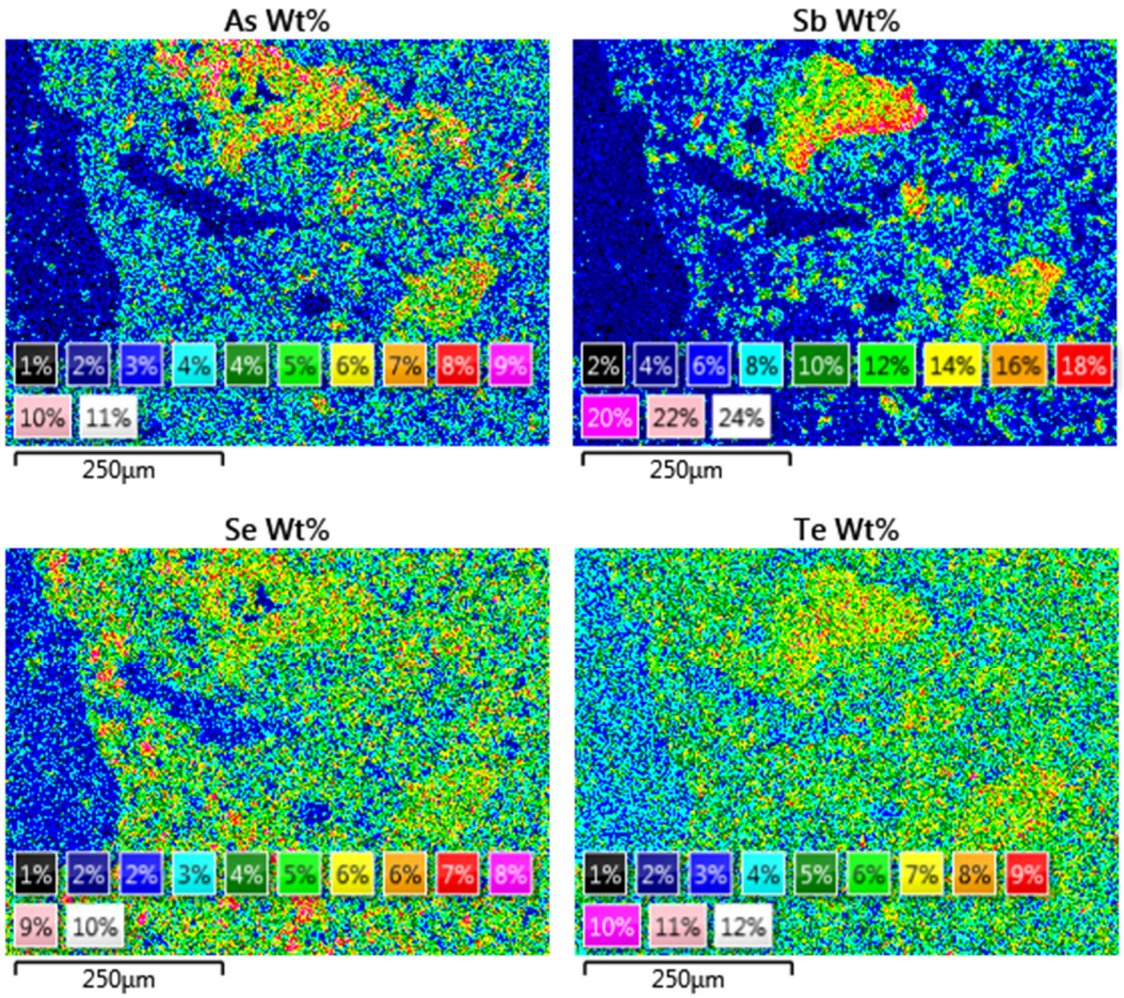

Figure 3-8: Element mappings for As, Sb, Se and Te, crude slime (area 1)

3.5.3 Iron and zinc

Figure 3-9 shows the element mappings for Fe and Zn in the crude slime (area 2). Fe and Zn arise in distinct areas. In the washed slime the Zn-rich areas are smaller and iron is distributed more equally across the section. This might be the result of the dissolution of Zn in the sulphatic solution. The mapping for the washed slime (area 3) is shown in the appendix (Figure A-2).

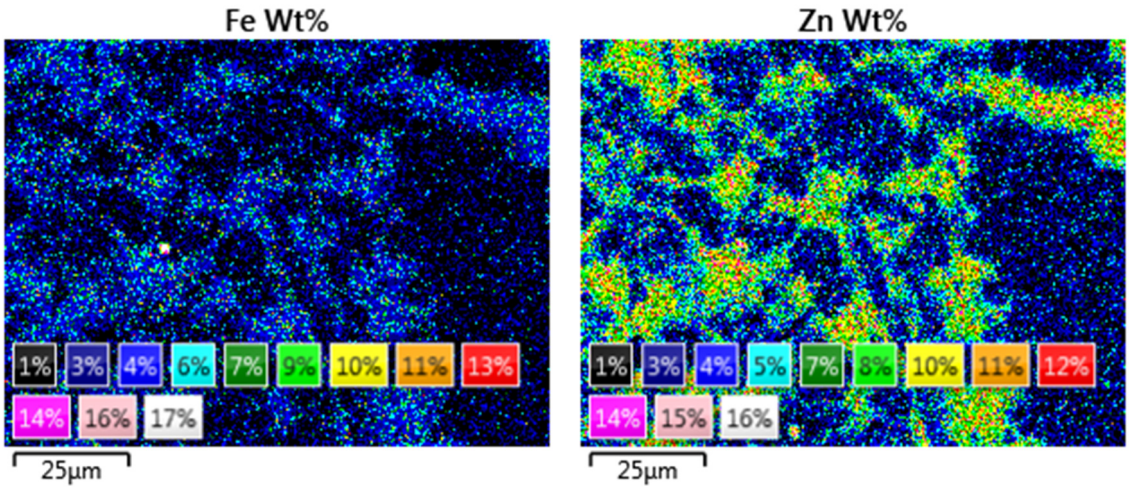

Figure 3-9: Element mappings for Fe and Zn, crude slime (area 2)

3.5.4 Aluminium and silicon

The most pronounced appearance is shown by Al and Si, whose distribution is presented in Figure 3-10 (crude slime, area 1). Both arise in the same, very distinct particles, while their concentration in the surrounding areas is extremely low. This allows the assumption that they form an independent phase without other metals. However, in the washed slime, Al is distributed almost equally across the section, while for Si just one very Si-rich particle can be found (see appendix, Figure A-3).

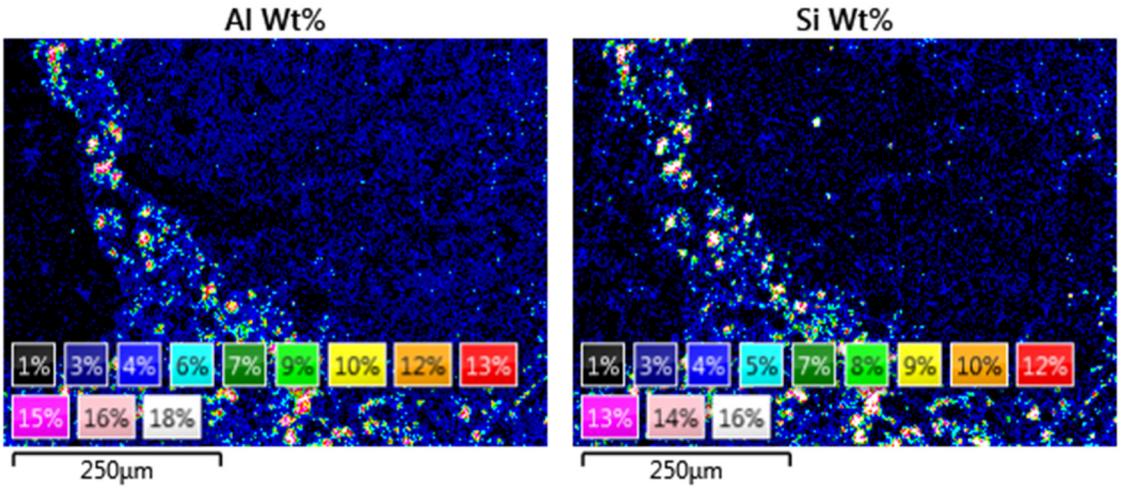

Figure 3-10: Element mappings for Al and Si, crude slime (area 1)

3.5.5 Silver, chlorine and tellurium

Figure 3-11 shows the element mappings of the crude slime (area 2) of Ag, Cl and Te. They partly seem to appear together, where Ag either correlates with Cl or Te. For Ag and Cl, the same can be observed in the washed slime (see appendix, Figure A-4).

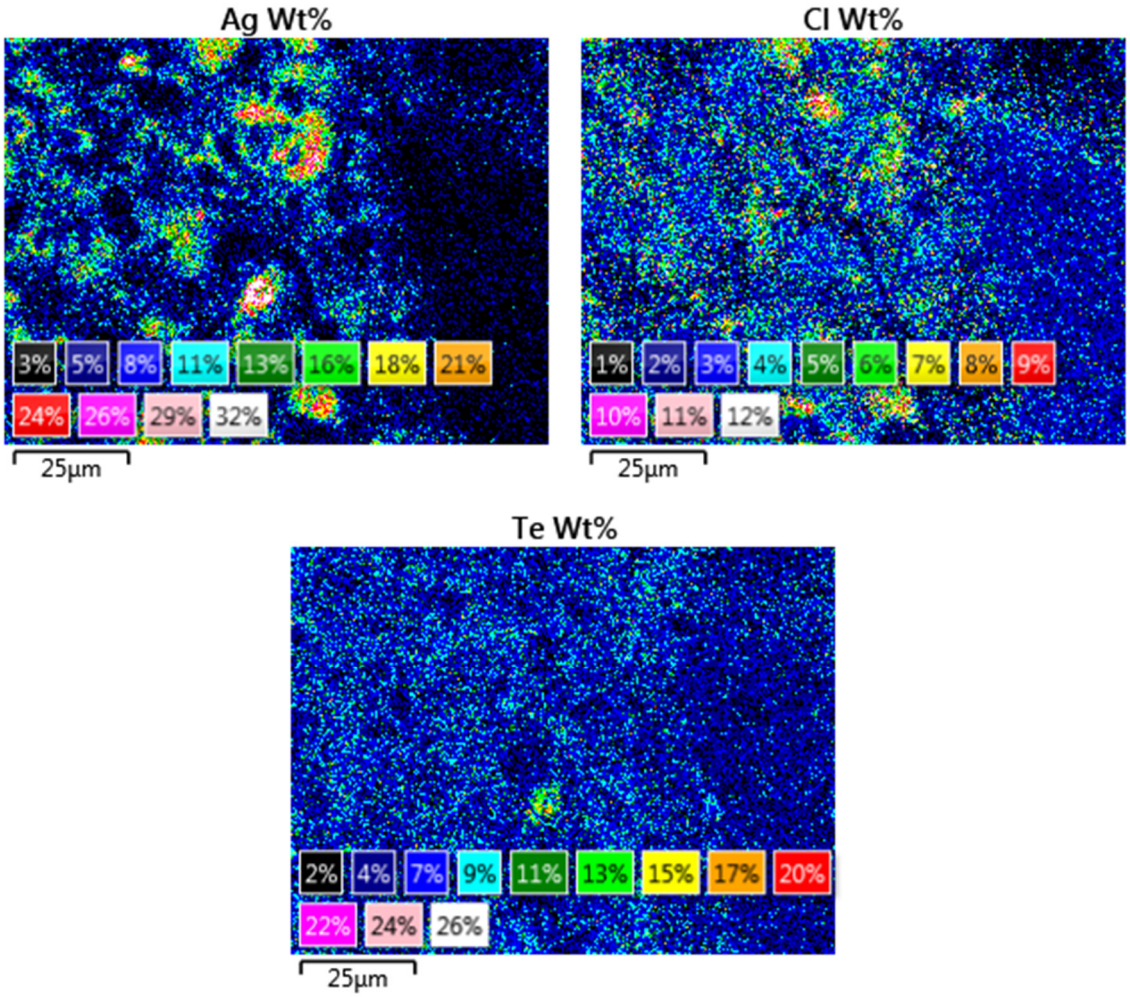

Figure 3-11: Element mappings for Ag and Cl, crude slime (area 2)

3.5.6 Copper, nickel and antimony

Cu, Ni and Sb show some similarities concerning their appearance. Figure 3-12 shows their mappings for the crude slime (area 2). They probably form a chemical compound with each other, as indicated by the needle-shaped body in the middle of the images in Figure 3-12. But one can be sure that all three are also present in other forms, as well. In the washed slime (area 3), the situation is similar (see appendix, Figure A-5).

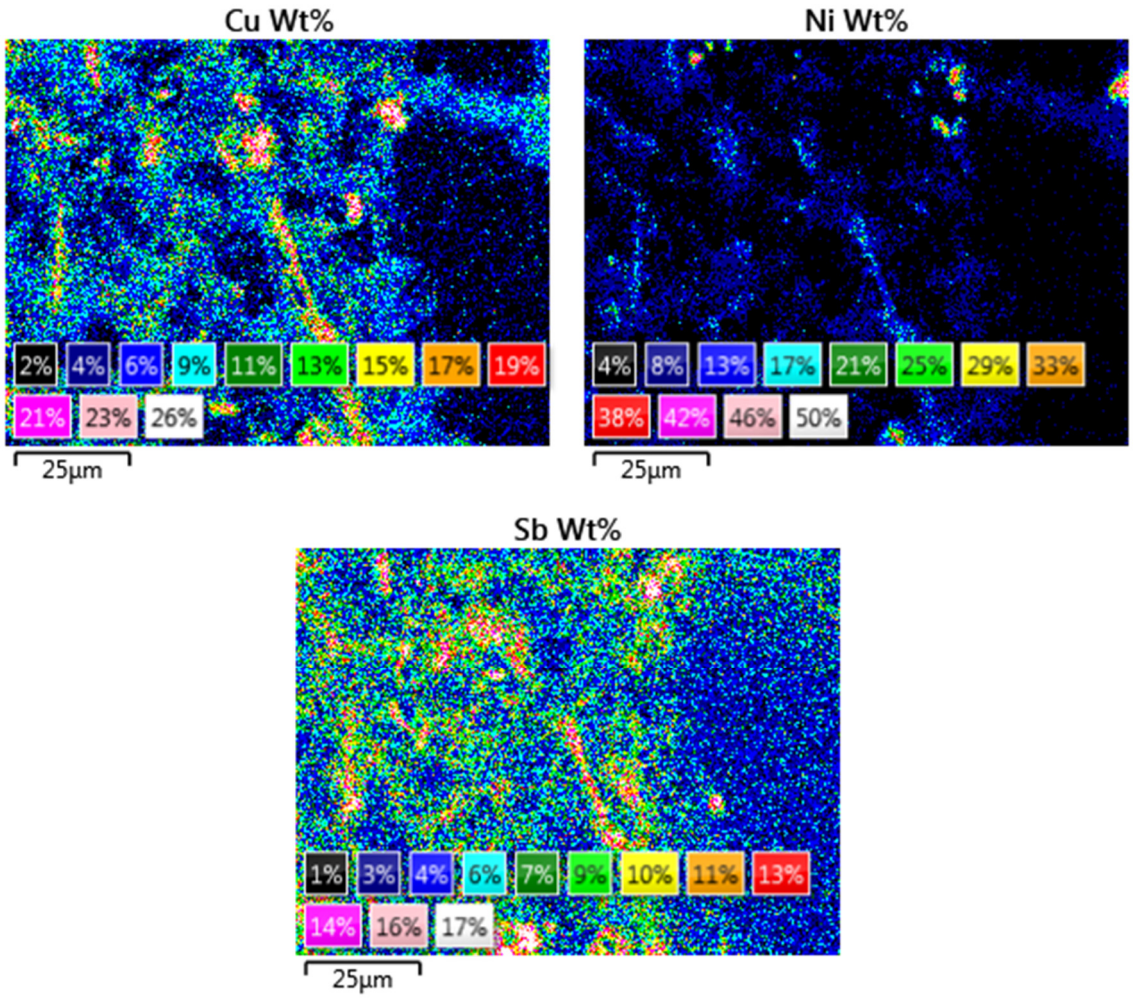

Figure 3-12: Element mappings for Cu, Ni and Sb, crude slime (area 2)

3.5.7 Tin

Tin occurs mainly in needle-shaped grains, as it can be observed in Figure 3-13 in the form of red-coloured elongated areas. Regions containing mainly As, Sb, Se and Te (compared to Figure 3-8) seem to be slightly enriched in Sn. As a consequence, Sn can be assumed to be present mainly in its own phase, but also in small amounts as impurity inside or around other phases. Considering the washed slime, nothing seems to change with Sn.

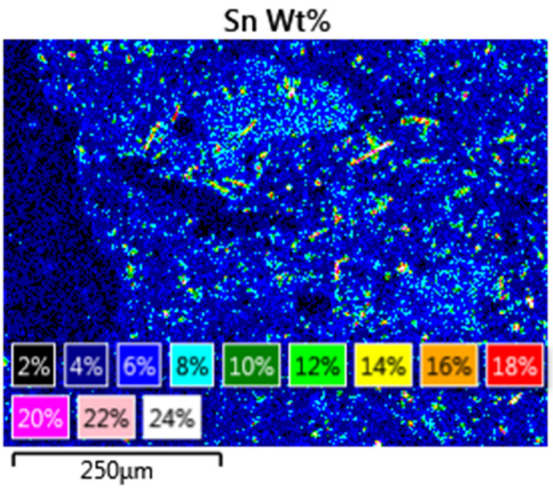

Figure 3-13: Element mapping for Sn, crude slime (area 1)

3.5.8 Gold

In Figure 3-14 the element mapping for Au is shown. This is remarkable as this element is the only one which does not seem to correlate with any of the other chemical elements. And it is the only one which is almost perfectly distributed all over the whole cross section. This is perfectly true for all three areas and implies that Au is mainly present in its elemental form, rather than associated in chemical compounds.

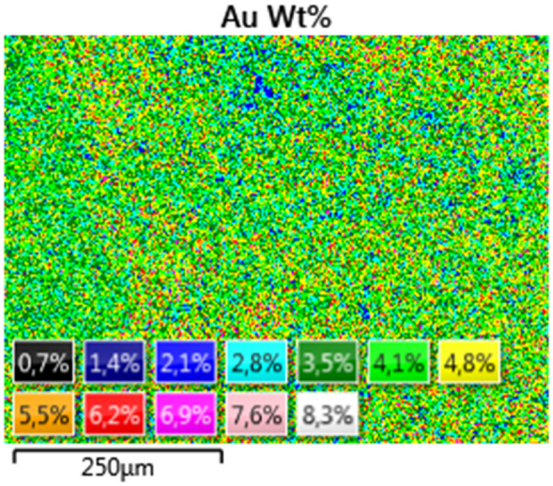

Figure 3-14: Element mapping for Au, crude slime (area 1)

3.5.9 Summary of element correlations

It can be concluded that there are groups of elements which appear together in the anode slime. These groups are indications as to which elements could form phases or chemical compounds with each other. Furthermore, it was observed that washing the anode slime in a

sulphatic solution changes the content of some of the elements but does not have a significant influence on the correlations of their appearance. To summarise, the following groups of elements were observed:

- Pb, Bi, Ba and S
- As, Sb, Se and Te
- Fe and Zn
- Al and Si
- Ag, Cl and Te
- Cu, Ni and Sb
- Sn
- Au

3.6 Compounds with sulphur and oxygen

The third step is the classification of the analysed elements with regard to a high affinity to either sulphur or oxygen. This seems to make sense, as regions with high oxygen concentrations tendentially refer to regions with low sulphur concentrations. Regions high in S still have O, as well. That way, elements that form sulphates can be seperated from those which are present as oxides. Figure 3-15 presents the occurrences of S and O.

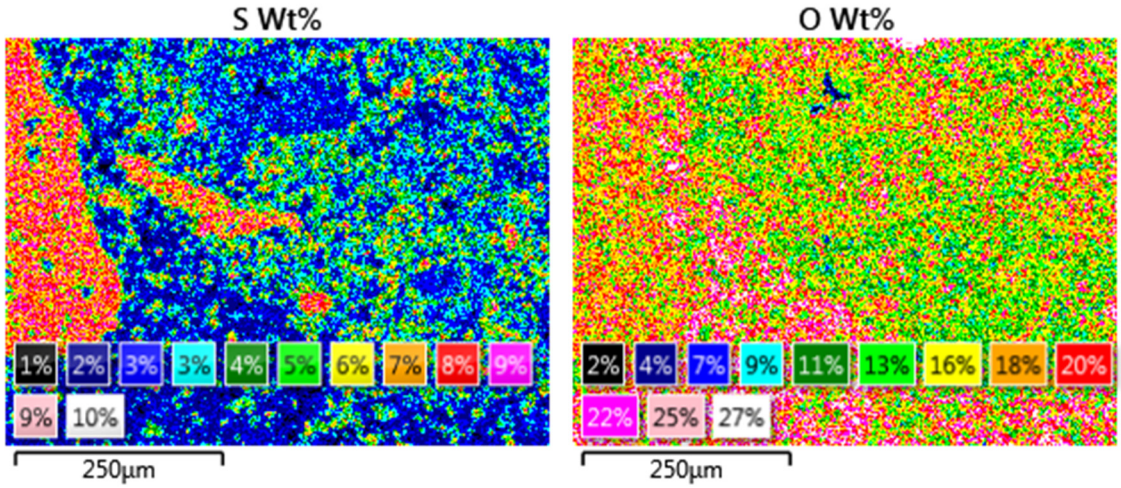

Figure 3-15: Element mappings of S and O

If the mappings of sulphur and oxygen are compared with those of the other elements, it is found that the following elements go with sulphur:

- Pb
- Bi
- Ba
- Ni

Ni shows correlations with both sulphur and oxygen; however, all other elements seem to only go with oxygen. These are:

- As
- Sb
- Se
- Te
- Fe
- Ni
- Al
- Si
- Cu
- Sn
- Zn

The noble elements Ag and Au correlate with neither sulphur nor oxygen. As a consequence, the constituents of anode slime can be classified according to their chemistry as follows into:

- Sulphates
- Oxides and hydroxides
- Halogenides
- Intermetallic compounds
- Elemental phases

3.7 Systematic SEM-EDX of single grains

The previous chapter focussed on the macroscopic analysis of the anode slimes. This provides important information concerning the basic chemistry of the material. But the mappings do not deliver any stoichiometric information and thus do not allow a conclusion regarding certain chemical compounds. Therefore, it is necessary to take a closer look at single grains.

The chemical analysis of the grains was done by SEM-EDX for both the crude and washed slime. Single grains were investigated under the SEM and then analysed. 39 spectra were recorded; 21 for the crude and 18 for the washed anode slime. Once the chemical analyses were performed, the mass values had to be converted into atomic percent to get the stoichiometric information. In Table 3-III and Table 3-IV, the compositions of grains of the crude slime and the washed slime respectively, are presented. The main element was detected for each grain along with all the elements appearing in a relevant amount. These were considered afterwards, when the stoichiometric amounts were derived into specific chemical compounds.

Table 3-III: Chemical analysis of selected single grains in the crude anode slime (composition in atomic %)

Spectr.	O	Al	Si	S	Cl	Ni	Cu	As	Se	Ag	Sn	Sb	Te	Ba	Pb	Main element	Suspected species
2	73.4	0.3	0.1	0.2		0.3	1.0	0.2			23.9	0.2	0.2		0.2	Sn	$Sn(OH)_2 + Sn(OH)_4$
3	76.7	0.3		0.7	0.2	0.7	2.5	0.9	0.2	0.7	15.8	0.8	0.1		0.5	Sn	$Sn(OH)_4$
4	73.3	0.1	0.3	1.7	1.1	0.4	6.4	4.5		1.9	0.3	7.4			1.9	Sb	Cu-As-Sb-O
5	63.9	0.6	0.3	5.7	1.0	0.5	6.2	1.9	2.0	9.1	0.6	1.5	1.2		5.4	Ag	Cu-Ag-Pb-SO_4
6	63.3	0.5	0.3	8.6	0.7	0.8	8.0	1.5		2.0	2.3	2.9	0.1	0.3	8.6	Pb	Cu-Ag-Pb-SO_4
7	72.3	0.5	0.2	7.1		0.5	3.9	1.6	0.2	1.1	0.2	3.6			8.9	Pb	$PbSO_4$
8	61.1	0.7	0.4	2.6	5.6	0.4	8.7	2.6	1.5	11.8		1.9	0.6	0.3	1.1	Ag	AgCl
9	60.9	0.6		1.8	0.3	8.8	15.7	1.2	0.3	0.6	1.1	6.0			2.1	Cu	$Cu_3Ni_{2-x}SbO_{6-x}$
10	74.5	0.4		10.0		0.3	1.5	0.8	0.2	0.8	0.0	0.5		10.2	0.7	Ba	$BaSO_4$
14	67.2		0.1	8.4		0.3	4.1	1.1			0.3	5.7			12.4	Pb	$PbSO_4 + PbSbO_2 + CuSO_4{\cdot}5H_2O$
15	69.1		0.1	15.0		0.2	0.3							15.1	0.1	Ba	$BaSO_4$
16	67.8		0.2	11.4		0.5	2.5	1.5			0.2	3.0			12.7	Pb	$PbSO_4$
17	30.1		0.2	2.1		0.5	2.6	1.1	10.4	40.2		2.1	9.2		1.6	Ag	$Ag_2(Se,Te)$
18	69.7		0.2	0.2	0.1	0.2	7.3	7.0		0.5	0.3	12.1			0.7	Sb	Cu-As-Sb-O
19	53.5		0.1	0.8	3.3	0.4	32.6	6.2	0.2	1.9		0.6	0.1		0.2	Cu	$Cu_3(AsO_4)_2{\cdot}4H_2O + Cu_2O$
20	41.7		0.0	4.0	14.6	0.4	8.2	2.1	2.4	23.8		0.6	0.7		0.5	Ag	$AgCl + CuSO_4{\cdot}5H_2O$
21	64.2	13.1	12.4		0.1		0.2					0.1				Al	$Al_2O_3{\cdot}2SiO_2{\cdot}2H_2O$
22	54.2					14.6	22.8	0.1			0.5	7.6			0.1	Cu	$Cu_3Ni_{2-x}SbO_{6-x}$
23	71.8			1.9		0.4	1.0	0.2			22.3	0.3			2.2	Sn	$Sn(OH)_2 + Sn(OH)_4$
25	63.8	12.8	12.6	0.2	0.1		0.3			0.0		0.1		0.1	0.0	Al	$Al_2O_3{\cdot}2SiO_2{\cdot}2H_2O$
26	13.7			0.7		0.9	1.7		9.4	55.5			17.0		0.6	Ag	$Ag_2(Se,Te)$

Table 3-IV: Chemical analysis of selectedsingle grains in the washed anode slime (composition in atomic %)

Spectr.	O	Al	Si	S	Cl	Ni	Cu	As	Se	Ag	Sn	Sb	Te	Ba	Pb	Main element	Suspected species
41	64.2	0.4	0.4	12.2	0.4	0.9	1.5	1.4	0.3	2.3	0.6	2.4	0.2	0.4	12.4	Pb	$PbSO_4$
42	59.9			13.0		0.9	2.2	1.8	0.3	2.5	0.7	4.4			14.3	Pb	$PbSO_4 + As_{0,172}Sb_{0,570}O_{1,113}$
43	64.7			9.7		0.8	2.0	3.6	0.6	3.3	0.6	4.2	0.4		10.1	Pb	$PbSO_4 + SbAsO_4$
44	60.2			11.6		1.1	2.0	1.7		2.7	0.7	6.6			13.5	Pb	$PbSO_4 + As_{0,172}Sb_{0,570}O_{1,113}$
45	63.5	0.2	0.4	12.5		0.8	1.7	1.7		1.9	0.7	2.7	0.3	0.3	13.2	Pb	$PbSO_4$
46	63.3			5.7	1.2	0.8	5.6	8.0	0.3	3.4	3.7	4.4	0.4		3.2	As	$(Sb_2O_3)_x \cdot (As_2O_5)_{1-x} + CuSO_4 + Sn(OH)_2$
47	48.5	0.5	0.3	3.0	0.5	23.2	11.0	1.8	0.5	1.9	0.7	5.1			2.3	Ni	$Cu_3Ni_{2-x}SbO_{6-x} + NiO$
48	63.7		2.0	12.4		1.0	1.5	1.3	0.2	1.4	0.9	1.6	0.2	10.6	2.4	Ba	$BaSO_4$
49	65.1			6.8	0.5	0.8	1.5	4.9		1.6	0.4	16.1			2.2	Sb	$Sb_2(SO_4)_3 + (Sb_2O_3)_x \cdot (As_2O_5)_{1-x}$
50	68.6			10.9		0.7	1.4	2.0	0.2	1.9	0.5	2.4		0.3	11.2	Pb	$PbSO_4$
51	69.4		0.3	9.1		1.0	2.3	1.9	0.3	2.5	0.7	3.0			9.1	Pb	$PbSO_4$
52	56.0	0.5		3.1	0.8	8.5	14.7	1.8	0.9	2.8	1.5	6.0	0.2	0.3	2.2	Cu	$Cu_3Ni_{2-x}SbO_{6-x}$
53	59.0		0.6	3.2	0.4	9.1	14.2	1.6		1.7	0.9	6.2		0.5	2.2	Cu	$Cu_3Ni_{2-x}SbO_{6-x}$
54	67.3			8.5		0.8	2.0	1.7	0.4	2.4	0.7	5.9			10.3	Pb	$PbSO_4 + Sb_2O_4$
55	68.8			9.0	1.6	0.9	2.0	1.9		3.4	0.6	2.7		0.4	8.6	Pb	$PbSO_4$
56	68.3		0.5	9.9		0.8	1.9	1.9		2.8	0.6	2.9		0.3	9.7	Pb	$PbSO_4$
57	65.2			7.4		1.1	2.0	2.1	1.3	5.7	0.8	4.8	0.7		8.8	Pb	$PbSO_4 + Ag_3Cu(Se,Te) + (Sb_2O_3)_x \cdot (As_2O_5)_{1-x}$
58	69.9	0.4	0.8	5.0	0.7	0.9	3.0	4.2	1.0	3.9	1.4	3.8		0.8	3.6	Ag	$PbSO_4 + Ag_3Cu(Se,Te) + (Sb_2O_3)_x \cdot (As_2O_5)_{1-x}$

As can be seen from the previous tables, in some cases it becomes obvious as to which compound is present, while in others it is quite ambivalent and can only be suspected. For some grains it is assumed that there is more than one chemical compound. There are a number of reasons for this assumption. Firstly, the SEM-EDX analysis of such small particles has a larger uncertainty than the usual chemical analysis. Secondly, it can hardly be determined what is underneath the particle. This is important because EDX has a certain penetration depth and thus always measures in the depth of the material, too. And thirdly, there are also grains which look homogenous, but in fact may consist of different phases grown together extremely tight.

The basis for the derivation of specific chemical compounds was the literature research on the constituents that have already been found in copper anode slimes by researchers in the past, summarised in Table 2-III and Table 2-V. To conclude, the following compounds could be suspected in both the crude and the washed slime:

- $PbSO_4$
- $Cu_3Ni_{2-x}SbO_{6-x}$
- $BaSO_4$
- $Sn(OH)_2$

According to the SEM spectra of the single grains, the following chemical compounds could be suspected in the crude anode slime only:

- $Sn(OH)_4$
- Cu-As-Sb-oxide
- Cu-Ag-Pb-sulphate
- AgCl
- $PbSbO_2$
- $CuSO_4 \cdot 5H_2O$
- $Ag_2(Se,Te)$
- $Cu_3(AsO_4)_2 \cdot 4H_2O$
- Cu_2O
- $Al_2O_3 \cdot 2SiO_2 \cdot 2H_2O$

According to the SEM spectra of the single grains, the following compounds could be suspected in the washed anode slime sample only:

- $As_{0,172}Sb_{0,570}O_{1,113}$
- $SbAsO_4$
- $(Sb_2O_3)_x \cdot (As_2O_5)_{1-x}$
- $CuSO_4$
- NiO
- $Sb_2(SO_4)_3$
- Sb_2O_4
- $Ag_3Cu(Se,Te)$

A more detailed discussion of each compound is found in section 4.

3.8 Behaviour of selected phases at high temperatures and in aqueous media

As one possible way to pretreat copper anode slimes is the evaporation of tramp elements, the vapour pressure of the constituents plays an important role. The curves in Figure 3-16 were calculated using HSC 6. This software is based on thermodynamic data and considers neither the actual evaporation kinetics nor possible reactions before reaching the boiling point in a real process. Nevertheless, it provides very useful information regarding which elements could possibly be removed by means of selective evaporation.

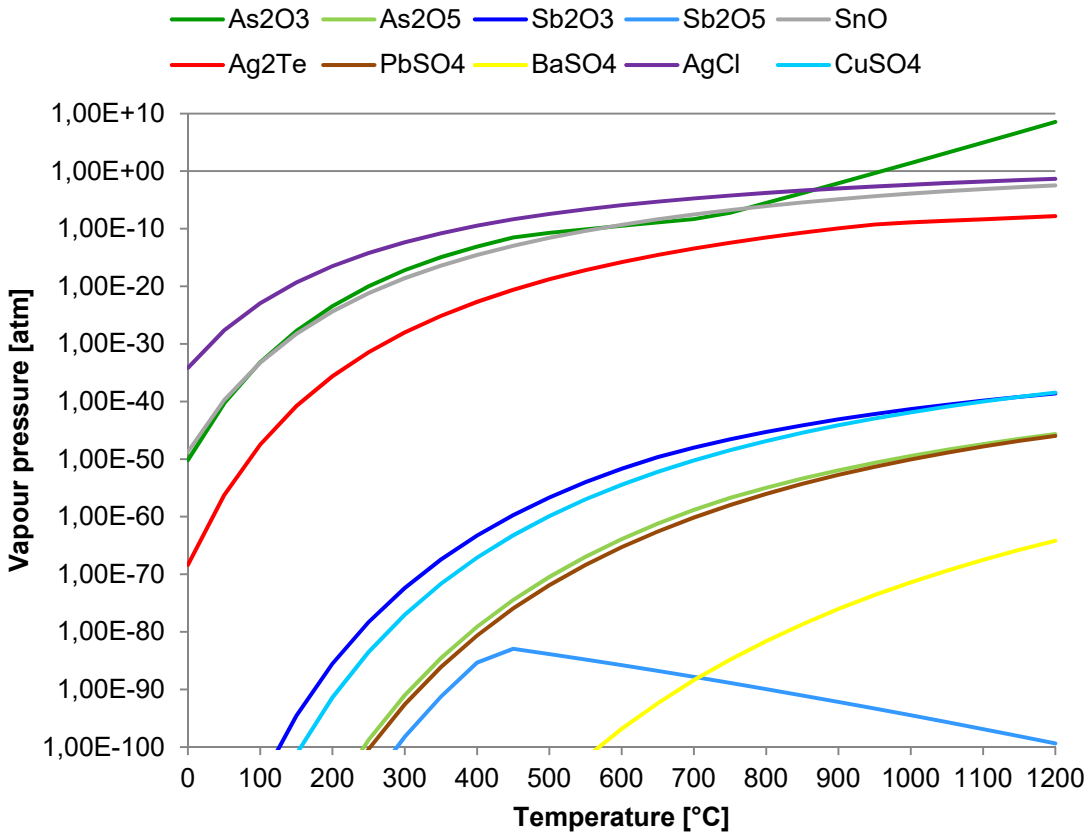

Figure 3-16: Vapour pressure of different constituents with temperature

From Figure 3-16 it can be seen that As_2O_3 is the only chemical compound which evaporates in considerable amounts at atmospheric pressure. The reaction constant for the evaporation reaches values higher than one at temperatures above 960 °C. AgCl and SnO also reach a high vapour pressure at high temperatures but the thermodynamic equilibrium remains on the side of the solid phase, even above 1000 °C. This behaviour is also reflected in the boiling point, which is low for As_2O_3, compared to the other compounds. Table 3-V summarises the melting and boiling points, the density as well as the solubility in water at

room temperature for the chemical compounds Figure 3-16 deals with. Those where the melting point is marked with a star (*) do not actually melt, but decompose at the designated temperature.

Table 3-V: Physical data of anode slime constituents [34]

Species	Melting point (T_M) [°C]	Boiling point (T_B) [°C]	Density [g/cm³]	Solubility in water [g/l]
As_2O_3	315	465	3.74	37
As_2O_5	315*		4.32	well soluble
Sb_2O_3	570	1425	5.58	insoluble
Sb_2O_5	380*		3.78	nearly insol.
SnO	1042	1527	6.45	insoluble
Ag_2Te	959		8.40	
$PbSO_4$	1170		6.29	0.0445
$BaSO_4$	1580		4.49	insoluble
AgCl	457	1547	5.56	0.00188
$CuSO_4$	560*		3.60	203

Especially the data from Table 3-V is significant concerning leaching experiments in aqueous media, as they were carried out within this diploma thesis and are described in greater detail below. It can be seen that while arsenic oxides are considered well soluble, oxides of antimony and tin are insoluble in pure water. However, according to the survey (compare Chapter 2.5.1), there are ways to also get antimony oxide into solution. It is supposed that this different behaviour concerning solubility in water can be exploited for a selective extraction, when the correct media and parameters are determined.

4 Discussion and phase identification

After having calculated the stoichiometry of the phases with a specific composition, the findings were proved with the help of element mappings. For this purpose, all elements contained in a certain compound must be present in one position in their mappings. Hydrogen and other very light elements are excluded, because they are not measurable with SEM-EDX. Subsequently, the phases and compounds found in the previous section are discussed. Furthermore, single grains that are visible in the electron images of the mappings are identified at the end of this section.

4.1 $Sn(OH)_2$ and $Sn(OH)_4$ – tin hydroxides

Figure 4-1 shows the relevant mappings for Sn and O in the crude slime. The yellow circles mark the positions of tin hydroxide phases. They can also be found in the washed slime (see appendix, Figure A-6). The stoichiometric calculation gives a pretty clear result with very low contents of tramp elements in the corresponding spectra of both the crude and the washed samples. $Sn(OH)_2$ was also determined by the XRD analysis. Therefore, $Sn(OH)_2$ can be considered as proved. No evidence for the presence of $Sn(OH)_4$ can be found, as it was only the result of stoichiometric calculations once, and even that was not a clear case. Moreover, it was not detected in the XRD analysis.

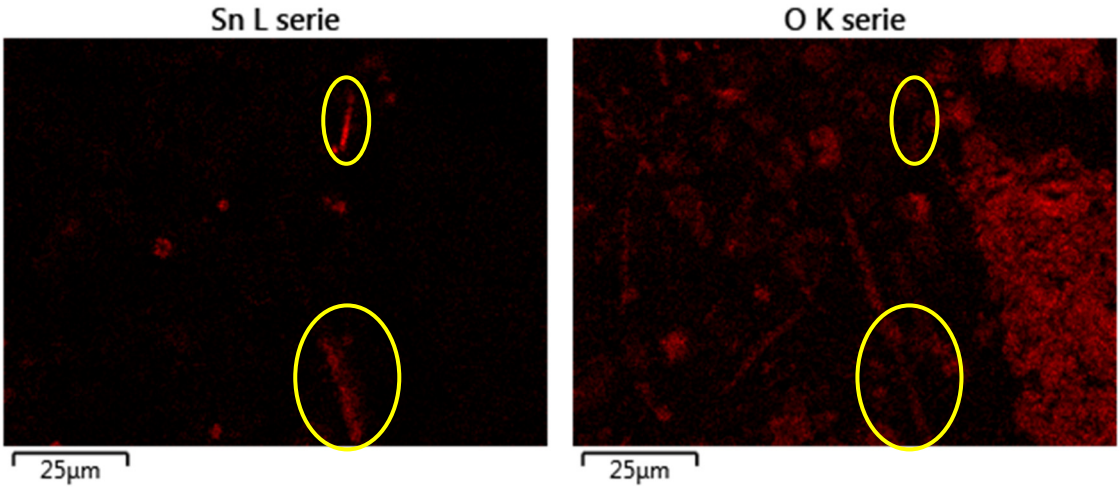

Figure 4-1: Element mappings for Sn and O, crude slime (area 2)

4.2 $PbSO_4$ – lead sulphate

Figure 4-2 shows the element mappings for Pb, S and O in the crude slime. The yellow circles mark the positions of the lead sulphate. The same compounds can be found in the washed sample (see appendix, Figure A-7). It was found many times in the stoichiometric calculations, as a pure phase as well as combined with others. $PbSO_4$ was found through the XRD analysis too, which is why $PbSO_4$ can also be considered proved.

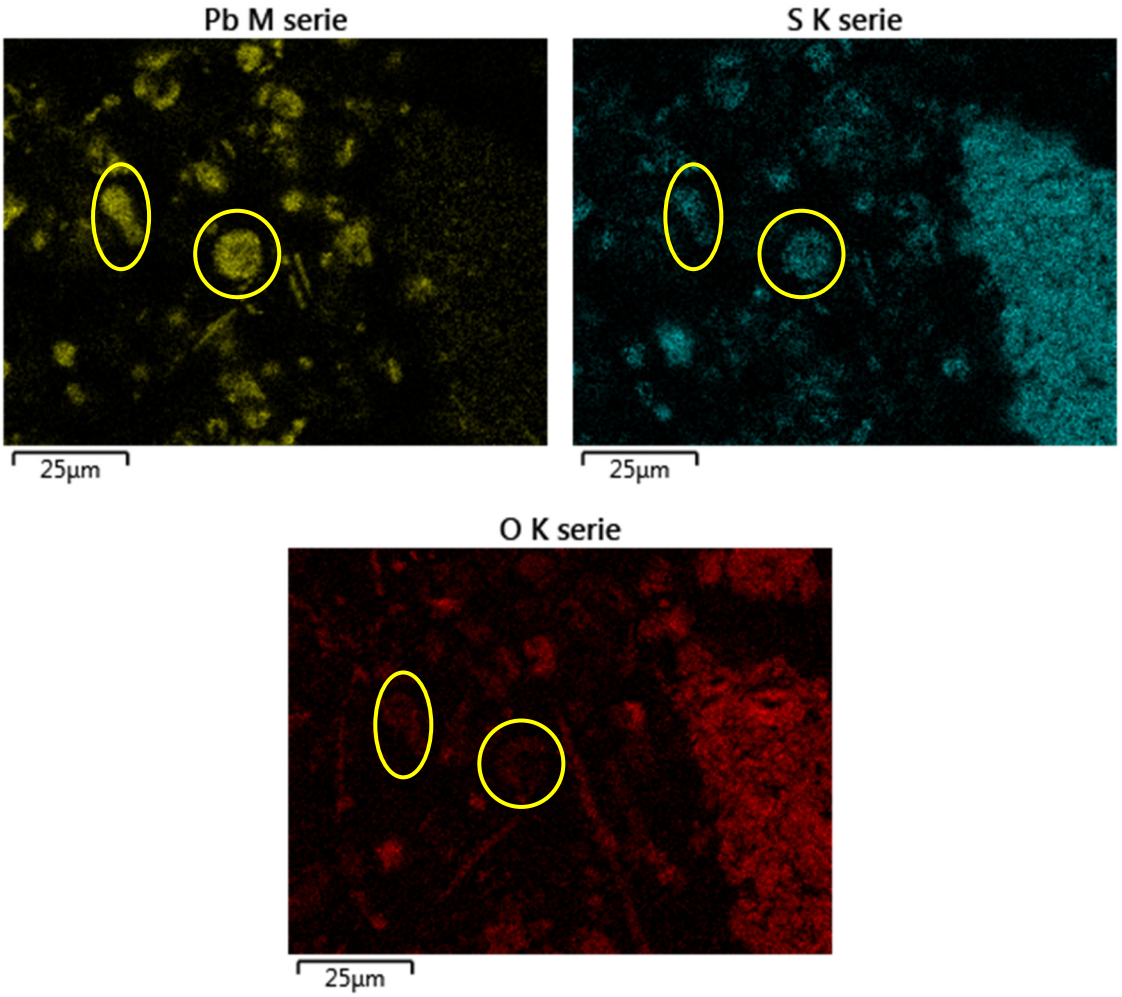

Figure 4-2: Element mappings for Pb, S and O, crude slime (area 2)

4.3 AgCl – silver chloride

Figure 4-3 displays the element mappings for Ag and Cl in the crude slime. The yellow circles mark the positions where the silver chloride is situated. The correlation can also be found very clearly in the washed sample (see appendix, Figure A-8). In the stoichiometric calculations of the crude slime, there were two particles found with high amounts of both Ag and Cl, besides Cu. In both cases, there was more Ag than Cl contained. It seems probable that in addition to AgCl, these grains also contain a metallic Cu-Ag-alloy or sulphatic compounds. AgCl was not identified by the XRD analysis, because of the comparably small amount of Ag. But as the mappings draw a very clear picture and the analysed spectra have comparably high Ag and Cl contents with low tramp element concentrations except Cu, AgCl can be considered as present.

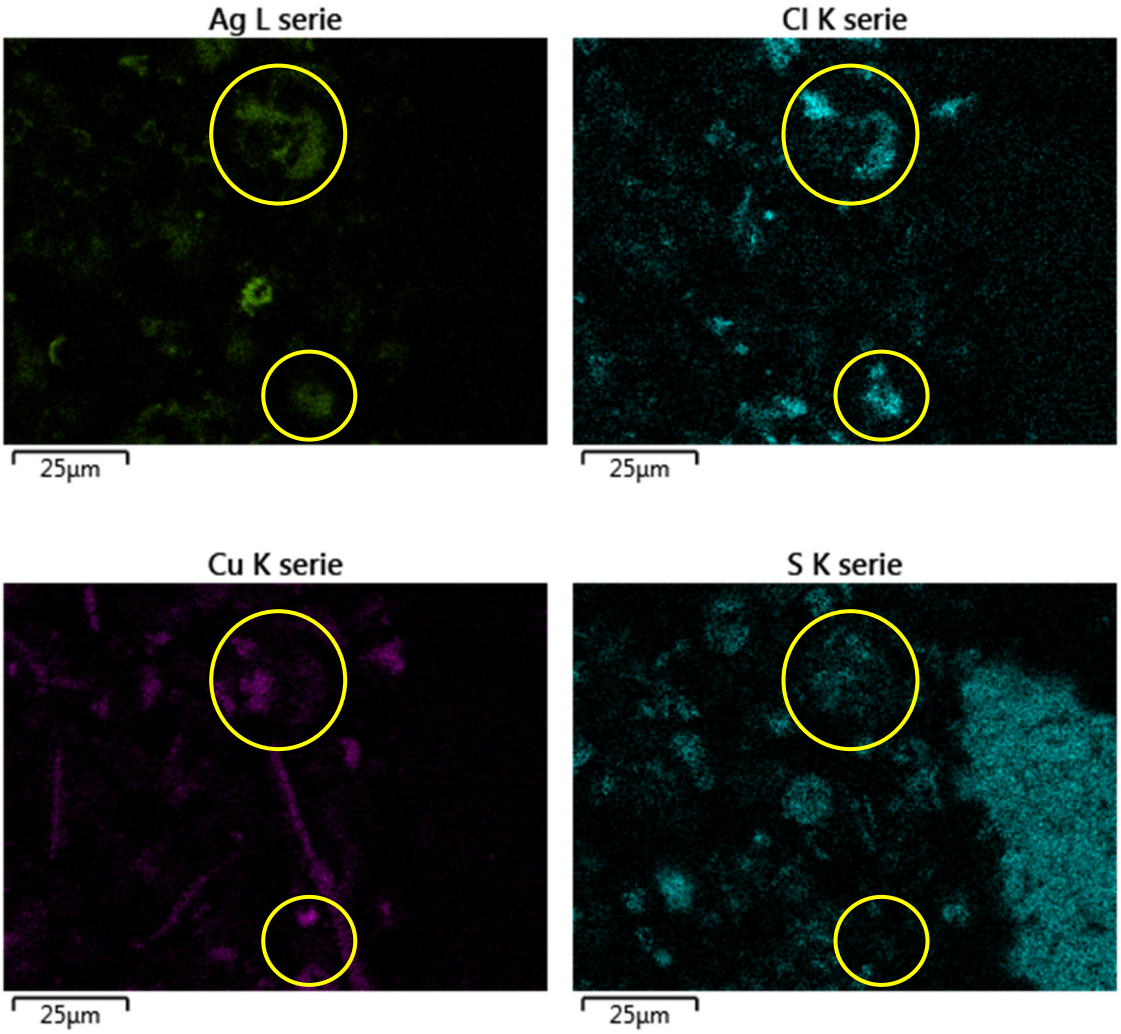

Figure 4-3: Element mappings for Ag, Cl, Cu and S, crude slime (area 2)

4.4 $Cu_3Ni_{2-x}SbO_{6-x}$ – “Kupferglimmer”

Figure 4-4 shows one of the mappings for Cu, Ni, Sb and O in the crude slime. In the crude slime, “Kupferglimmer” appears all over the scanned section in the form of acicular phases. The situation is just the same for the washed slime, but not as needles; there, it is present as more compact grains (see appendix, Figure A-8, marked with yellow circles). “Kupferglimmer” could be found by stoichiometric calculation multiple times, partly pure with little tramp elements and quite accurate stoichiometry and sometimes with hyperstoichiometric amounts of Ni or Sb, and once combined with a sulphatic lead phase. $Cu_3Ni_{2-x}SbO_{6-x}$ could not be identified by the XRD analysis, but the mappings reveal a good correlation over a wide range, which can be observed in many places in the mappings, and the stoichiometry was partly exact.

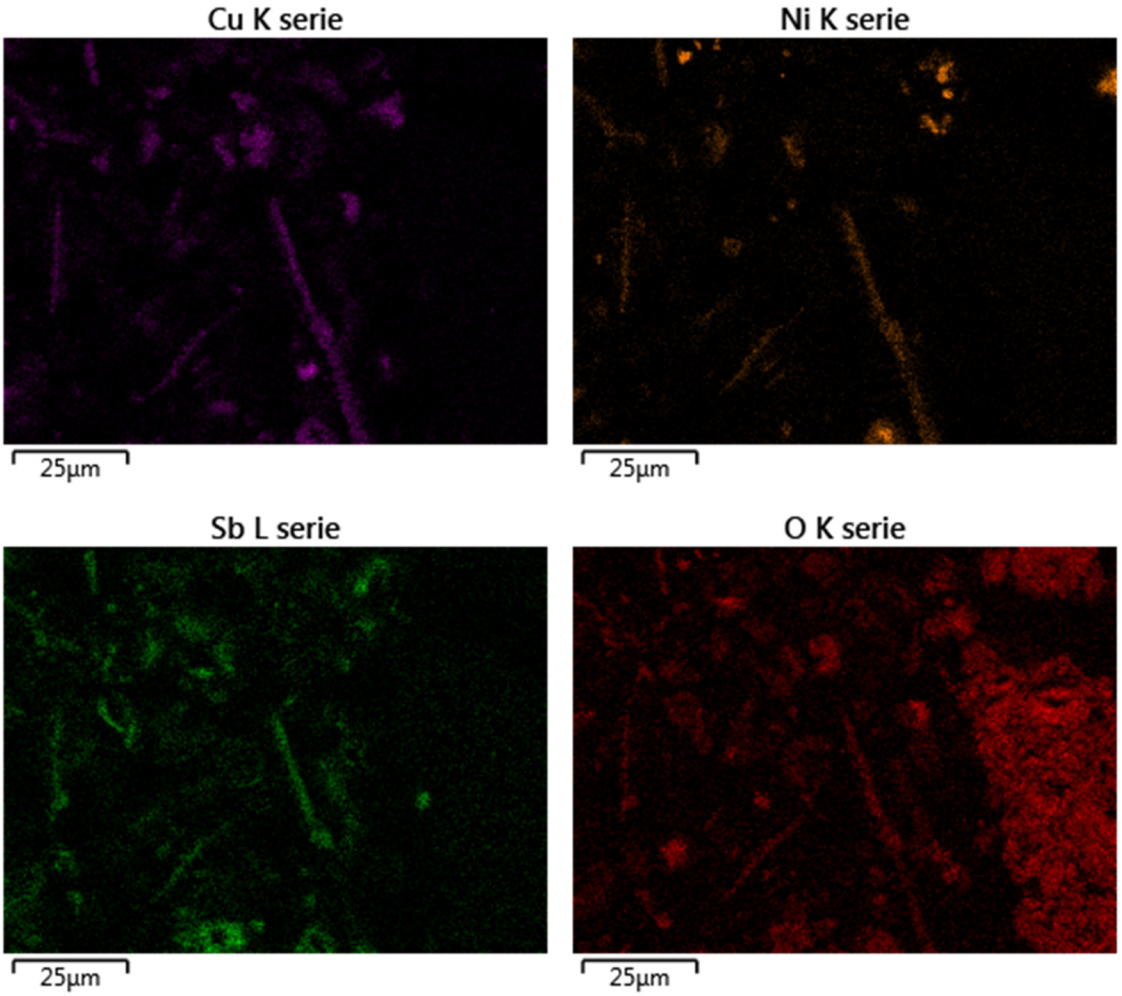

Figure 4-4: Element mappings for Cu, Ni, Sb and O, crude slime (area 2)

4.5 $BaSO_4$ – barium sulphate

Barium sulphate is one of the main constituents of these slimes. This is true for the crude as well as for the washed anode slime. In Figure 4-5 the congruence of the concentration profiles of Ba, S and O can be seen very clearly for the example of the crude slime. The same can be observed for the washed slime in Figure A-10 (appendix). $BaSO_4$ was found by XRD analysis as well as several times by stoichiometric calculations of the results of microscopic EDX analysis of both slimes. Therefore, the presence of barium sulphate is evident, both in the crude as well as in the washed slime, originating from chemicals used in the casting mould to avoid sticking.

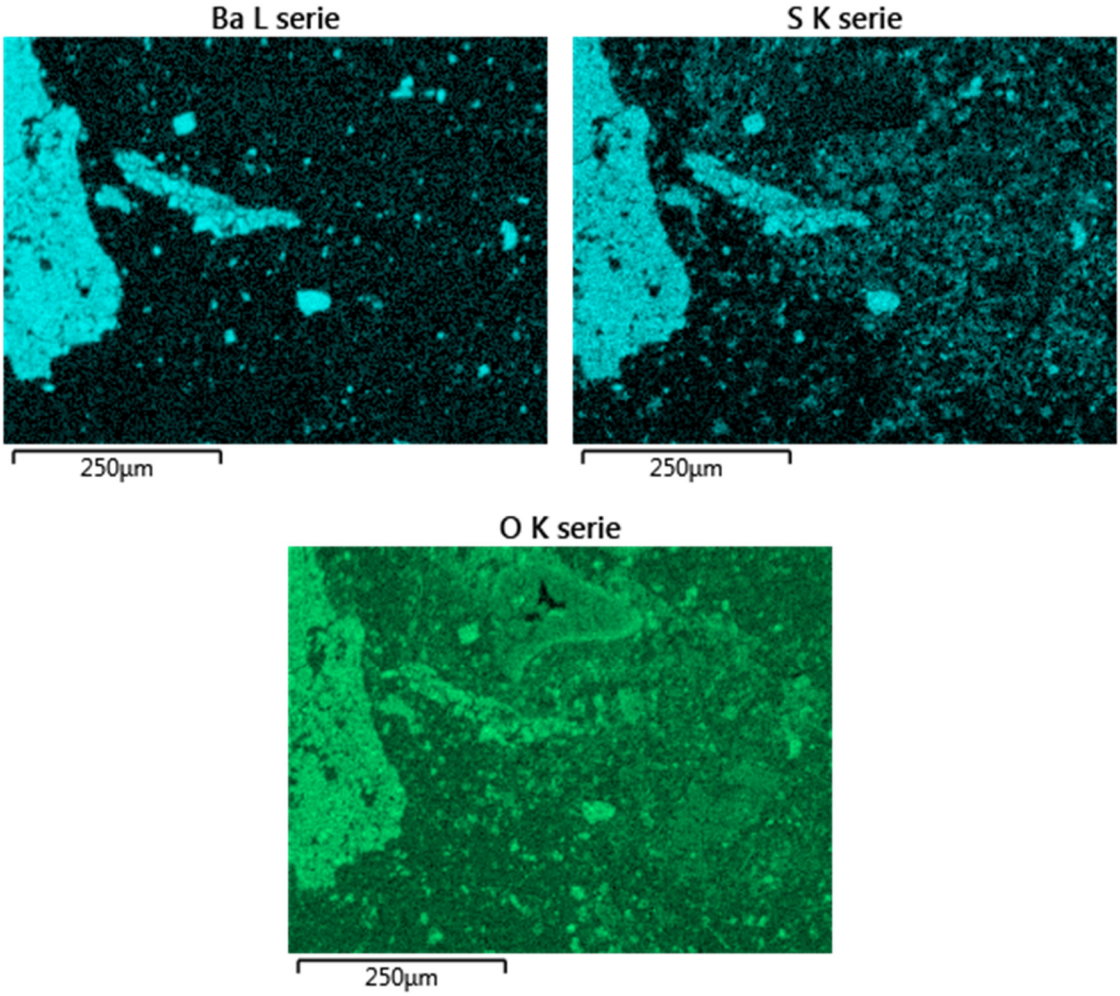

Figure 4-5: Element mappings for Ba, S and O, crude slime (area 1)

4.6 $CuSO_4$ and $CuSO_4 \cdot nH_2O$ – copper sulphate (hydrate)

Copper sulphate was also a possible result of the stoichiometric calculations, but always in combination with other species or as mixed sulphates. In Figure 4-6 there is one grain visible which could be copper sulphate, marked with a yellow circle. However, copper sulphate could not be identified in the XRD analysis. To conclude, the presence of copper sulphates can be considered as most likely but it was not definitely proved in the investigated samples.

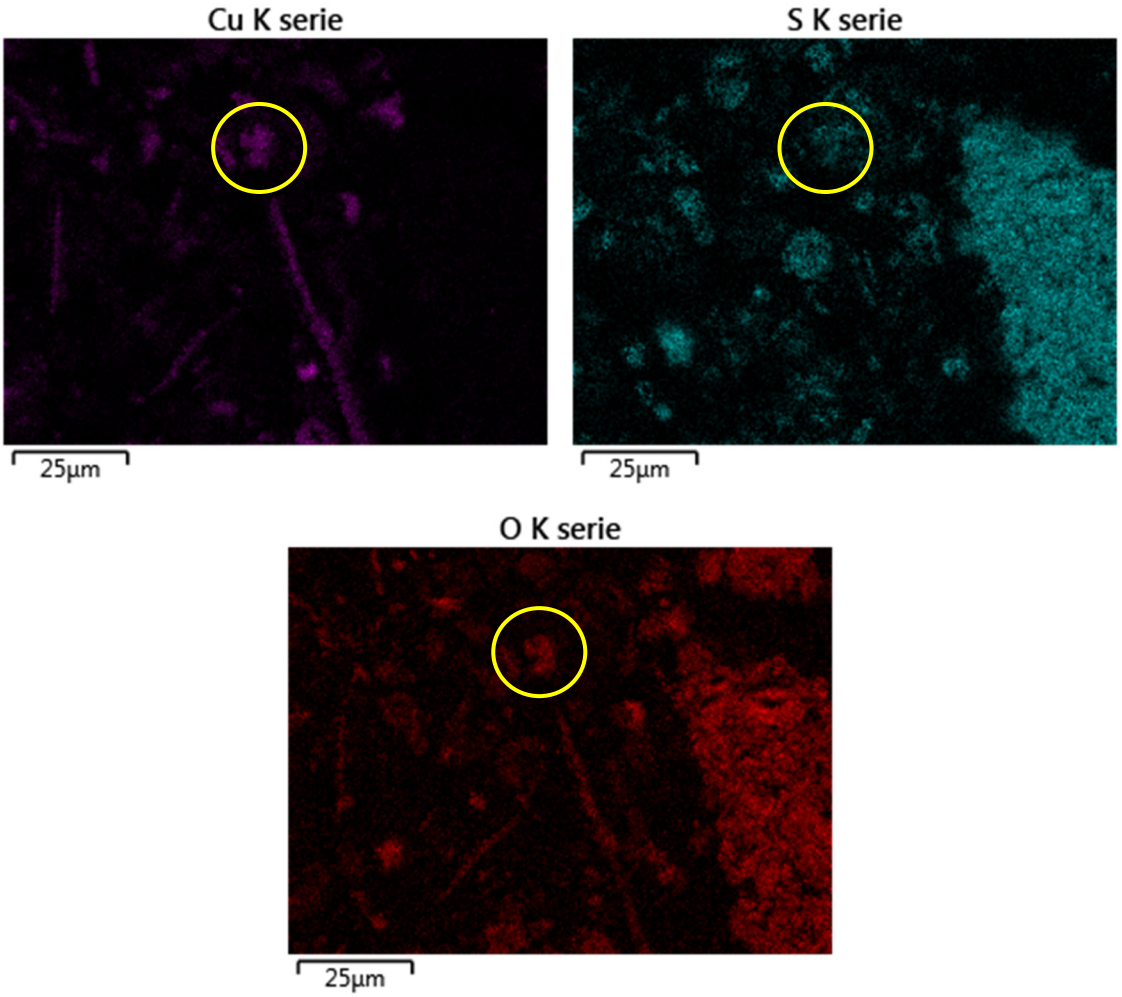

Figure 4-6: Element mappings for Cu, S and O, crude slime (area 2)

4.7 $(Ag,Cu)_2(Se,Te)$ – silver/copper-di-selenide/telluride

Silver telluride was identified in the XRD analysis and silver mixed selenides/tellurides were identified multiple times in the stoichiometric calculations of both slimes. Ag, Se and Te also show a large congruency in Figure 4-7 (yellow circles). At least silver selenides and tellurides are seen as proved to be present in the crude slime. Mixed copper/silver selenide also seems to be plausible, as a certain congruency can be observed in the red circles, but evidence by XRD or distinct stoichiometry in the microscopic EDX analysis is missing. Consequently, $Cu_2(Se,Te)$ cannot be seen as proved although it is likely to be present in crude and washed slime. A silver selenide particle could be identified in the washed slime, as can be seen in the appendix in Figure A-11.

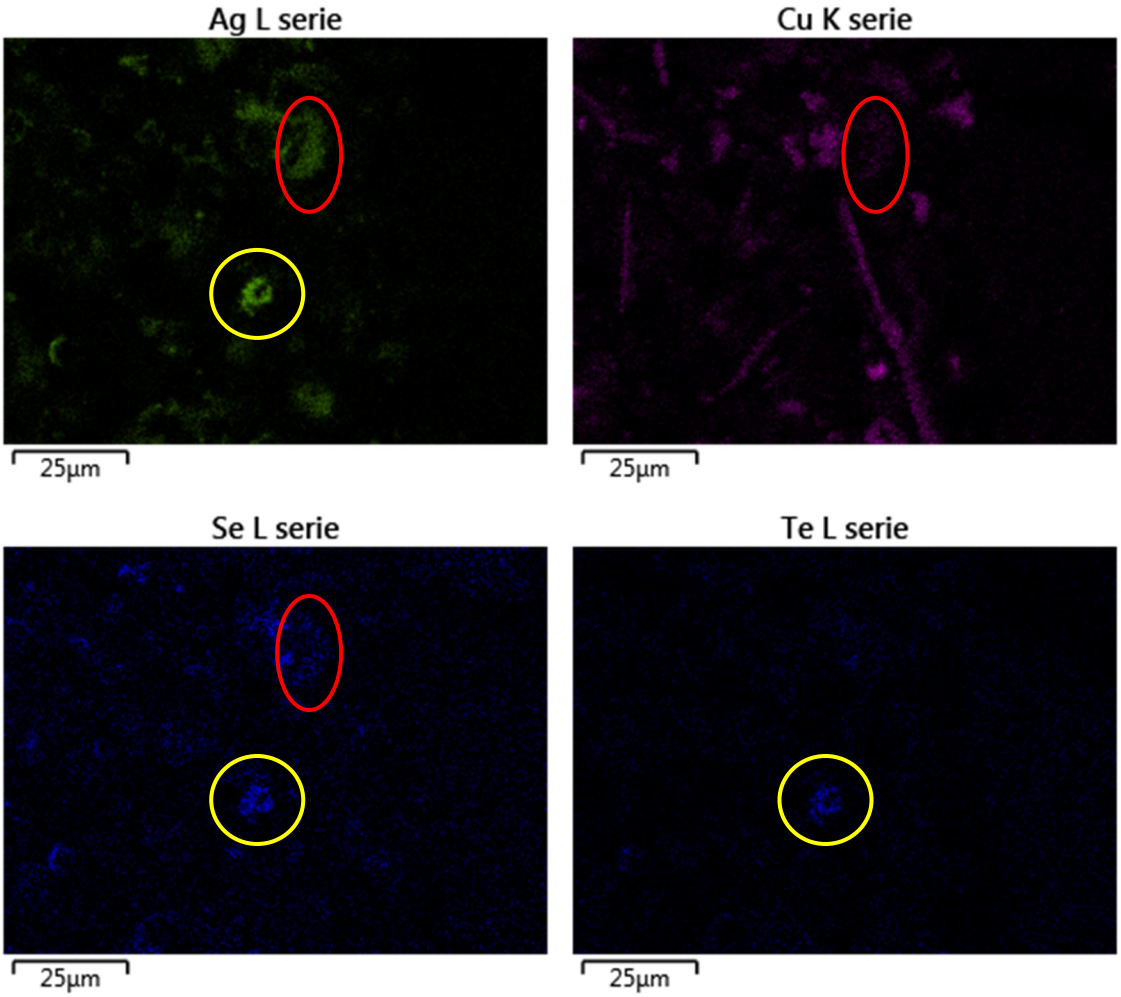

Figure 4-7: Element mappings for Ag, Cu, Se and Te, crude slime (area 2)

4.8 $Al_2O_3 \cdot 2SiO_2 \cdot 2H_2O$ – aluminium-silicon-oxide-hydrate

Aluminium-silicon-oxide-hydrate was found twice in the stoichiometric calculation, and in some other EDX spectra Al and Si have almost equal concentrations. In Figure 4-8 the congruency of Al, Si and O can be seen very distinctly (yellow circles). Therefore, it can be considered as proved, even though it was not found by XRD. Beside areas high in Si and Al, particles high in Si (see red circles), obviously without Al or O, were also observed. These spots do not fit any of the other element mappings analysed. Thus, they are probably metallic Si particles but there is not sufficient evidence for this theory. Both appearances could also be found in the mapping of the washed slime (see Figure A-12).

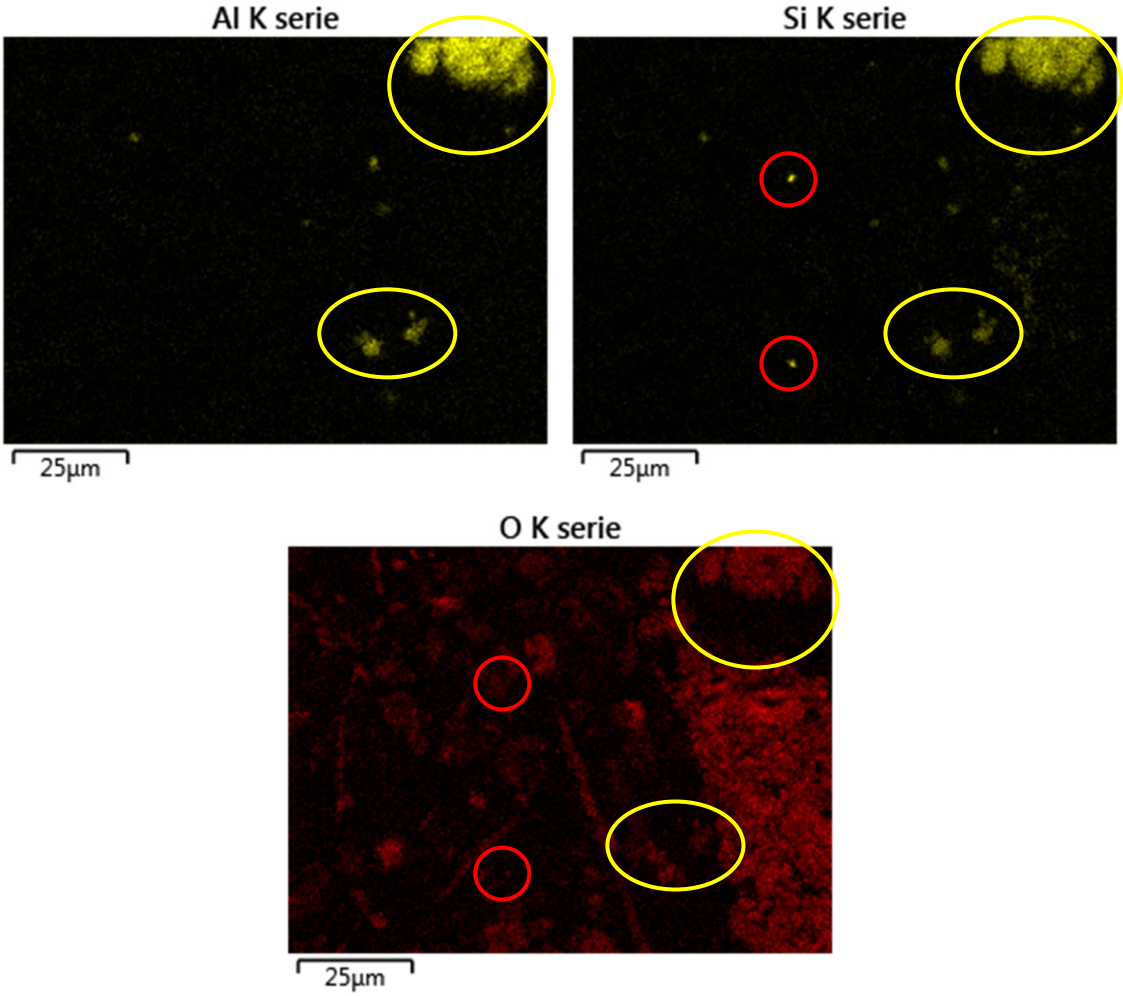

Figure 4-8: Element mappings for Al, Si and O, crude slime (area 2)

4.9 $(Sb_2O_3)_x \cdot (As_2O_5)_{1-x}$ – arsenic-antimony mixed oxides

Figure 4-9 shows the mappings for Sb, As and O. In the yellow circles, their congruency with each other can be observed quite well. Arsenic-antimony mixed oxides were identified in both the XRD analysis and the microscopic EDX spectra. Congruency in the mapping was found for both the crude slime (see Figure 4-9) and the washed slime (see Figure A-13 in the appendix). They are often reported [5,8,18,21,23–26] to be present in anode slimes in literature. For that reason, they can be considered as proved. However, it is important to keep in mind that arsenic-antimony oxides appear in a wide range of their stoichiometric relation, according to literature. This could be the reason why no definite proportion between them could be found in the EDX spectra.

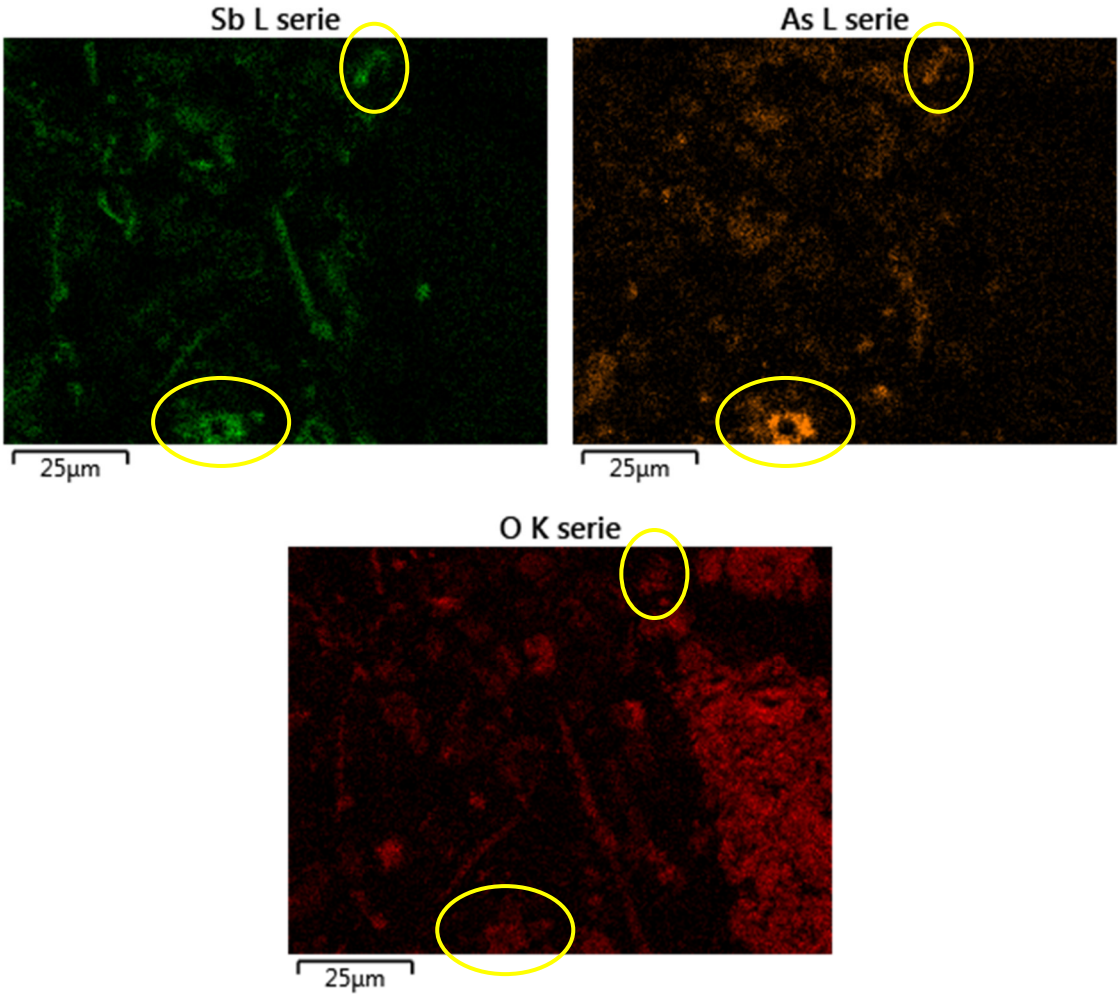

Figure 4-9: Element mappings for Sb, As and O, crude slime (area 2)

4.10 Summary

In the section above, the different suspected and partly proved phases were discussed. In Table 4-I the results of this investigation are summarised. The row “XRD” indicates if one phase was found in the XRD analysis or not. “Calc.” is the number of times one phase was the result of the stoichiometric calculations of the EDX spectra. “Mapping” gives the number of grains that are plausible to fit the various different phase compositions. These are listed seperately for crude and washed slime. The last row gives an idea, as to whether the phase could be proved in the slimes with the characterisation carried out for the material investigated.

Table 4-I: Summary of the phase identification

Phase	XRD	Crude		Washed		Presence
		Calc.	Mapping	Calc.	Mapping	
$Sn(OH)_2$	yes	3	>3	none	1	proved in crude
$PbSO_4$	yes	5	>3	12	>3	proved
AgCl	no	2	>3	none	>3	likely
$Cu_3Ni_{2-x}SbO_{6-x}$	no	2	>3	3	>3	very likely
$BaSO_4$	yes	2	>3	1	>3	proved
$CuSO_4$	no	4	1	1	none	likely in crude
$(Ag,Cu)_2(Se,Te)$	yes	2	2	2	>3	proved
$Al_2O_3 \cdot 2SiO_2 \cdot 2H_2O$	no	1	3	none	1	likely
$(Sb_2O_3)_x \cdot (As_2O_5)_{1-x}$	yes	none	>3	6	>3	proved

Figure 4-10 and Figure 4-11 summarise the mappings for both the crude slime and the washed slime. Wherever possible, the phases were identified according to their stoichiometric composition, based on the findings of the XRD analysis, the information from the literature survey, the stoichiometric calculations from section 3.4, and based on the congruency of certain elements described in the sections before. The images are the same as those that were the basis for the discussion of the different phases and the images in the appendix (see Figure A-6 to Figure A-13), respectively.

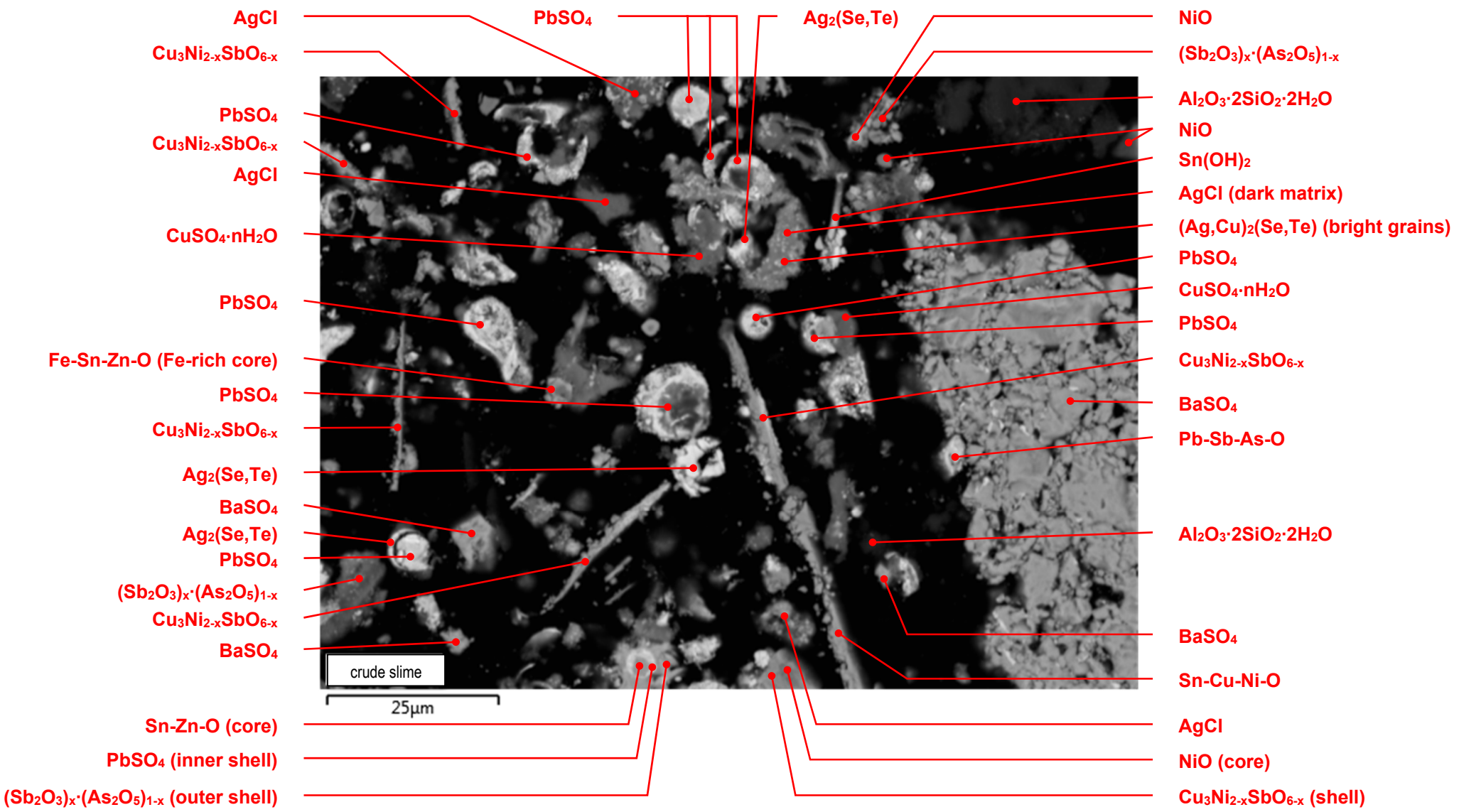

Figure 4-10: Phase identification in the crude anode slime (area 2)

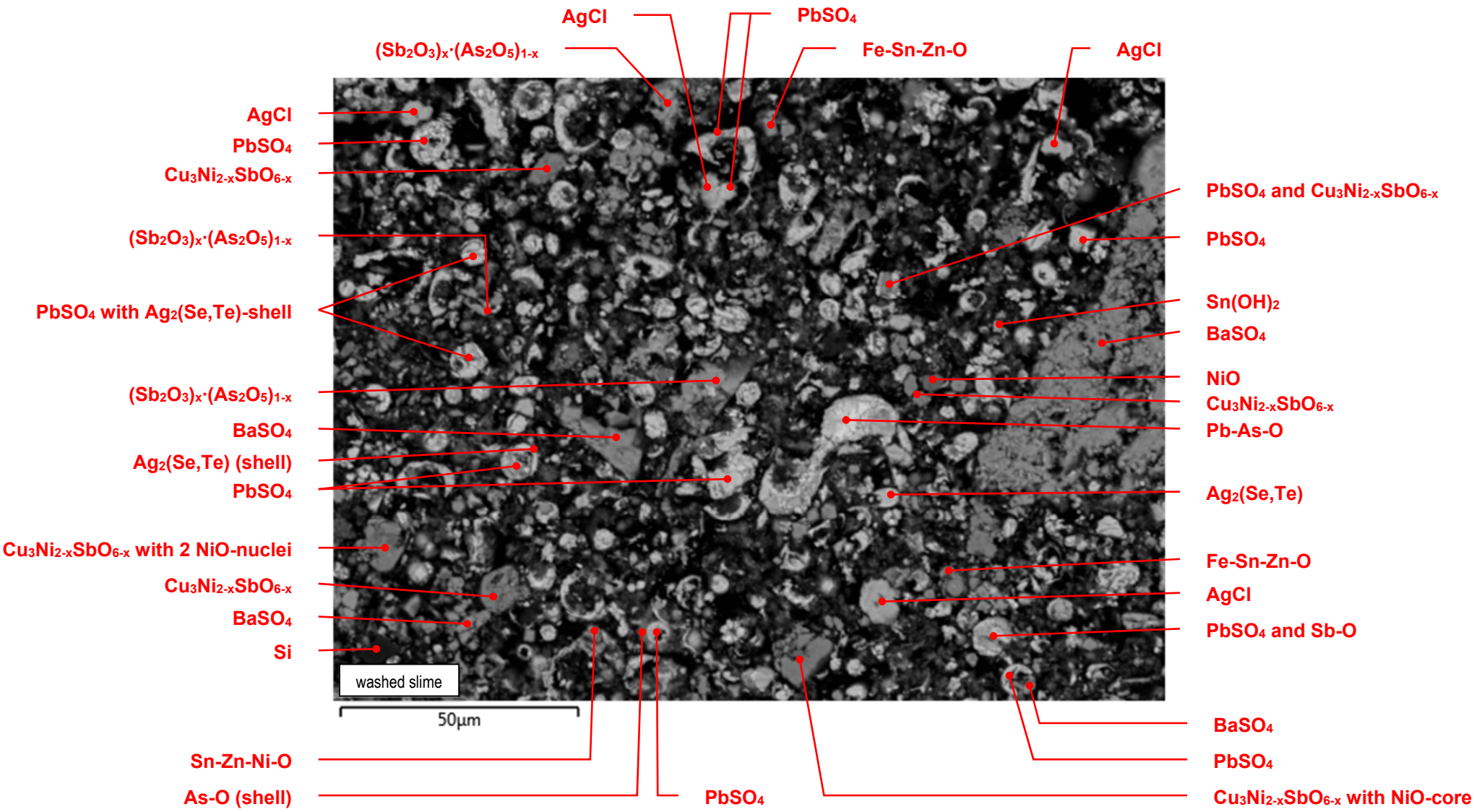

Figure 4-11: Phase identification in the washed anode slime (area 3)

5 Leaching experiments

As already mentioned in the introduction, it would be favourable to have a pretreatment method which is able to extract all undesired elements separately from each other. So the purpose of these leaching experiments was to find out a possible way to extract several fractions enriched in As or Sb or Sn, respectively, and in the best case, a total separation of them. The leaching was carried out in a 4 M KOH aqueous solution at temperatures between room temperature and 80 °C with solid/liquid ratios between 1/4 and 1/20. Detailed experimental parameters are listed in Table 5-I. All experiments were carried out at atmospheric pressure, so neither vacuum technique nor high-pressure apparatuses were needed. A detailed description of the setup and parameters is given in the subsequent sections.

5.1 Basic considerations

For all experiments, the washed slime was used due to the fact that this washing step is state of the art worldwide and helps to keep copper losses low. The slime was stored at atmospheric conditions before the experiments, so it can be presumed to be partly oxidised by the atmospheric oxygen.

The principal setup of the leaching experiments was based on the publication by Fernández et al. [9], described in section 2.5.1. Aside from their considerations, the process parameters were chosen in a way to find out if a separate winning of As and Sb could be possible. It was also focussed on how Sn would behave during leaching, although a positive effect on Sn was not really expected, as Fernández et al. did not consider Sn as a point of interest in their studies.

However, according to the findings of Fernández et al., Sb is less soluble in KOH than As at temperatures below 80 °C. This is shown in Figure 5-1. The solubilities of As are marked with green horizontal lines; those of Sb with blue. As mentioned before, the slime is oxidised, which is why the lines for the OXID sample are relevant in all further considerations. It can be assumed that the difference in solubility is even stronger at lower temperatures, for example at 40 or 20 °C. Therefore, experiments even at room temperature seemed to be a useful attempt.

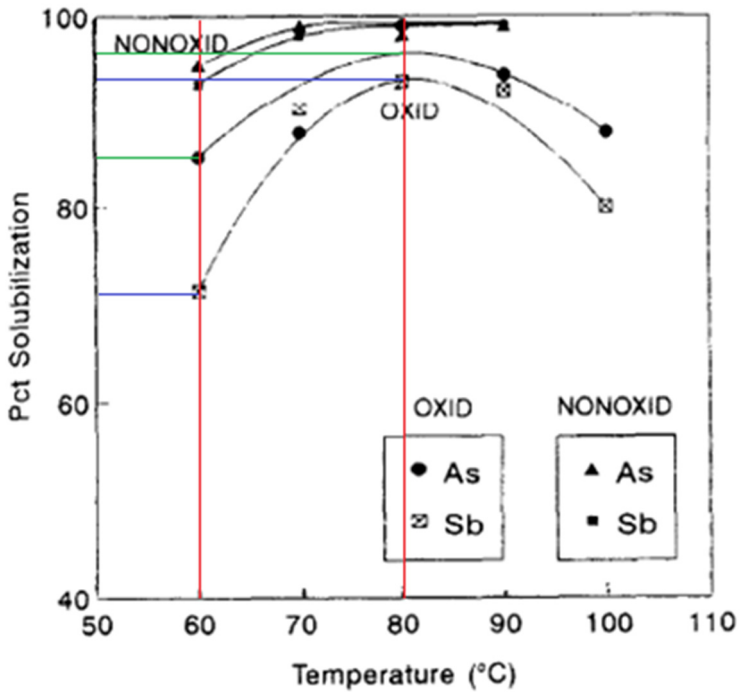

Figure 5-1: Effect of the leaching temperature on the solubilisation of As and Sb from oxidised (OXID) and non-oxidised (NONOXID) anode slimes. Conditions: 4 M KOH, 30 min, S/L ratio = 1/40, 5 g of anode slime [9]

The second important influence parameter for the solubility of As and Sb in KOH is the solid/liquid ratio. For the oxidised sample, the solubility of Sb gets smaller with an increasing solid/liquid ratio, exhibited in Figure 5-2.

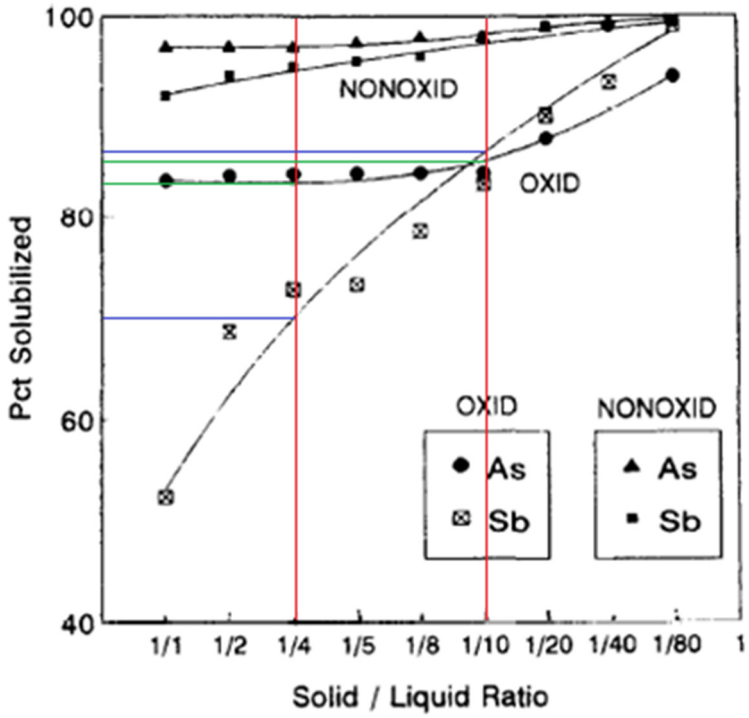

Figure 5-2: Effect of the solid/liquid ratio in the pulp on the solubilisation of As and Sb from oxidised (OXID) and non-oxidised (NONOXID) anode slimes. Conditions: 80 °C, 4 M KOH, 30 min, 5 g of anode slime [9]

If both effects are now combined, the difference in the solubility of As and Sb might even be stronger. So the temperature and the solid/liquid ratio are the important parameters that must be optimised to achieve the best possible separation between As and Sb. For that reason, both parameters were varied within the present experimental series. Detailed parameters are listed below, in Table 5-I.

5.2 Experiment setup

As neither high pressure, vacuum nor temperature above the boiling point of water were necessary, the experiment setup could be kept quite simple. The first step was the leaching of a defined amount (30 g in all experiments) of anode slime in aqueous KOH solution. At the beginning the required amount of KOH was prepared in a beaker and set onto a heating plate with a magnetic stirrer. The solution was heated to the desired temperature and then kept constant by an electronic temperature control device during the whole leaching process. After reaching the experiment temperature, the slime was added and the suspension was continuously stirred to ensure a quick reaction progress. The leaching setup is shown in Figure 5-3.

Figure 5-3: Leaching setup

In all experiments the leaching time was kept constant at 30 min. Afterwards the suspension had to be filtered to separate the solution from the solid leaching residue. This was carried out using laboratory filter paper and a filtering flask. The filtering procedure can be seen in Figure 5-4.

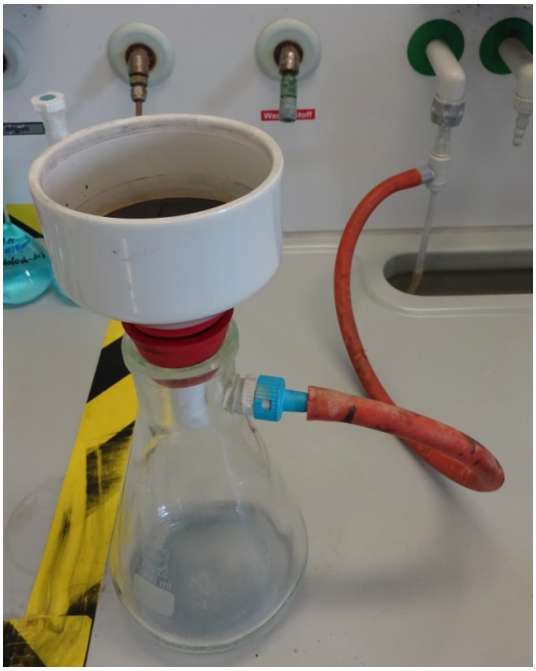

Figure 5-4: Filter setup

What remains is on the one hand the solution and on the other hand the solid filter cake on the filter paper. The filter cake was weighed, dried at 105 °C and weighed once again. Weighing twice was important to get a correct mass balance, as a small amount of solution remained trapped in the solid after filtering. The solution had to be weighed too and both the solution and the filter cake were sent to an external laboratory for chemical analysis.

5.3 Experiment parameters

The series consisted of six experiments with the parameters listed in Table 5-I. As mentioned already, the temperature and the solid/liquid ratio varied in the range between room temperature and 80 °C and between 1/4 and 1/20, respectively. It can be seen as two experimental series; one with varying temperature and a constant solid/liquid ratio of 1/4 (experiments № 4, 1, 2 and 3) and the other with a varying solid/liquid ratio and constant temperature of 80 °C (experiments № 3, 5 and 6). Leaching duration and the KOH concentration were kept constant at 30 min and 4.0 mol/l, respectively, in all experiments.

Table 5-I: Experiment parameters

Experiment parameters	**Dimension**	**Experiment №**					
		4	**1**	**2**	**3**	**5**	**6**
T	°C	**RT**	**40**	**60**	**80**	80	80
t	min	30	30	30	30	30	30
S/L	1	1/4	1/4	1/4	**1/4**	**1/10**	**1/20**
c(KOH)	mol/l	4.0	4.0	4.0	4.0	4.0	4.0

6 Experimental results and discussion

The results of the leaching experiments are presented in this section. Special attention is paid to the success of the removal of As, Sb and Sn, as this is, in addition to the detailed characterisation, the main focus of the experimental part of the diploma thesis. The influence of the variation of the temperature and the solid/liquid ratio is discussed, as well.

6.1 Removal rates

Table 6-I lists the percentage removal rates for selected elements from the anode slime by leaching in KOH, according to the previously-described parameters for all executed experiments. The removal rate quotes what percentage of the initial amount of each element contained in the anode slime could be removed by the leaching procedure.

Table 6-I: Removal rates of selected elements by leaching

***Parameters* / Element**	**Dimension**	**Experiment №**					
		4	**1**	**2**	**3**	**5**	**6**
T	*°C*	***RT***	***40***	***60***	***80***	*80*	*80*
S/L	*1*	*1/4*	*1/4*	*1/4*	***1/4***	***1/10***	***1/20***
Ag	%	6.1	14.7	14.0	14.6	23.8	9.6
As	%	37.2	45.9	47.9	70.5	84.0	87.7
Cu	%	9.0	6.5	15.5	15.1	24.3	29.1
Ni	%	3.4	0.0	8.0	9.2	0.0	0.0
Sb	%	2.3	0.0	0.0	0.0	25.3	37.2
Se	%	0.0	1.8	2.9	2.8	11.4	0.0
Sn	%	15.9	30.1	36.9	48.0	80.1	79.8
Te	%	18.2	18.9	19.4	23.6	33.8	25.9

The basis for the data shown is the chemical analysis of the washed anode slime and the dried filter cakes. In order to validate the results, the filtered solutions were also analysed. Those results correspond with the figures shown above quite well.

6.2 Variation of the leaching temperaure

In this section the results of experiments № 4, 1, 2 and 3 are compared. The solutions from the leaching, after filtering change significantly in colour with the changing process temperature from a deep blue, with room temperature leaching, to a slightly yellow-greenish colour with leaching at 80 °C. These can be seen in Figure 6-1.

Figure 6-1: Solutions from experiments with varying temperature (from left to right: RT, 40, 60, 80 °C)

The chart in Figure 6-2 shows the removal rates of As, Sb and Sn with an increase in temperature from room temperature to 80 °C.

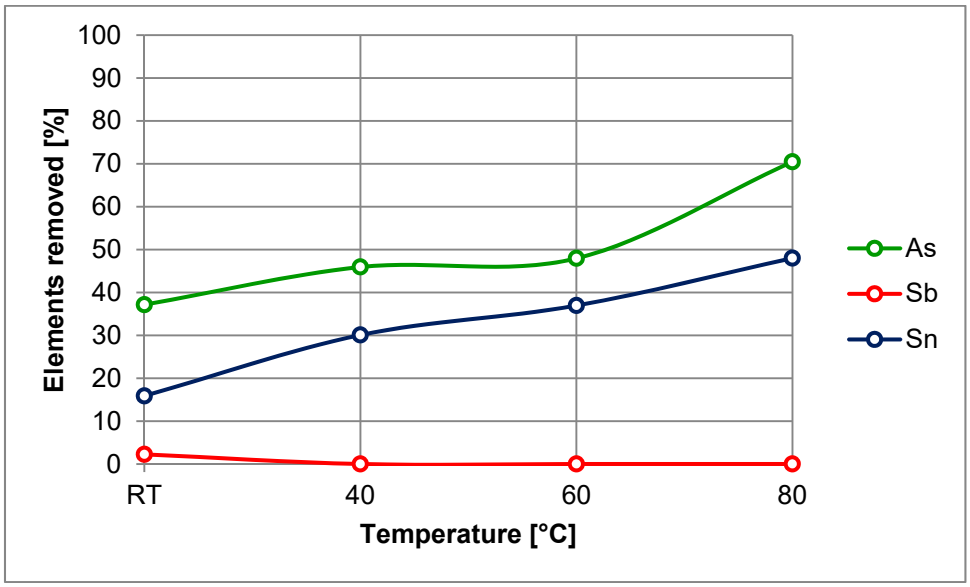

Figure 6-2: Removal rates of As, Sb and Sn depending on the leaching temperature (experiments № 4, 1, 2 and 3), S/L = 1/4, t = 30 min, c(KOH) = 4.0 mol/l

About 70 % of the As content was able to be removed at 80 °C. This is slightly below the expected yield of over 80 %, which Fernández et al. reached with the same parameters, but still acceptable. It is remarkable that almost half of the Sn content could be leached. Even more noticeable is the fact that obviously no Sb was leached with a solid/liquid ratio of 1/4, regardless of which temperature was applied during leaching. This is a complete contrast to the results of Fernández et al., who published a 70 % leaching rate at these conditions (compare to Figure 6-3).

Besides As, Sb and Sn, a significant amount of Ag and Cu (up to 15 %) was also leached, moreover up to 10 % of the Ni at temperatures exceeding 60 °C, and up to 24 % of the Te. Se was not leached in significant amounts at all temperatures. Especially the loss of Ag is a problem to be solved with regard to a future industrial application because precious metals like silver are the cash cow in the processing of anode slimes.

However, the attempt at the seperate winning of As and Sb from the anode slime was successful and can certainly be improved in selectivity by further optimisation of the process parameters.

6.3 Variation of the solid/liquid-ratio

In the following section, the results of experiments № 3, 5 and 6 are compared. A significant change in the colour of the filtered solutions appears here, as well. They are shown in Figure 6-3. The solution on the left in this figure is the same as the one on the right in Figure 6-1. The colour changes from yellow-greenish to blue with a decreasing solid/liquid ratio.

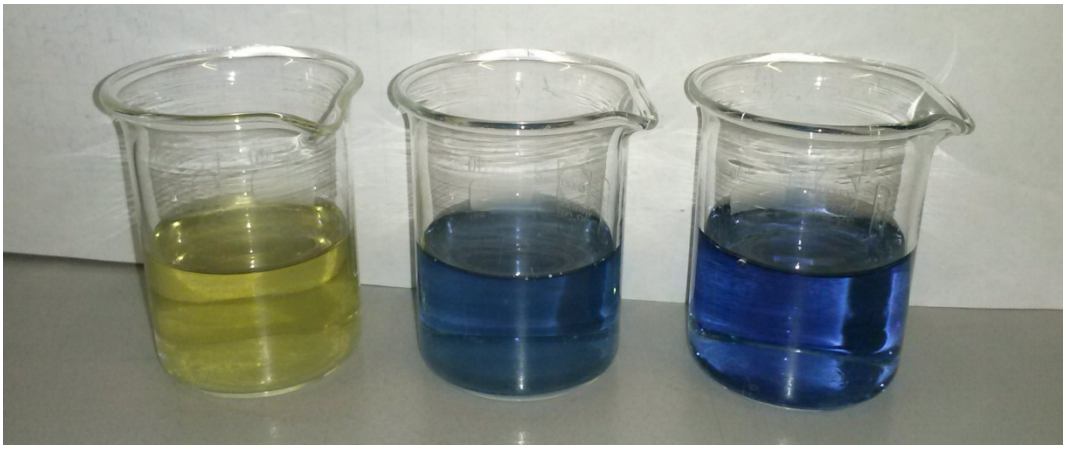

Figure 6-3: Solutions from experiments with a varying solid/liquid ratio (from left to right:1/4, 1/10, 1/20)

The removal rates for As, Sb and Sn with decreasing solid/liquid ratio at a constant temperature of 80 °C can be observed in Figure 6-4.

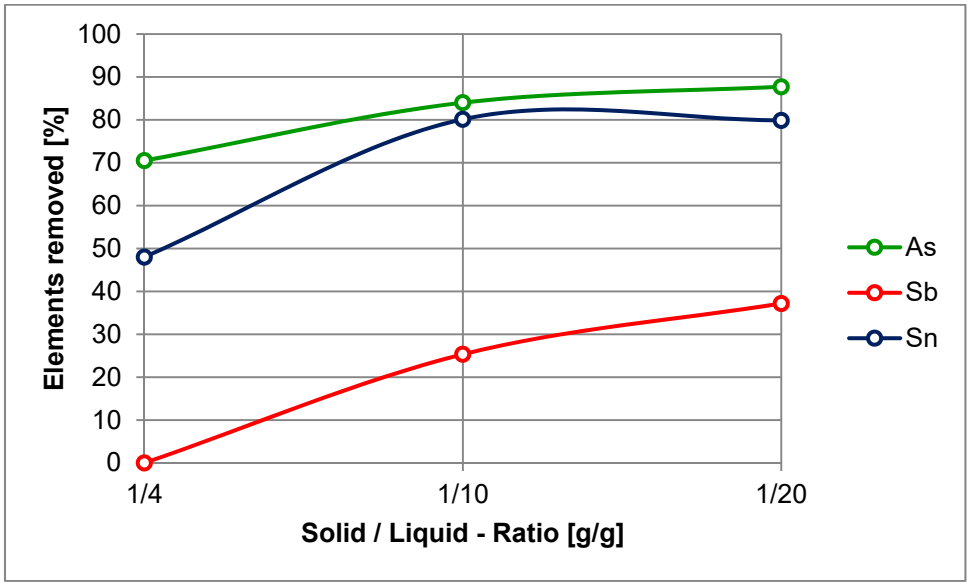

Figure 6-4: Removal rates of As, Sb and Sn depending on the solid/liquid ratio (experiments № 3, 5 and 6), T = 80 °C, t = 30 min, c(KOH) = 4,0 mol/l

When more KOH solution is available for the same amount of anode slime, it can of course be expected that greater amounts can be leached. As a consequence, the yield of As rises to nearly 90 % if 20 times more KOH solution is present than slime. This figure corresponds rather well with what was found in literature (compare to Figure 6-3). The leaching rate of Sn can obviously also be increased up to 80 % that way.

The removal rate of Sb is now increasing. At a solid/liquid ratio of 1/20 it reaches nearly 40 %. But this is far below the expected value of about 90 % that was found during the literature survey (compare to Figure 6-3). The reason for such an unsatisfying yield could be found in the temperature sequence after leaching during the process of filtering. According to Fernández et al. (compare with Figure 5-1), the removal rate of Sb is strongly dependent on the temperature. It decreases with decreasing temperature. If one extrapolates the curve for the solubility of Sb in KOH solution down to room temperature, the solubility of Sb is estimated to be nil. In fact, the solution is cooled down during filtering because the filtering flask could not be heated.

The suspected consequence is the reprecipitation of Sb phases during filtering. Thus, in the first seconds of filtering, the solution is still hot and precipitation takes place after filtering. These precipitates can be found in the solution afterwards (see Figure 6-5). The chemical analysis of the dried precipitates is shown in Table 6-II. Seeing as the rest of the liquid still needs to be filtered, precipitates that occur above the filter remain in the solid filter cake. The chemical analysis of the sediments from the solution revealed that Sb is its main metallic constituent, thus supporting this theory.

Table 6-II: Chemical analysis of Sb-rich precipitates

Element	Dimension	Conc.	Element	Dimension	Conc.
Ag	%	0.063	**Sb**	%	16
As	%	5.1	**Se**	%	< 0.08
Cu	%	3.6	**Sn**	%	2.3
Ni	%	< 0.08	**Te**	%	0.63

Figure 6-5: Sb-rich sediments from solution after leaching (experiment № 5)

As a consequence, filtering must take place at the same temperatures as leaching in order to assure that Sb is successfully removed from the anode slime. The aforementioned effect could also be exploited in a very useful way if selective leaching of As without any Sb is desirable.

6.4 Proposal for future experiment layout

As shown by the experimental results presented above, selective removal of As and Sb by KOH leaching is definitely possible. Within this process, Sn also is leached and can be mainly found in the As-rich fraction. Selective leaching requires a two-step process, in which the first step has to be designed in such a way that a maximum of As (and Sn) can be extracted, while the carryover of Sb must be prevented. Only in the second step should Sb (and the rest of As and Sn) be dissolved. Hence, the following process parameters seem to be useful for this purpose:

- Leaching at T = 80 °C and S/L =1/4 or higher
- Cooling
- Filtering

This first step leaves an Sb-free, As and Sn-rich solution and a filter cake. The filter cake undergoes the second leaching step:

- Leaching at T = 80 °C and S/L = 1/20 or even lower
- Filtering at a constant temperature of 80 °C

This should prevent Sb from precipitating and leaves an Sb-rich solution as well as a pretreated anode slime poor in As, Sb and Sn ready for further processing.

7 Conclusion and outlook

This section provides a brief summary of the points dealt with previously. The literature research comprises a basic flowchart for secondary materials from the copper production route, a brief description of the formation of anode slime in copper refining, possible methods and recent research activities in the field of anode slime pretreatment, as well as methods for the scientific analysis of powdery anorganic substances like anode slime. In this case, ICP-OES, XRD and SEM-EDX were the relevant analysis techniques.

The characterisation of the two anode slimes, one crude, as taken from the electrolysis cell, and one washed in sulphatic milieu, was carried out using the following steps. Besides a chemical analysis, firstly XRD was used to get an idea of what phases to search for in detail. There it was found out that the washing obvieously does not change the basic composition of the phases, as the XRD spectra of both slimes have quite similar characteristics. In a second step, SEM-EDX was applied to receive element-specific mappings of slime samples. At that point, groups of elements which appear together and will likely also form chemical compounds with each other could be named. For further verification in the third step, microscopic SEM-EDX spectra were recorded for a number of single grains visible in the SEM images. That gives stoichiometric information about the single grain composition. By doing this, many phases detected by the XRD analysis, and further ones, could be confirmed or found.

This way, $Sn(OH)_2$, $PbSO_4$, $BaSO_4$, $(Ag,Cu)_2(Se,Te)$ and $(Sb_2O_3)_x \cdot (As_2O_5)_{1-x}$ could be successfully proved by both XRD and microscopic SEM-EDX. Furthermore, AgCl, $Cu_3Ni_{2-x}SbO_{6-x}$, $CuSO_4$ and $Al_2O_3 \cdot 2SiO_2 \cdot 2H_2O$ were found by stoichiometric relation, but not by XRD. The reason is most likely the low concentration of them, which makes it impossible to find their characteristic peaks in the spectrum. The SEM images reveal that $Sn(OH)_2$ and $Cu_3Ni_{2-x}SbO_{6-x}$ change their appearance from needle-shaped to a more globular shape in the washing step. The other phases dealt with seem to keep their shape. Apart from that, only the absolute concentrations of some elements change from washing but not the basic composition of the phases. This makes perfect sense insofar as the milieu in a copper refining electrolysis cell is sulphatic as well as the medium used for washing.

Besides characterisation, the topic of this diploma thesis is also a multi-metal recovery. In that context, the goal was to execute a small experimental series designed to investigate a possibility for removing Sn, As and Sb from the anode slime. According to the literature research, the easiest way is leaching in KOH solution. In studying the literature sources, the idea was born that it must also be possible to remove either As alone or both As and Sb. The

behaviour of Sn had to be investigated because the literature sources do not deal with Sn. A series of six leaching experiments was done, varying the leaching temperature as well as the solid/liquid ratio of the suspension, producing promising results.

The removal rates for As named in literature could be widely confirmed by the experiments with the investigated sample material. Secondly, parameters were detected where either no Sb or nearly half of the Sb contained can be removed. In the case of Sn, it turned out that much more than half of the amount contained is leachable. Maximum removal rates of 88 % for As, 37 % for Sb and 80 % for Sn could be achieved with leaching parameters of 80 °C, a solid/liquid ratio of 1/20, 30 min leaching time and 4.0 mol/l KOH. If the solid/liquid ratio is changed to 1/4, the amount of Sb leached is nil, but 71 % of the As and 48 % of Sn can still be removed. The temperature control while filtering after the leaching step turned out to be crucial for the success of leaching Sb. It was found that Sb can reprecipitate in the filter when the filtering time is long and so the solution cools down before filtering. This can completely inhibit Sb removal. It is believed that this effect is one reason why the removal rates for Sb are much lower than those for As and Sn, as heating while filtering was not available and thus the solution was always cooled to a certain degree. However, based on these findings, a two-step process can be proposed which removes As and partly Sn in one step and Sb with residual As and Sn in the second by varying temperature and the solid/liquid ratio.

By optimising the temperature control, the results will certainly be better, especially for Sb. Moreover, for further investigation it would be of interest to also vary the concentration of KOH and the leaching time to see their influence. The proposed two-step version for a selective winning of As and Sb would have to be tested in experiments, as well. All experiments carried out within this diploma thesis used the washed anode slime, because the initial concentration levels were lower. Another future topic could be to try all of this using crude slime. In literature it is mentioned that the removal rates are even better if anode slime does not have time to oxidate after being taken from the cells. So another future research approach could be to use reducing agents like SO_2 purging during the leaching step or try with slime straight from the electrolysis cell.

To sum up, the characterisation proved, amongst others, those phases containing the elements focussed on, Sn, As and Sb. The experimental approach of leaching in KOH worked, even though unexpectedly in the case of Sn, for all three of these elements. And at the end, a proposal for a practical process design could be provided.

Literature

[1] Amer, A.M.: Processing of copper anodic-slimes for extraction of valuable metals, Waste Management 23 (2003), 8, 763–770.

[2] Ludvigsson, B.M. and S.R. Larsson: Anode slimes treatment: The boliden experience, JOM 55 (2003), 4, 41–44.

[3] Petkova, E.N.: Mechanisms of floating slime formation and its removal with the help of sulphur dioxide during the electrorefining of anode copper, Hydrometallurgy 46 (1997), 3, 277–286.

[4] Hait, J., R.K. Jana and S.K. Sanyal: Processing of copper electrorefining anode slime: a review, Miner. Process. Ext. Metall. 118 (2010), 240–252.

[5] Antipov, N.I. and A.V. Tarasov: Hydrometallurgical Methods of Recycling Interelectrode Slime, Metallurgist 46 (2002), 229–233.

[6] Guo, X.Y., C.M. Xiao, J.Y. Zhong and Q.H. Tian: Behaviors of precious metals in process of copper anode slime treatment, Chin. J. Nonferrous Met. 20 (2010), 5, 990–998.

[7] Liu, W., T. Yang, D. Zhang, L. Chen and Y. Liu: Pretreatment of copper anode slime with alkaline pressure oxidative leaching, International Journal of Mineral Processing 128 (2014), 48–54.

[8] Lin, D. and K. Qiu: Removing arsenic from anode slime by vacuum dynamic evaporation and vacuum dynamic flash reduction, Vacuum 86 (2012), 8, 1155–1160.

[9] Fernández, M.A., M. Segarra and F. Espiell: Selective leaching of arsenic and antimony contained in the anode slimes from copper refining, Hydrometallurgy 41 (1996), 2-3, 255–267.

[10] Qiu, K., D. Lin and X. Yang: Vacuum Evaporation Technology for Treating Antimony-Rich Anode Slime, JOM 64 (2012), 11, 1321–1325.

[11] Antrekowitsch, H.: Metallhüttenkunde II, Vorlesungsskriptum, Leoben, 2011.

[12] Mukongo, T., K. Maweja, B. wa Ngalu, I. Mutombo and K. Tshilombo: Zinc recovery from the water-jacket furnace flue dusts by leaching and electrowinning in a SEC-CCS cell, Hydrometallurgy 97 (2009), 1-2, 53–60.

[13] Solnordal, C.B., F.R. Jorgensen, P.T. Koh and A. Hunt: CFD modelling of the flow and reactions in the Olympic Dam flash furnace smelter reaction shaft, Applied Mathematical Modelling 30 (2006), 11, 1310–1325.

[14] Montenegro, V., H. Sano and T. Fujisawa: Recirculation of high arsenic content copper smelting dust to smelting and converting processes, Minerals Engineering 49 (2013), 184–189.

[15] Agrawal, A. and K.K. Sahu: Problems, prospects and current trends of copper recycling in India: An overview, Resources, Conservation and Recycling 54 (2010), 7, 401–416.

[16] Ranjbar, R., M. Naderi, H. Omidvar and G. Amoabediny: Gold recovery from copper anode slime by means of magnetite nanoparticles (MNPs), Hydrometallurgy 143 (2014), 54–59.

[17] Wang, X., Q. Chen, Z. Yin, M. Wang, B. Xiao and F. Zhang: Homogeneous precipitation of As, Sb and Bi impurities in copper electrolyte during electrorefining, Hydrometallurgy 105 (2011), 3-4, 355–358.

[18] Kilic, Y., G. Kartal and S. Timur: An investigation of copper and selenium recovery from copper anode slimes, International Journal of Mineral Processing 124 (2013), 75–82.

[19] Chen, T.T. and J.E. Dutrizac: Mineralogical characterization of a copper anode and the anode slimes from the la caridad copper refinery of mexicana de cobre, Metall and Materi Trans B 36 (2005), 2, 229–240.

[20] Mastyugin, S.A. and S.S. Naboichenko: Processing of copper-electrolyte slimes: Evolution of technology, Russ. J. Non-ferrous Metals 53 (2012), 5, 367–374.

[21] Chen, T. and J. Dutrizac: Mineralogical characterization of anode slimes: Part 10. Tellurium in raw anode slimes, Canadian Metallurgical Quarterly 35 (1996), 4, 337–351.

[22] Chen, A., Z. Peng, J.-Y. Hwang, Y. Ma, X. Liu and X. Chen: Recovery of Silver and Gold from Copper Anode Slimes, JOM (2014).

[23] Yannoupoulus, J. C., Agrawal, J. C. (Ed.): Factors affecting the quality of electrorefining cathode copper, New York, 1976.

[24] Nishimura, T. and K. Tozawa: Behaviour of antimony and arsenic in sulfuric acid solution, Metall. Rev. MMIJ 3 (1986), 2, 131–145.

[25] Noguchi, F., T. Nakamura and Y. Ueda: Behaviour of anode impurities in copper electrorefining - effect of bismuth and oxygen in anode, Metall. Rev. MMIJ 7 (1990), 2, 93–107.

[26] Zhao, T.C.: Metallurgy of heavy metals (part 1), Metallurgical Industry Press (1981).

[27] Dutrizac, J.E. and T.T. Chen: Mineralogical characterisation of anode slimes, Can. Metall. Q. 27 (1988), 2, 91–115.

[28] Scott, J.D.: Electrometallurgy of copper refinery anode slimes, Metallurgical Transactions B 21 (1990), 4, 629–635.

[29] Bragg diffraction, https://commons.wikimedia.org/w/index.php?curid=17543875, Accessed on: 03.05.2016.

[30] Schematic of SEM, https://commons.wikimedia.org/w/index.php?curid=9643934, Accessed on: 03.05.2016.

[31] Avramovic, L. et al.: Production of selenium powder from anode slimes, Metal Powder Report 57 (2002), 11, 41.

[32] Fan, Y., Y. Yang, Y. Xiao, Z. Zhao and Y. Lei: Recovery of tellurium from high tellurium-bearing materials by alkaline pressure leaching process: Thermodynamic evaluation and experimental study, Hydrometallurgy 139 (2013), 95–99.

[33] Xue-Wen, W., C. Qi-Yuan, Y. Zhou-Lan and X. Lian-Sheng: Identification of arsenato antimonates in copper anode slimes, Hydrometallurgy 84 (2006), 3-4, 211–217.

[34] Institut für Arbeitschutz der Deutschen Gesetzlichen Unfallversicherung (IFA), GESTIS-Stoffdatenbank.

Acronyms

APOL	Alkaline pressure oxidative leaching
Approx.	Approximately
c	Concentration
Calc.	Calculation
Conc.	Concentration
Cont.	Continuation
E^0	Standard electrode potential
EDX	Energy dispersive X-ray spectrometry
i	Current density
ICP-OES	Inductively coupled plasma-optical emission spectrometry
M	Molar concentration
p	Pressure
p_{atm}	Atmospheric pressure
rpm	Rotations per minute
RT	Room temperature
PGM	Platinum group metals
SAL	Sulphuric acid leaching
SEM	Scanning electron microscopy
SEM-EDX	Scanning electron microscopy-energy dispersive X-ray spectrometry
S/L ratio	Solid/liquid ratio
T	Temperature
TBRC	Top blown rotary converter
XRD	X-ray diffractometry

Index of Tables

Index of Figures

Appendix

Figure A-1 to Figure A-5 show the mappings of the washed slime sample of the systematic study of element correlations dealt with in section 3.5.

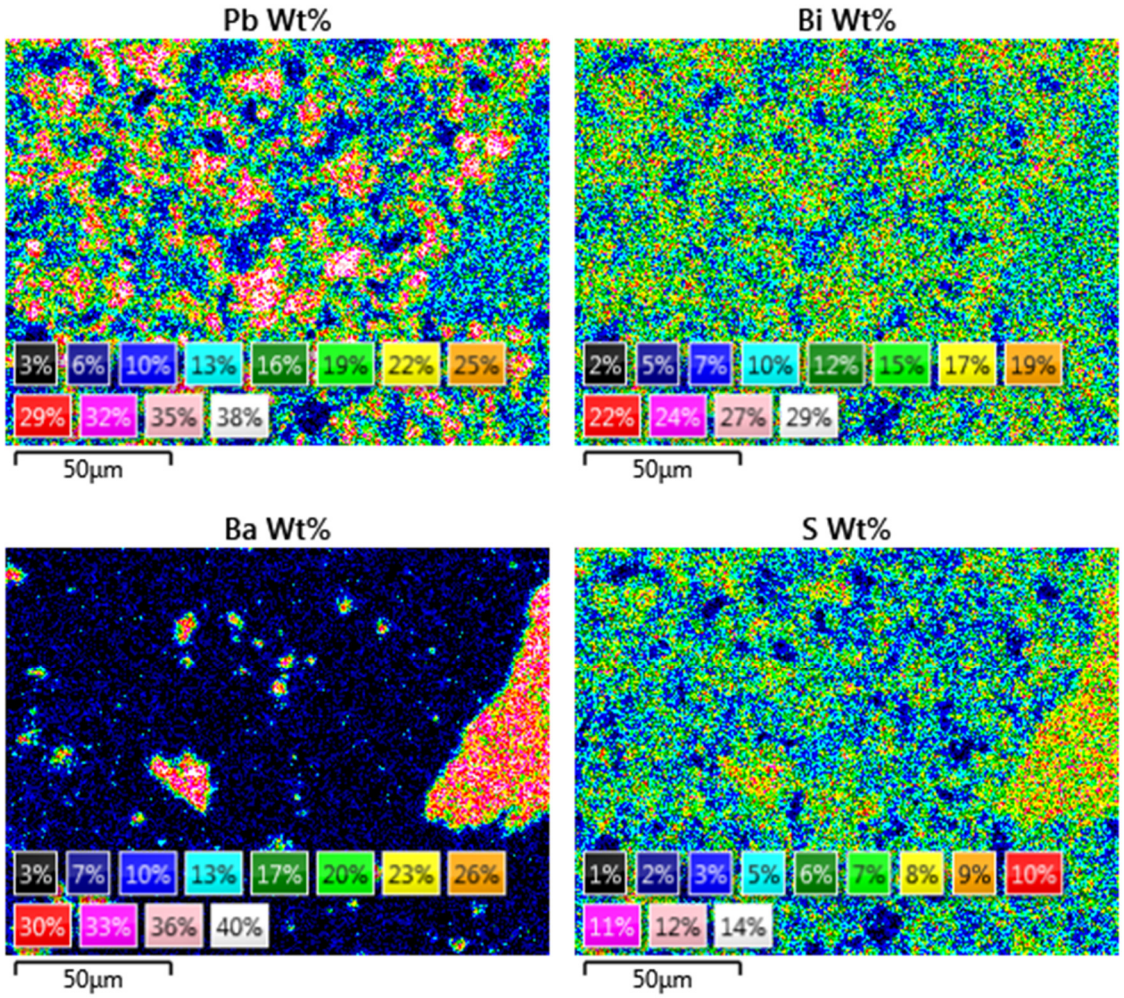

Figure A-1: Element mappings for Pb, Bi, Ba and S, washed slime (area 3)

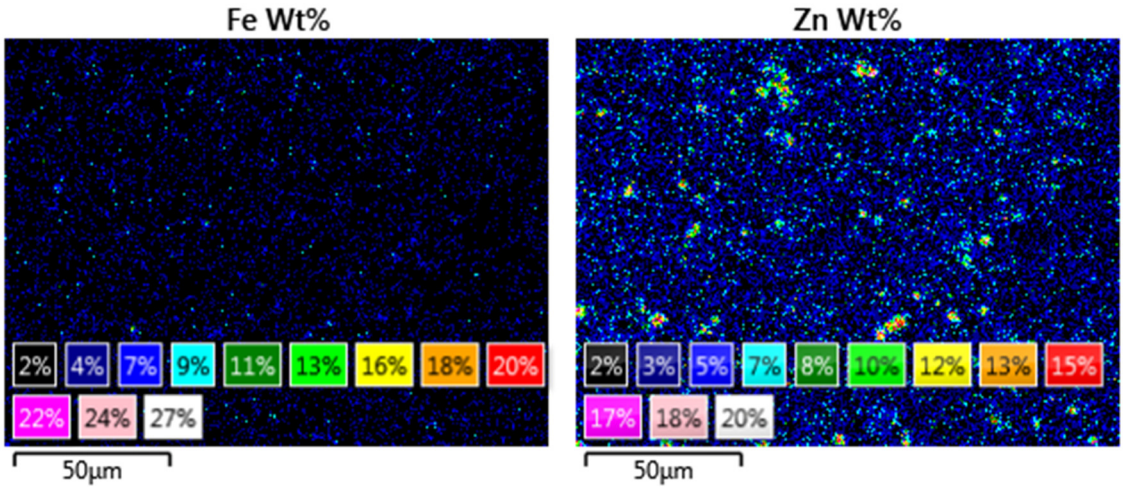

Figure A-2: Element mappings for Fe and Zn, washed slime (area 3)

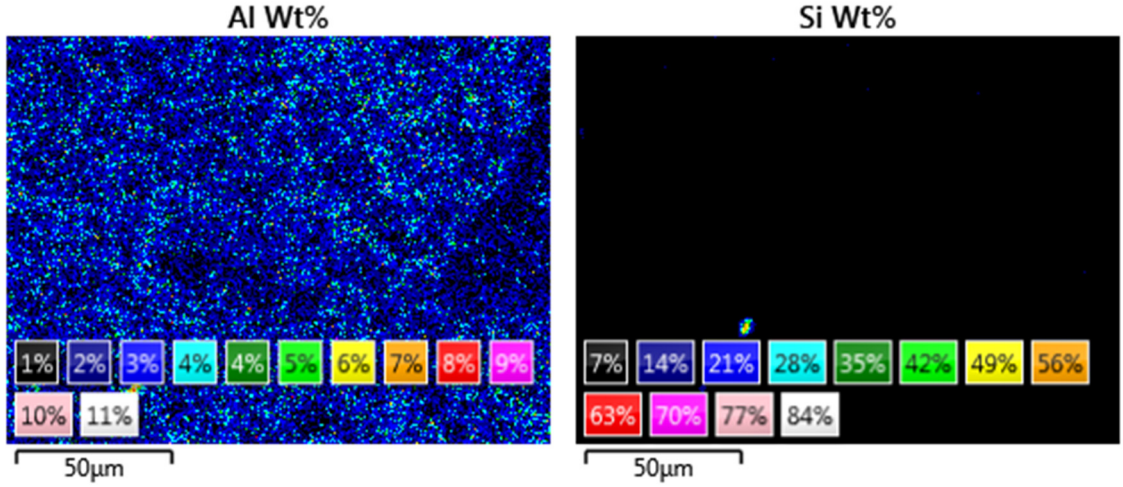

Figure A-3: Element mappings for Al and Si, washed slime (area 3)

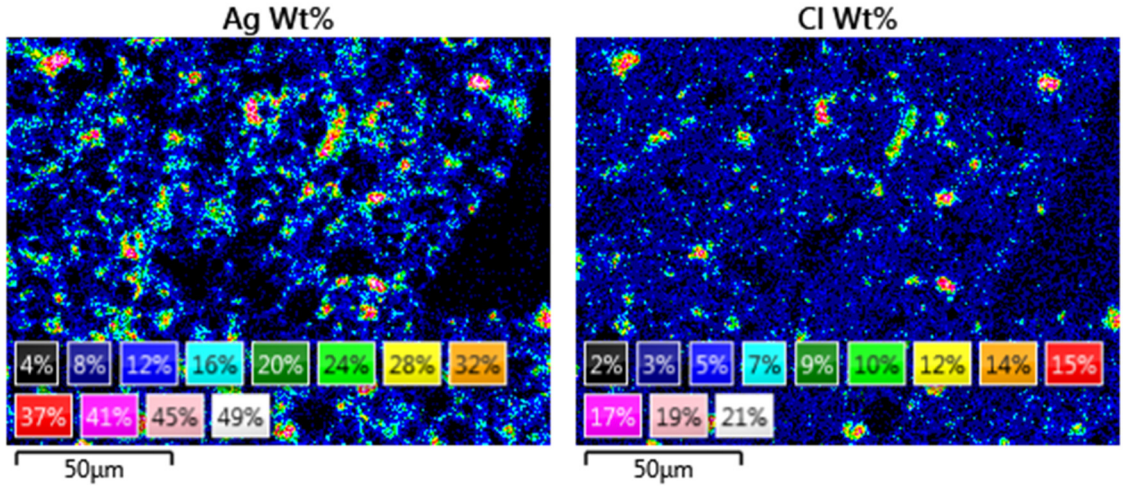

Figure A-4: Element mappings for Ag and Cl, washed slime (area 3)

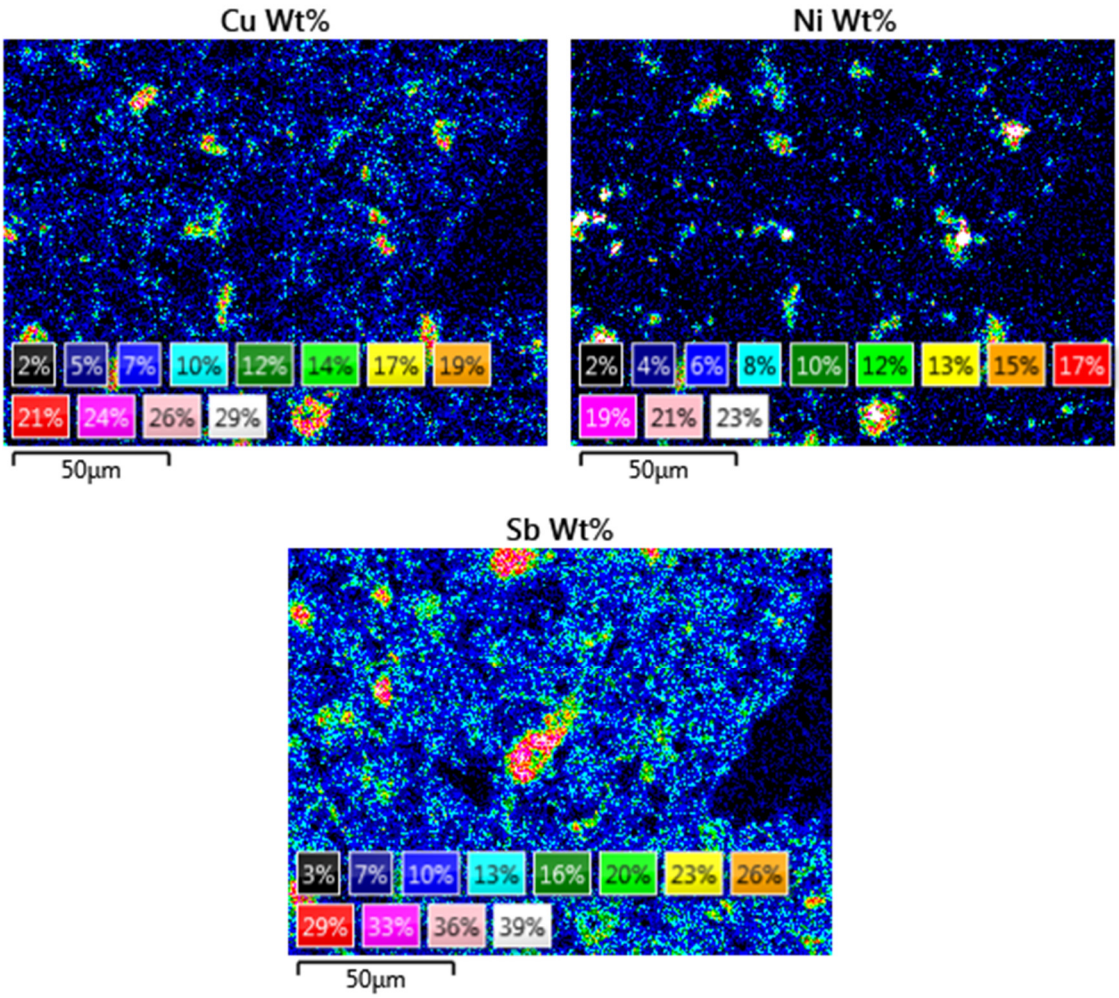

Figure A-5: Element mappings for Cu, Ni and Sb, washed slime (area 3)

Figure A-6 to Figure A-13 show the mappings for single elements of the washed slime, which were used to prove certain phases.

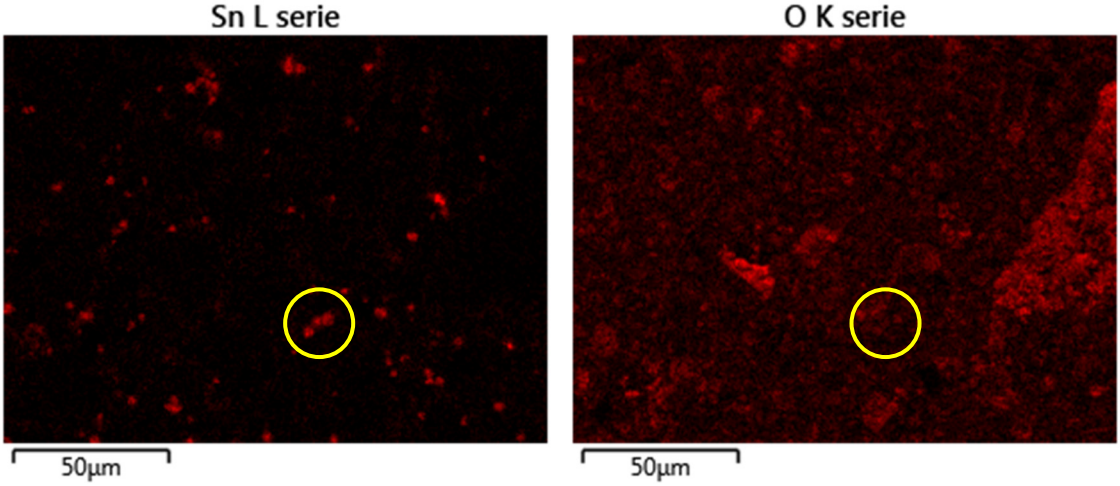

Figure A-6: Element mappings for Sn and O, washed slime (area 3)

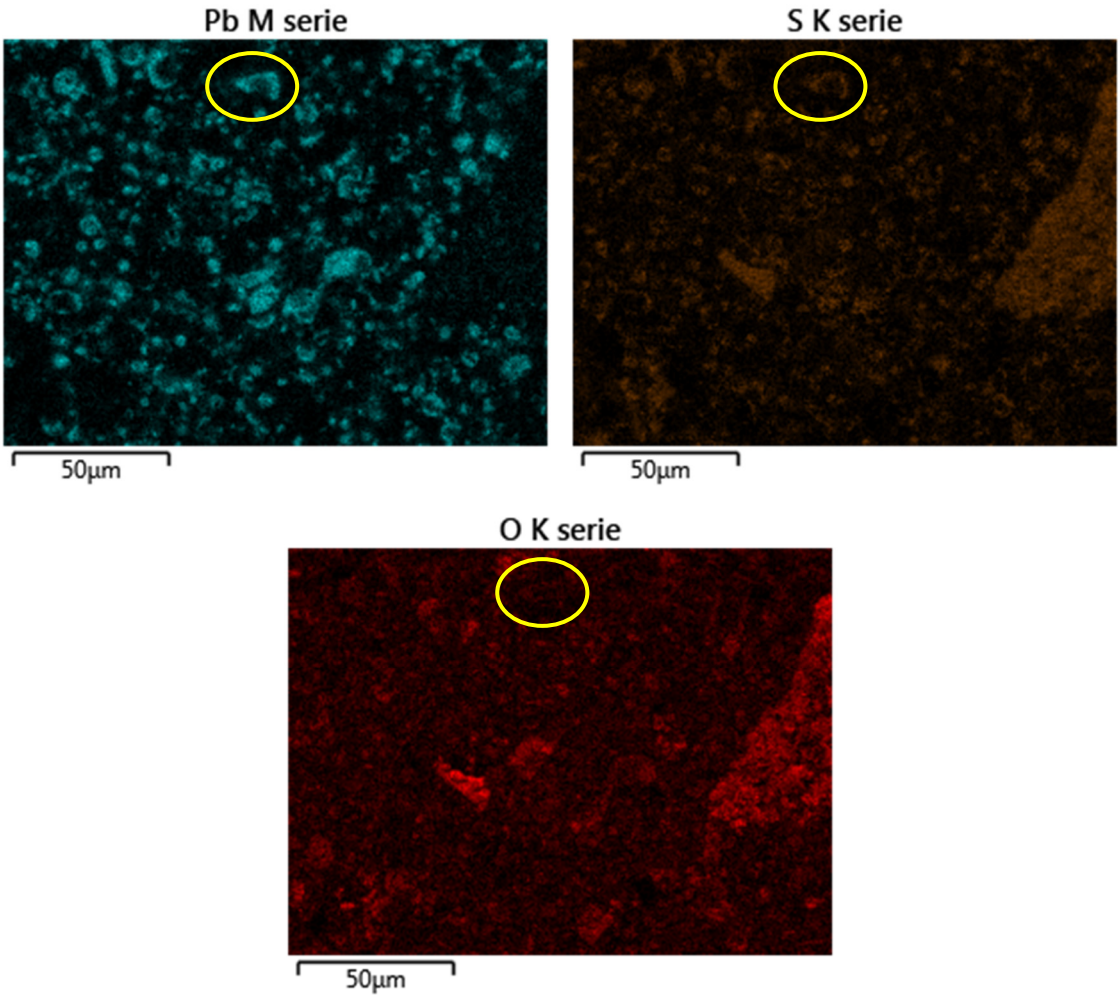

Figure A-7: Element mappings for Pb, S and O, washed slime (area 3)

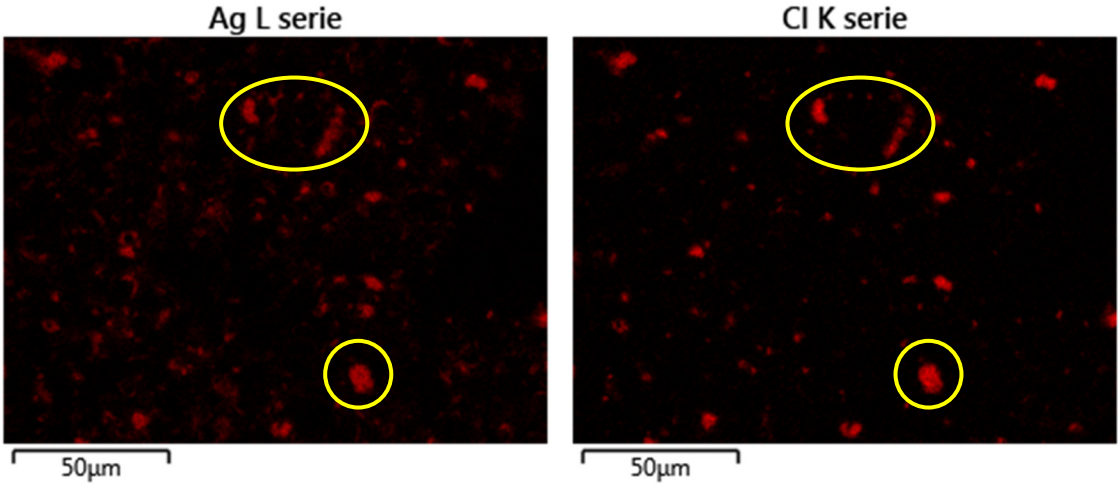

Figure A-8: Element mappings for Ag and Cl, washed slime (area 3)

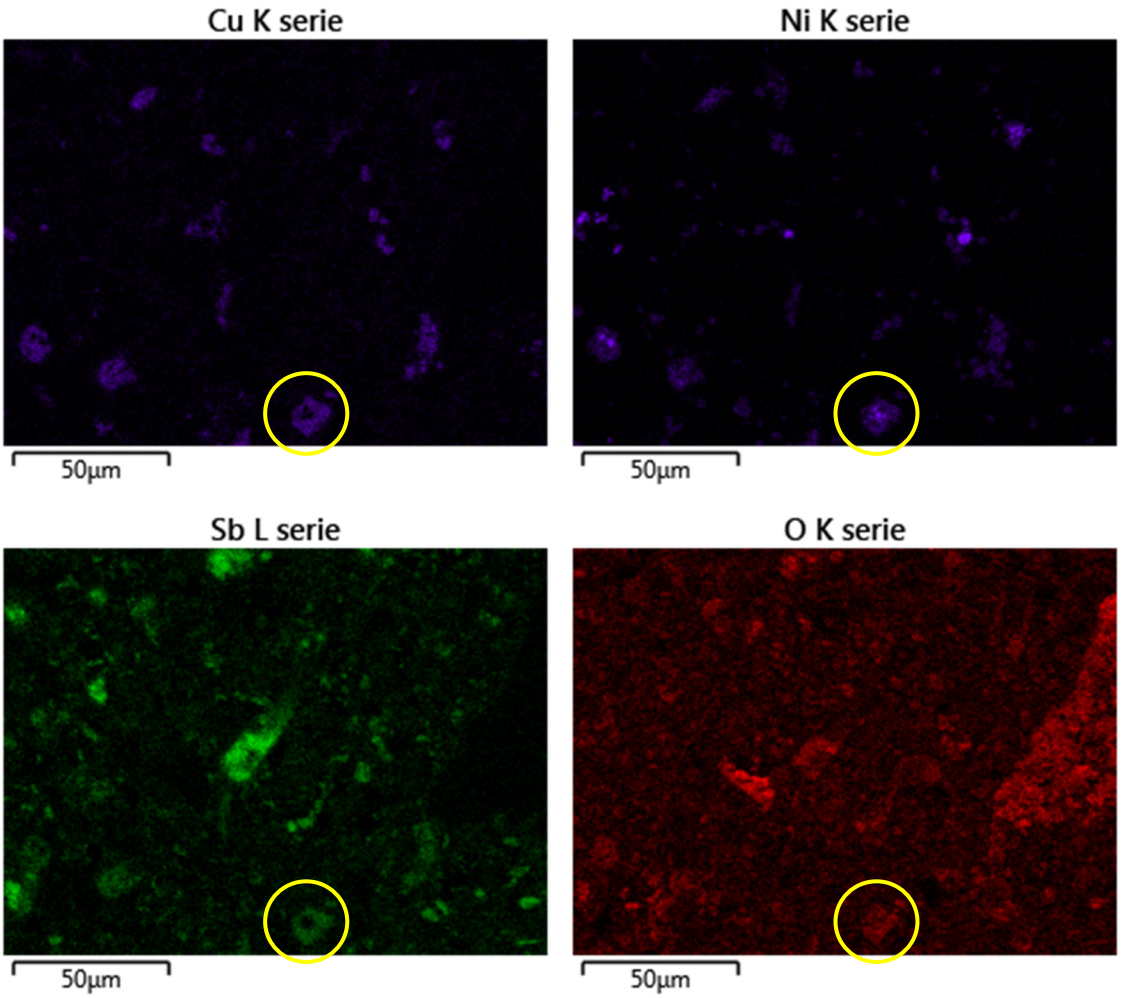

Figure A-9: Element mappings for Cu, Ni, Sb and O, washed slime (area 3)

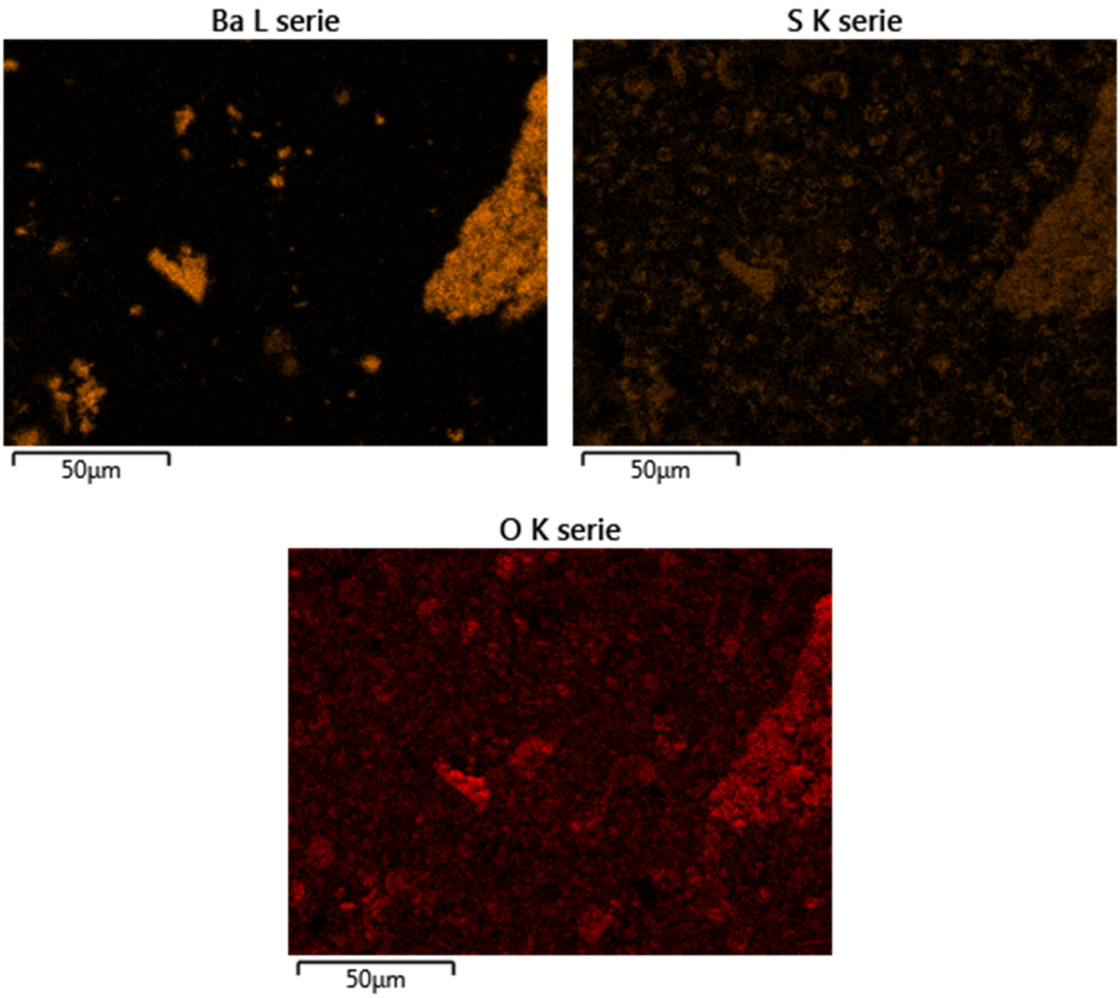

Figure A-10: Element mappings for Ba, S and O, washed slime (area 3)

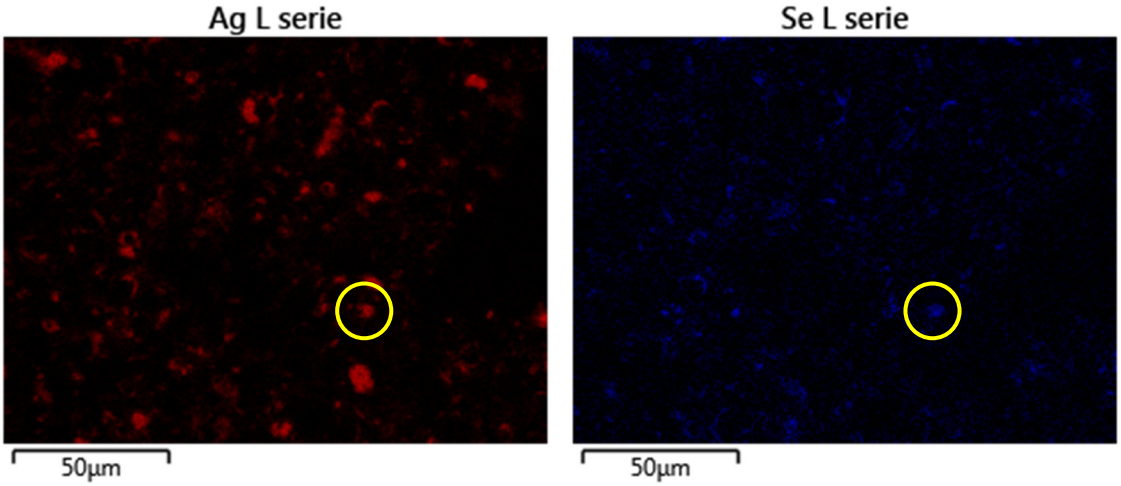

Figure A-11: Element mappings for Ag and Se, washed slime (area 3)

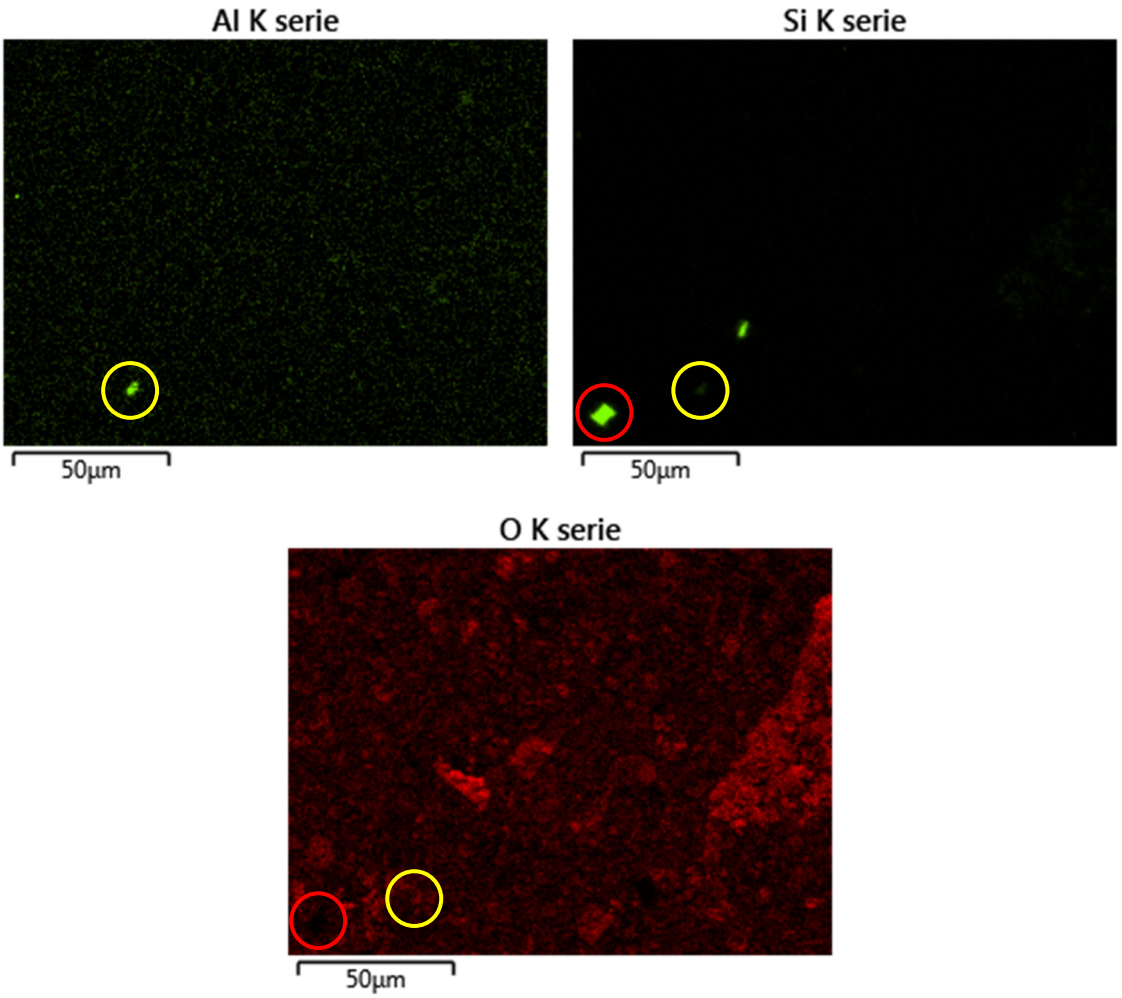

Figure A-12: Element mappings for Al, Si and O, washed slime (area 3)

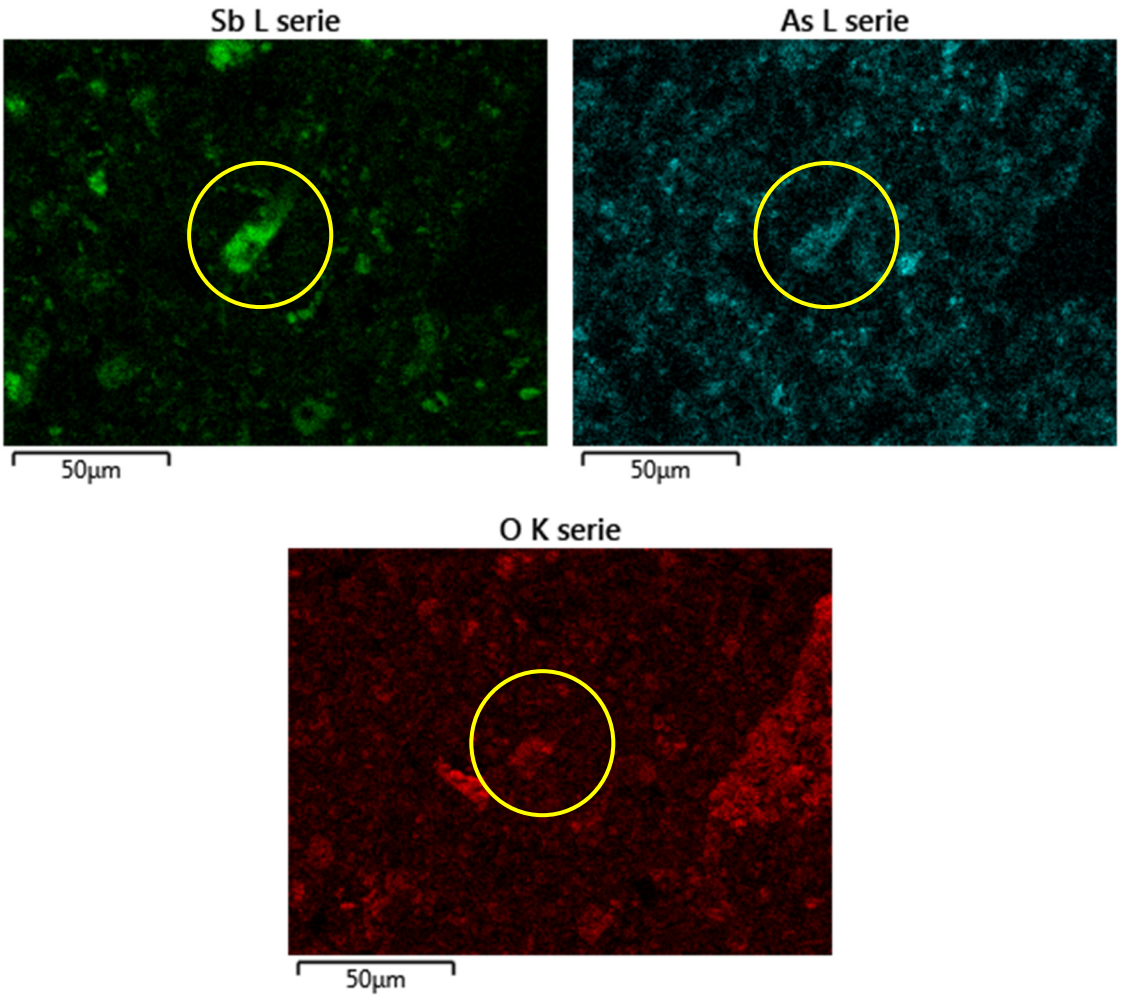

Figure A-13: Element mappings for Sb, As and O, washed slime (area 3)